
TDP-43 and Translational Regulation in Amyotrophic Lateral Sclerosis and Related Neurodegenerative Diseases

Dissertation with the aim of achieving a doctoral degree at the Faculty of Mathematics,
Informatics and Natural Sciences Department of Biology
of Universität Hamburg

Submitted by Katharine K. Miller

2014 in Hamburg, Germany

Evaluation Committee

1st reviewer: Prof. Dr. Christian Lohr

2nd reviewer: PD Dr. Sabine Hoffmeister-Ullerich

Date of Oral Defense: September 5th, 2014

TABLE OF CONTENTS

i	ACKNOWLEDGEMENTS.....	vii
ii	ABSTRACT.....	viii
iii	ZUSSAMMENFASSUNG.....	ix
1	INTRODUCTION – TDP-43.....	1
1.1	OVERVIEW OF TDP-43 RELEVANT NEURODEGENERATIVE DISEASE	1
1.1.1	AMYOTROPHIC LATERAL SCLEROSIS	1
1.1.2	FRONTOTEMPORAL LOBAR DEGENERATION	3
1.1.3	ADDITIONAL TDP-43 PROTEINOPATHIES	4
1.1.3.1	ALZHEIMER’S DISEASE	4
1.1.3.2	PARKINSON’S DISEASE	5
1.1.3.3	CHRONIC TRAUMATIC ENCEPHALOPATHY	5
1.2	TRANSLATION	5
1.2.1	mRNA STRUCTURE	6
1.2.2	RIBOSOME STRUCTURE	7
1.2.3	RIBOSOMAL SCANNING	10
1.2.4	INITIATION	11
1.2.5	ELONGATION	12
1.2.6	TERMINATION AND RECYCLING	14
1.3	TRANSLATIONAL REGULATION	15
1.3.1	GENERAL TRANSLATIONAL CONTROL	15
1.3.2	mRNA-SPECIFIC TRANSLATIONAL CONTROL	16
1.3.3	INTERNAL RIBOSOME ENTRY SITES	18
1.4	TAR DNA-BINDING PROTEIN 43 (TDP-43)	19
1.4.1	TDP-43 DOMAINS	19
1.4.2	NUCLEAR TO CYTOPLASMIC SHUTTLING ABILITY	20
1.4.3	RNA-BINDING ABILITY	22
1.4.4	ALTERNATIVE SPLICING REGULATION	22
1.4.5	PROTEIN-BINDING ABILITY	23
1.4.6	PATIENT MUTATIONS	23
1.4.7	LARGE NUMBER OF NEURODEGENERATIVE DISEASES SHOW TDP-43 PATHOLOGY	24
1.4.8	RNA-BINDING FUNCTION NEEDED FOR TOXICITY	25
1.5	RNA-BINDING PROTEINS	25
1.5.1	RNA-BINDING PROTEINS INVOLVED IN SPLICING	26
1.5.2	RNA-BINDING PROTEINS INVOLVED IN TRANSLATION	27
1.5.3	RNA-BINDING PROTEINS INVOLVED IN NEURODEGENERATIVE DISEASES	28
1.6	THESIS HYPOTHESIS	28
2	MATERIALS AND METHODS – TDP-43	29
2.1	MN1 CELL CULTURE	29
2.1.1	CHARACTERISTICS OF MN1 CELLS	29
2.1.2	CELL CULTURE PRACTICES FOR MN1 CELLS	29

2.2	SUBCELLULAR FRACTIONATION	31
2.3	RNA INTERFERENCE	32
2.3.1	siRNA TRANSFECTION	32
2.3.2	siRNA IMMUNOBLOT	33
2.4	Flp-In T-REx STABLE CELL	34
2.4.1	TRANSFECTION AND STABILIZATION OF MN1 CELLS	34
2.4.2	X-GAL TEST OF LacZ EXPRESSION	36
2.4.3	GALACTO STAR SYSTEM FOR DETECTION OF β-GALACTOSIDASE	37
2.4.4	SOUTHERN BLOT	37
2.4.5	LUCIFERASE ASSAY	39
2.5	PLASMID CLONING	39
2.6	TRANSIENT TRANSFECTION	46
2.7	WESTERN BLOT ANALYSIS	46
2.8	POLYSOME PROFILING FROM MN1 CELLS	48
2.9	POLYSOME PROFILING FROM MOUSE BRAINSTEMS	50
2.10	POLYSOME TO MONOSOME RATIO CALCULATION	50
2.11	PROTEIN ISOLATION FROM POLYSOME FRACTIONS	51
2.12	RNA PURIFICATION AND cDNA SYNTHESIS FROM POLYSOME FRACTIONS	53
2.13	REAL-TIME PCR	54
2.14	Click-iT NASCENT PROTEIN SYNTHESIS MEASUREMENT	54
2.15	BacTRAP IMMUNOPRECIPITATIONS FROM MN1 CELLS AND MOUSE BRAINSTEM	55
2.16	RIBOSOME FOOTPRINTING	56
2.17	ANTIBODIES	62
3	RESULTS – TDP-43	63
3.1	KNOCKDOWN OF TDP-43 IN MN1 CELLS DOES NOT SIGNIFICANTLY ALTER GLOBAL TRANSLATION	63
3.1.1	MOTOR NEURON-LIKE MN1 CELLS EXPRESS ENDOGENOUS TDP-43 MOSTLY IN THE NUCLEUS	63
3.1.2	ROBUST POLYSOME PROFILING FROM MN1 CELL EXTRACTS	64
3.1.3	TDP-43 IS EFFICIENTLY KNOCKED DOWN BY siRNA IN MN1 CELLS	68
3.1.4	TDP-43 REDUCTION DOES NOT AFFECT GLOBAL TRANSLATION IN MN1 CELLS	69
3.2	TRANSIENT EXPRESSION OF TDP-43 VARIANTS IN MN1 CELLS DOES NOT ALTER GLOBAL TRANSLATION	72
3.2.1	STABLE-INDUCIBLE “Flp-In T-REx” MN1 CELL LINE EXPRESSED TDP-43 VARIANTS AT VERY LOW LEVELS	72
3.2.2	GENERAL TRANSLATION IS NOT ALTERED IN MN1 CELLS TRANSIENTLY TRANSFECTED WITH TDP-43 VARIANTS	80
3.3	TRANSLATIONAL EFFICIENCY OF SELECTED CANDIDATE mRNAs WAS NOT AFFECTED BY TDP-43 KNOCKDOWN	82
3.4	TDP-43 IS ASSOCIATED WITH RIBOSOMES AND POLYSOMES	86
3.4.1	TRANSIENTLY TRANSFECTED TDP-43 PROTEIN ASSOCIATES WITH POLYSOMES	86
3.4.2	GFP-TAGGED RIBOSOMAL PROTEIN L10a EXPRESSED IN MOUSE Chat-POSITIVE NEURONS IS INCORPORATED INTO RIBOSOMES	92
3.4.3	IMMUNOPRECIPITATION OF GFP-TAGGED L10a FROM TRANSIENTLY TRANSFECTED MN1 CELLS IS HIGHLY EFFICIENT	95

3.4.4	REAL-TIME PCR OF SELECTED SET OF GENES SHOWS CLEAN AND ROBUST IMMUNOPRECIPITATION FROM Chat BacTRAP MOUSE BRAINSTEMS	97
3.4.5	CO-IMMUNOPRECIPITATION OF V5-TAGGED TDP-43 WITH GFP-TAGGED L10a INDICATES THAT TDP-43 ASSOCIATES WITH RIBOSOMES	100
3.5	RIBOSOME FOOTPRINTING METHOD IN MN1 CELLS AFTER TDP-43 KNOCKDOWN CAN BE USED AS AN ADDITIONAL GENOME-WIDE APPROACH	102
4	DISCUSSION – TDP-43	106
4.1	TDP-43 ASSOCIATES WITH RIBOSOMES/POLYSOMES	106
4.2	KNOCKDOWN OF TDP-43 IN MN1 CELLS DOES NOT ALTER GENERAL TRANSLATION	109
4.3	TRANSIENT EXPRESSION OF TDP-43 VARIANTS – INCLUDING hTDP-43, hTDP-43 WITH AN EXTRA NES, AND hTDP-43 WITH THE A315T PATIENT MUTATION – IN MN1 CELLS DOES NOT ALTER GENERAL TRANSLATION	111
4.4	REAL-TIME PCR ASSAY FOR SELECTED GENES AFTER TDP-43 KNOCKDOWN SHOWED NO ALTERED POLYSOME ASSOCIATION	112
4.5	ESTABLISHMENT OF SEVERAL GENOME-WIDE METHODS FOR FURTHER ANALYSIS OF TDP-43 TRANSLATIONAL REGULATION	114
4.6	GENERAL CONCLUSIONS	116
5	INTRODUCTION – DOHH	118
5.1	HYPUSINATION	118
5.2	eIF5A	119
5.3	DHS	120
5.4	DOHH	120
5.5	GENERATION AND CHARACTERIZATION OF CONDITIONAL DOHH KNOCKOUT IN MICE AND 3T3 CELLS	121
5.6	HYPOTHESIS	122
6	MATERIALS AND METHODS – DOHH	123
6.1	CELL CULTURE	123
6.2	POLYSOME PROFILE GENERATION	123
6.3	POLYSOME TO MONOSOME RATIO CALCULATION	125
6.4	STATISTICAL ANALYSIS	126
7	RESULTS – DOHH	127
7.1	DOHH KO IN 3T3 CELLS SHOWS A DEFECT IN TRANSLATION INITIATION	127
7.2	INHIBITION OF DHS SHOWS EXAGGERATED DEFECT IN TRANSLATION INITIATION	128
7.3	DEFECT IS NOT DUE TO A CELLULAR GROWTH PHENOTYPE	128
7.4	SIMILAR TRANSLATION INITIATION DEFECT PHENOTYPE IS SEEN IN MEF CELLS AFTER REMOVAL OF DOHH	131

8	DISCUSSION – DOHH	133
8.1	DOHH REMOVAL FROM 3T3 AND MEF CELLS CAUSES AN INITIATION DEFECT	133
8.2	GENERAL CONCLUSION	135
9	REFERENCES	136
10	STATEMENT OF CONTRIBUTION	146
11	EIDESSTÄTTLICHE VERSICHERUNG	146
12	EIDESSTÄTTLICHE ERKLÄRUNG	146

ACKNOWLEDGEMENTS

I first have to heartily thank Prof. Dr. Christian Lohr and PD Dr. Sabine Hoffmeister-Ullerich for agreeing to co-supervise this thesis and to additionally thank PD Dr. Sabine Hoffmeister-Ullerich for her incredible guidance, support, and scientific suggestions that made the writing of this thesis possible.

I would like to thank Dr. Kent Duncan for the opportunity to do this thesis in his lab, for discussions, and the opportunity to visit international conferences. I would like to also thank the other members of the lab, as well as the collaborators from the laboratories of Prof. Dr. Stefan Balabanov (including Dr. Henning Sievert) and Prof. Dr. Manuel Friese (including Dr. Benjamin Schattling and Constantin Volkmann), for their insight and input on this project.

Many thanks also go to the Hans und Ilse Breuer Stiftung for selecting me to receive the Graduate Student Stipend for the past two years. This support was a great honor.

The graduate student community at ZMNH has been extremely supportive, and there are too many great people with whom I have had the pleasure of becoming friends and colleagues to name them all. I must, however, thank Andrea Merseburg and Anna Katharina Schlusche in particular for their friendship and help during the writing of this thesis (in particular their assistance with the German language).

My parents, my brothers, my in-laws, and my sisters-in-law (and Coda) have been steadfast in their support during the entirety of my PhD. Everyone in the world should have such a loyal cheering section. So many “thank yous”.

And most importantly, to my husband. Thank you doesn't cover it. Seni çok seviyorum, Canım.

ABSTRACT

Transactive Response (TAR) DNA-Binding Protein 43 (TDP-43) is a ubiquitously expressed RNA-binding protein that is normally localized in the nucleus, but relocates to the cytoplasm of affected cells under disease conditions. TDP-43 was identified as the major protein component of cytoplasmic aggregates found in amyotrophic lateral sclerosis (ALS) and frontotemporal lobar degeneration (FTLD). Additionally, several TDP-43 mutations were identified in ALS patients, indicating that TDP-43 may be a major cause of disease. Whether TDP-43 is causing disease due to a nuclear loss of function, a cytoplasmic gain of function, or a combination of the two is not yet known. TDP-43 binds to approximately 30% of the mouse transcriptome, and participates in splice regulation for many of these mRNAs. However, it was revealed that TDP-43 frequently binds cytoplasmically localized mRNAs at their 3' UTRs. Previous research has identified several RNA-binding proteins that bind to the 3' UTR's of cytoplasmic mRNAs as translational regulators. It would be of great interest to the field of neurodegenerative disease research to identify whether TDP-43 plays such a role, and if so, what mRNAs are translationally regulated by TDP-43.

This thesis shows that both knockdown of TDP-43 and transient expression of several TDP-43 variants (human TDP-43, human TDP-43 targeted to the cytoplasm, and human TDP-43 containing a patient mutation) in cell culture do not show any effects on general translation under normal conditions. Additionally, a focused look at a subset of genes with TDP-43 3' UTR binding sites showed no altered specific translation for these genes. However, since TDP-43 does bind to such a large percentage of mRNAs, it is likely that experimentation on a genome-wide scale would be needed in order to identify mRNAs that are specifically regulated by TDP-43. To this end, multiple genome-wide translation assays – including polysome profiling, BacTRAP analysis, and ribosome footprinting – were established during the time of this work using motor neuron-like cell culture and ChAT-positive neurons in mouse brainstems. These assays are robustly functional, and will provide major insight into what mRNAs TDP-43 translationally regulates.

Intriguingly, the work done in this thesis showed that TDP-43 associates with polysomes and can be immunoprecipitated with ribosomes. This is a very important finding as it is the first time that TDP-43 has been shown to associate with translational machinery without the addition of stress-inducing agents, thus supporting the idea that TDP-43 may be involved in translational regulation. This thesis provides important new data showing TDP-43's association with polysomes/ribosomes and a strong starting point for continued study of TDP-43's involvement with translation, particularly with regard to the specific mRNAs that TDP-43 may translationally regulate. Such research is of great interest to the neurodegenerative disease research community, as it could provide possible drug targets.

ZUSAMMENFASSUNG

Das „Transactive Response“ (TAR) DNA-Bindeprotein 43 (TDP-43) ist ein RNA-Bindeprotein welches ubiquitär im Organismus exprimiert wird und im Zellkern lokalisiert ist. Unter Krankheitsbedingungen kann es jedoch vom Nucleus ins Zytoplasma betroffener Nervenzellen relokalisiert werden. Bei Amyotropher Lateralsklerose (ALS) und Frontotemporaler Demenz (FTD) wurde TDP-43 als ein Hauptproteinbestandteil der in den Nervenzellen vorliegenden zytoplasmatischen Aggregate identifiziert. Darüber hinaus wurden in ALS-Patienten verschiedene TDP-43-Mutationen gefunden, weswegen TDP-43 als eine der Hauptursachen dieser Erkrankungen gilt. Ob sie dadurch verursacht werden, dass TDP-43 seine Funktion im Zellkern nicht mehr wahrnehmen kann, oder dadurch, dass es zu einer überhöhten Funktion im Zytoplasma kommt oder durch eine Kombination aus beidem, ist jedoch noch nicht bekannt. TDP-43 bindet an etwa 30% des murinen Transkriptom, und ist an der Spleißregulation vieler dieser mRNAs beteiligt. Es konnte zusätzlich gezeigt werden, dass TDP-43 häufig an die 3'-UTR zytoplasmatisch lokalisierter mRNAs bindet. Frühere Studien konnten verschiedene RNA-Bindeproteine identifizieren, welche an die 3'-UTR zytoplasmatischer mRNAs binden und somit als Translationsregulatoren fungieren. Entsprechend wäre es für die Forschung im Bereich neurodegenerativer Erkrankungen von großem Interesse zu ermitteln, ob TDP-43 ebenfalls solch eine Rolle bei der Translationsregulation spielt, und welche mRNAs von TDP-43 potentiell reguliert werden.

Die vorliegende Arbeit zeigt, dass sowohl das Herunterregulieren von TDP-43 als auch eine transiente Expression verschiedener TDP-43-Varianten (humanes TDP-43, humanes zytoplasmatisches TDP-43, und humanes TDP-43 mit einer Patientenmutation) in Zellkultur unter normalen Bedingungen keinen Effekt auf die Translation ausüben. Die Untersuchung einer Auswahl von Genen mit TDP-43 3'-UTR-Bindestelle zeigte auch für diese jeweils spezifische Translation keine Veränderung. Da TDP-43 sehr viele mRNAs bindet, muss also systematisch eine genomweite Untersuchung durchgeführt werden, um mRNAs zu identifizieren, welche spezifisch durch TDP-43 reguliert sind. Aus diesem Grund wurden in dieser Arbeit mehrere genomweite Translationsstudien unter Verwendung motorneuronartiger Zellen und aus dem murinen Hirnstamm gewonnener ChAT-positiver Zellen etabliert; darunter Polysomanalyse, BacTRAP-Analyse, und Ribosom-Footprinting-Analyse. Mit Hilfe dieser funktional sehr robusten Assays ist es möglich, einen genauen Einblick über die von TDP-43 potentiell regulierten mRNAs zu gewinnen.

Bemerkenswerterweise konnte hier gezeigt werden, dass TDP-43 sowohl mit Polysomen assoziiert als auch mit Ribosomen immunpräzipitiert werden kann. Dies ist der erste Beleg dafür, dass TDP-43 auch ohne zusätzliche Stressinduktion mit dem Translationsapparat assoziiert, wodurch die Vermutung, dass TDP-43 bei der Translationskontrolle eine Rolle spielt, stark unterstützt wird. Die in dieser Arbeit gefundene Assoziation von TDP-43 mit Polysomen/Ribosomen liefert einen wichtigen Ausgangspunkt für weitere Untersuchungen hinsichtlich der Rolle von TDP-43 bei der Translation, insbesondere im Hinblick auf spezifische mRNAs, welche von TDP-43 reguliert werden könnten. Solche Untersuchungen sind vor allem für die Erforschung neurodegenerativer Erkrankungen von großer Bedeutung, da sie Hinweise für potentielle Therapieansätze und Wirkstoffziele liefern könnten.

1 INTRODUCTION – TDP-43

1.1 OVERVIEW OF TDP-43 RELEVANT NEURODEGENERATIVE DISEASE

1.1.1 AMYOTROPHIC LATERAL SCLEROSIS

Amyotrophic lateral sclerosis (ALS), also known as motor neuron disease or Lou Gehrig's disease, is the most frequently occurring motor neuron disease, affecting 2-3 people per 100,000. Age of onset ranges widely, but on average falls between 55 and 70 years of age (Logroscino et al., 2010), and life expectancy after diagnosis is approximately 3-5 years (Traynor et al., 2000). Progressive loss of motor function results in death, frequently due to malfunction of the diaphragm resulting in the inability to breathe. Despite many years of research, the molecular mechanisms behind this debilitating disease are not yet known (For a review see Kiernan et al., 2011).

Jean-Martin Charcot first described ALS in 1874. One common pathological marker of the disease is the appearance of aggregates in the motor neurons of affected patients. Aggregates are a unifying factor in patients, as there are more than 20 types of ALS, and many different genetic mutations have been found to be associated with ALS. The first major mutation to be identified was the SOD1 mutation, identified in 1993 (Rosen et al., 1993). Over 150 mutations in SOD1 have been identified, and have been extensively studied in animal models. Unfortunately, while much has been learned about SOD1, this has not led to a cure for the disease. Likely, this is because mutations in SOD1 are not the primary cause for ALS.

In 2006, several years after the discovery of the SOD1 mutation, the major protein content of the aggregates was identified as TAR DNA binding protein 43 (TDP-43) (Arai et al., 2006; Neumann et al., 2006). TDP-43 was found to be in aggregates of around 90% of ALS cases, but not in cases of ALS that present with SOD1 mutations (Mackenzie et al., 2007). This separation of the disease into sections suggests the possibility that the disease commonly known as ALS may actually be a collection of similarly presenting diseases.

Concomitant with the discovery of TDP-43 in the aggregates of ALS, it was found that TDP-43 was also a major protein content of aggregates found in frontotemporal lobar degeneration (FTLD) (Arai et al., 2006; Neumann et al., 2006). Most interestingly, it was also shown that there is frequently an overlap in patients presenting with ALS and FTLD, suggesting that ALS and FTLD may not be two separate diseases, but rather a disease continuum (For a review, see Geser, Lee, & Trojanowski, 2010). The common factor of TDP-43 positive aggregates links the two diseases.

<u>TYPE</u>	<u>ASSOCIATED GENE</u>
ALS1	SOD1
ALS2	ALS2
ALS3	-----
ALS4	SETX
ALS5	-----
ALS6	FUS
ALS7	-----
ALS8	VAPB
ALS9	ANG
<u>ALS10</u>	<u>TARDBP</u>
ALS11	FIG4
ALS12	OPTN
ALS13	ATXN2
ALS14	VCP
ALS15	UBQLN2
ALS16	SIGMAR1
ALS17	CHMP2B
ALS18	PFN1
ALS19	ERBB4
ALS20	HNRNPA1
ALS-FTD	C9ORF72

Fig 1.1 ALS types and associated genes

There are more than 20 types of ALS. Many of the associated genes have been identified, including TARBDP – the gene coding for TDP-43. However, several genes still remain unidentified.

Shortly after the discovery of TDP-43 as a major protein involved in ALS and FTLD pathology, another protein with many similar characteristics, FUS/TLS, was found to be involved in ALS (Kwiatkowski et al., 2009). FUS/TLS is a second RNA-binding protein

identified in aggregates in patients with ALS and FTLD. However, while TDP-43 pathology accounts for around 90% of all ALS patients, FUS/TLS pathology does not overlap with TDP-43 pathology, and accounts for a much smaller percentage of patients. Because of their RNA-binding ability, the association of TDP-43 and FUS/TLS with ALS strongly indicates that altered RNA processing may be a common factor in ALS disease progression.

Recently, in 2011, the C9Orf72 hexanucleotide repeat expansion was identified as the largest known cause for ALS, accounting for around 6% of all ALS cases (DeJesus-Hernandez et al., 2011; Renton et al., 2011). This repeat expansion shows TDP-43 pathology in carriers. There have been several suggestions as to how the C9Orf72 expansion affects disease progression, including recent studies that have shown that it can be involved in repeat associated non-ATG (RAN) translation, producing multiple versions of dipeptide repeats (Mori et al., 2013).

With so many different genes associated with ALS, it has been difficult for researchers to identify the common cause of the disease. However, it seems likely that RNA metabolism is involved, since many of the major factors (TDP-43, FUS/TLS, C9Orf72) are involved in RNA processing. TDP-43's presence in the aggregates of 90% of patients, including in the pathology of C9Orf72 patients, makes it a strong candidate for focused research. It is of great interest how TDP-43 may be involved in altered RNA processing under disease conditions.

1.1.2 FRONTOTEMPORAL LOBAR DEGENERATION

Frontotemporal lobar degeneration (FTLD) is a group of several different behavioral and speech disorders associated with dementia (For a review, see Neary, Snowden, & Mann, 2005). These disorders include behavioral variant frontotemporal dementia (bvFTD), semantic dementia (SD), and progressive nonfluent aphasia (PNFA). Briefly, bvFTD patients exhibit lethargy and an inability to care for themselves alongside verbal inhibition, which causes them to make inappropriate comments. SD patients have the ability to pronounce words and form sentences, but they lose the ability to recognize word meanings. PNFA patients, on the other hand, lose pronunciation and articulation abilities, as well as the ability to form sentences, however they maintain word meaning. Despite having very different behavioral presentations, these disorders are linked together by progressive degeneration of the frontal and temporal lobes of the brain.

FTLD is the fourth most common dementia, and the second most common young onset dementia after Alzheimer's disease (Feldman et al., 2003). Like ALS, most cases of FTLD present with aggregates in the affected neuronal subtypes. Three major proteins are found in separate sets of this disease: Tau, TDP-43, and FUS/TLS (Slegers, Cruts, & Van Broeckhoven, 2010). As mentioned above, there is a significant overlap between ALS and FTLD. Many patients that present with ALS also develop symptoms associated with FTLD and vice versa. Again, like ALS, there are many different genetic causes for FTLD. These include mutations in Tau, progranulin, chromatin-modifying protein/charged multivesicular body protein 2B (CHMP2B), and valosin-containing protein (VCP). While rare TDP-43 mutations have been found in FTLD, it is not considered a main cause of disease, and the overlap between ALS and FTLD may account for these mutations being present in FTLD at all (Geser et al., 2010).

1.1.3 ADDITIONAL TDP-43 PROTEINOPATHIES

While TDP-43 mutations and pathology are most frequently associated with ALS and FTLD due to the prevalence of TDP-43 positive aggregates found in these diseases, several other neurodegenerative diseases have been identified that show TDP-43 pathology. These diseases have come to be known as "TDP-43 Proteinopathies". There are many other diseases that have been identified as TDP-43 proteinopathies, but detailed in this section are three that have particularly strong ties with TDP-43 pathology.

1.1.3.1 ALZHEIMER'S DISEASE

Alzheimer's disease (AD) is the most frequently occurring dementia, predicted to affect 1 in 85 people by 2050 (Brookmeyer, Johnson, Ziegler-Graham, & Arrighi, 2007). Age of onset is most frequently after 65 years, and life expectancy is around 7 years after diagnosis. While the behavioral phenotype of AD varies greatly, it most often presents with memory loss and disorientation (For a review, see Ballard et al., 2011).

While the molecular causes of AD are not fully understood, there are several standing hypotheses. One such hypothesis is that the extracellular amyloid beta ($A\beta$) that is generated from amyloid precursor protein (APP) forms plaques that are a fundamental factor in AD

development. While there are many variations on this theory, as well as additional theories including misregulation of Tau protein, it is clear that the underlying cause is not yet known. Recently, it has been shown that TDP-43 pathology was found in approximately 50% of all Alzheimer's cases, indicating the possibility that TDP-43 may play a role in disease etiology (Arai et al., 2010). The identification of TDP-43's function in disease may help to shed light on the molecular characteristics of Alzheimer's disease.

1.1.3.2 PARKINSON'S DISEASE

Parkinson's disease (PD) is a neurodegenerative disorder affecting the dopaminergic neurons in the substantia nigra section of the brain. This neurodegeneration manifests as a shaking movement disorder early on, with development of dementia in later years. Adult onset PD is most common, with the average age of onset around 65 years. While PD is not considered fatal, complications can affect life expectancy (For a review, see Davie, 2008).

Accumulation of α -synuclein into Lewy bodies is the most prominent pathology of PD. However, how these Lewy bodies cause disease is not known. Recent research has shown that TDP-43 is also misregulated in PD (Nakashima-Yasuda et al., 2007). How TDP-43 misregulation may be involved in PD is not yet clear.

1.1.3.3 CHRONIC TRAUMATIC ENCEPHALOPATHY

Chronic traumatic encephalopathy (CTE) is a degenerative disease often found in athletes who perform in sports that incur frequent head injuries, or in persons with careers that result in similar injuries. Dementia and aggression are two of the major manifestations of this disease. Pathology of this disease is widely varied, and includes Tau and A β deposits, as well as TDP-43 aggregation (McKee et al., 2010).

1.2 TRANSLATION

RNA-binding proteins (RBPs) have the ability to alter normal RNA processing, and may eventually lead to diseases. One such RNA process that has been shown to lead to disease is

the process of protein translation. In order to investigate the function of RBPs on translation and how their altered expression might affect protein expression, the basic steps of translation must be understood. The basic steps of translation are scanning, initiation, elongation, termination, and ribosome recycling. Each of these steps requires unique factors to insure the integrity of the process. Translation differs between prokaryotes and eukaryotes, and small differences within eukaryotic translation have also been identified (For a review, see Malys & McCarthy, 2011). Since the research in this thesis focuses on mammalian models, this section will concentrate on the details of mammalian translation.

1.2.1 mRNA STRUCTURE

Messenger RNA (mRNA) is the molecule that transfers the genetic information from DNA in the nucleus to the ribosomes in the cytoplasm for translation into protein. mRNA is made up of nucleotides, and the nucleotide sequence is transcribed from the DNA as the matching base pairs of the gene, except that uracil (U) is substituted for thymine (T).

As pre-mRNA is transcribed from the DNA, it is modified in several important ways. The first way is mRNA splicing: removing introns from the pre-mRNA sequence and joining exons together. This is done by the spliceosome, a complicated multi-protein complex that recognizes sequences in the pre-mRNA that indicate that it should be spliced. The spliceosome loops the intronic RNA together and removes it while positioning the adjacent exons in position for a nucleophilic attack to join the two exons together (Brody & Abelson, 1985).

In addition to splicing, the mRNA normally also has the addition of a 5' 7 methylguanosine cap at the 5' end (Muthukrishnan, Both, Furuichi, & Shatkin, 1975). The addition of this cap assists in export of the mRNA from the nucleus and protects the mRNA from degradation. It also importantly promotes translation of this mRNA under canonical translational methods.

At the 3' end of the mRNA, most mRNAs (the exception being mRNAs for histones) are polyadenylated by a specific polymerase (Munroe & Jacobson, 1990). This adenylation helps to protect the mRNA from degradation, and also assists in translation of the mRNA.

Other important features of the mRNA are the 5' untranslated region (UTR), the 3' UTR, and the coding sequence (CDS). The 5'UTR is located upstream of the CDS, and contains many sites for RBP binding as well as cues for where the ribosome should start translation. The CDS is the sequence of nucleotides that actually encodes for the amino acid sequence of the protein that will be translated. CDS's usually begin with a start site (Methionine, AUG) and end with one of several stop sites. After the stop site, the 3'UTR continues downstream until the polyadenylated tail of the mRNA (For a review, see Gebauer & Hentze, 2004).

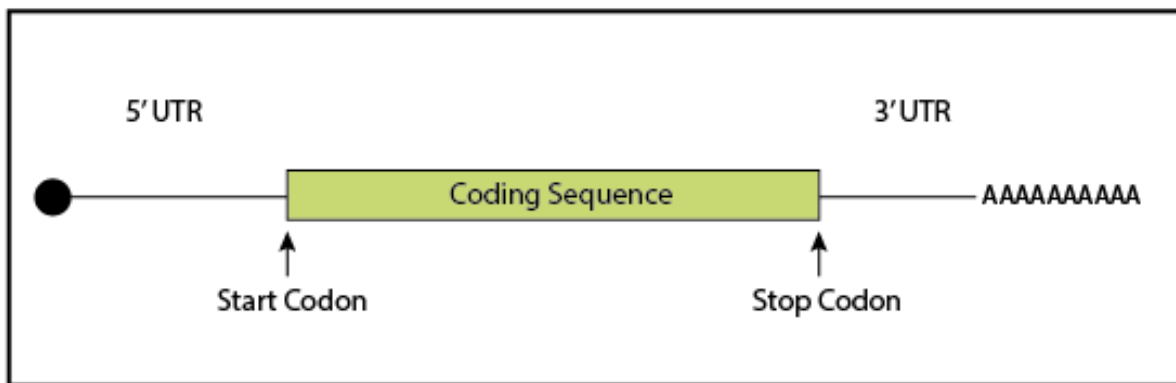


Fig 1.2 General structure of mRNA

An overview of the basic structure of an mRNA. mRNAs contain a 5' 7 methylguanosine cap (black ball) at the 5' end to aid in mRNA export and to help protect the mRNA from degradation. Similarly, it contains a poly(A) tail (string of As) at the 3' end, also to protect from degradation as well as to assist in translation. mRNAs also contain a 5' untranslated region (UTR) and a 3' UTR that flank the coding sequence (CDS). The CDS is what codes for the protein that will be translated. The CDS begins with the start codon and ends with a stop codon.

Prior to being translated, the mRNA is circularized. This circularization promotes scanning and translation initiation. The circularization takes place due to the binding of several RBPs to the mRNA's 5' and 3' UTRs. The poly-(A) binding protein (PABP) binds to the poly(A) tail, while eIF4E binds to the 5'UTR. They both bind to eIF4G, which forms a circularized version of the mRNA (Wells, Hillner, Vale, & Sachs, 1998).

1.2.2 RIBOSOME STRUCTURE

The structure of the ribosome differs between prokaryotes and eukaryotes (and even slightly between different eukaryotes such as yeast and mammals). Since this thesis will be focusing

on proteins and diseases found in mammals, only a description for the eukaryotic mammalian ribosome will be given.

The ribosome consists of RNA and proteins that are organized into two subunits: the 40S small ribosomal subunit and the 60S large ribosomal subunit. When they are joined together, they form the 80S monosome, which is able to translate mRNA into protein. Both subunits are made up of ribosomal RNA (rRNA) and ribosomal proteins that allow them to function in translation. The number of ribosomal proteins is approximate, and continues to fluctuate as experimental methods change (Nazar, 2004).

The 40S subunit, or the small subunit, is made up of the 18S rRNA as well as ~33 ribosomal proteins. The 40S subunit is important for matching the codon of the mRNA with the anti-codon of the tRNA holding the next amino acid. When separate from the 60S subunit, it can bind with several eukaryotic initiation factors, and has the ability to scan the 5'UTR of mRNAs until it reaches the start codon of the coding sequence (Ben-Shem et al., 2011).

The 60S subunit, or the large subunit, is made up of three rRNAs, the 5S, 5.8S and the 28S rRNAs, as well as ~49 ribosomal proteins. The 60S subunit contains the tunnel for the nascent polypeptide chain to pass through. Likely, this tunnel is important for formation of the secondary structure of the polypeptide chain (Ben-Shem et al., 2011).

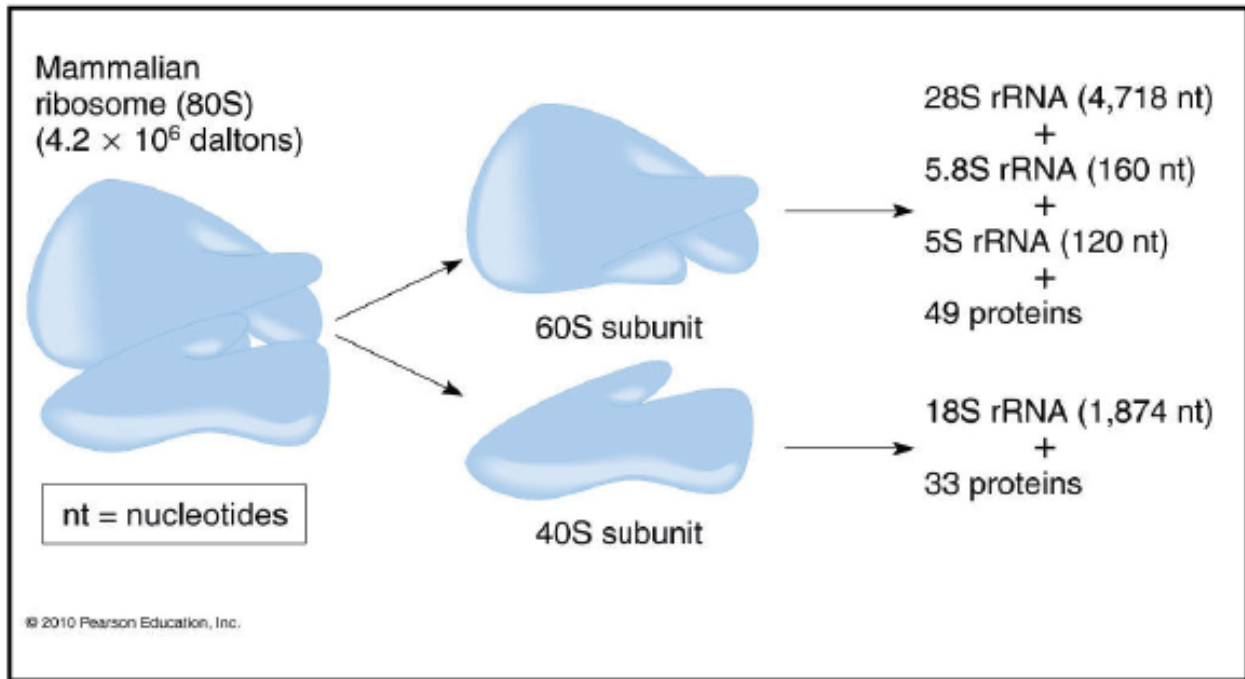


Fig 1.3 General structure of the eukaryotic ribosome

The eukaryotic ribosome is made up of two subunits; the 60S large ribosomal subunit, and the 40S small ribosomal subunit. The 60S subunit is made up of three ribosomal RNAs (the 28S, 5.8S and 5S rRNAs) as well as ~49 proteins. The 40S subunit is made up of the 18S rRNA and ~33 ribosomal proteins. These two subunits join together to form the 80S monosome, or ribosome, which can function to translate mRNA to protein. (Figure modified from Russell, 2009)

When these two subunits join together at the start codon of the coding sequence, they form the 80S monosome. As the monosome is translating an mRNA, the ribosome structure rearranges itself over and over in order to allow tRNA binding and translocation and ribosome movement along the mRNA.

The 80S monosome has three tRNA sites: the aminoacyl site (A site), the peptidyl site (P site) and the deacylated or exit site (E site). These sites accommodate the respective types of tRNA (aminoacyl-tRNA, peptidyl-tRNA and deacylated-tRNA, respectively).

1.2.3 RIBOSOMAL SCANNING

In order to identify the start codon of the mRNA, the 40S ribosomal subunit joins up with eukaryotic initiation factors (eIFs) 1, 1A, 3, and 5 as well as with the so-called ternary complex. The ternary complex is made up of initiator tRNA, which is bound to the methionine that will match the AUG start codon for the start of the protein, as well as eIF2 bound to GTP. Once the 40S, eIFs, and the ternary complex are bound together, they are called the 43S pre-initiation complex. With the attachment of eIF4, the 43S subunit begins scanning the mRNA starting at the 5' cap and moving along the 5' UTR (Pestova & Kolupaeva, 2002).

During scanning of the 5'UTR, the 43S pre-initiation complex will reach the “Kozak sequence” (Kozak, 1987). The Kozak sequence is a nucleotide sequence surrounding the start codon that indicates to the pre-initiation complex that it should join with the 60S subunit and initiate translation. The Kozak sequence consensus is (gcc) gccRccAUGG. The Kozak sequence can vary from this specific sequence, but the closer to the sequence it is, the stronger the chances of initiation (Iida, 1996).

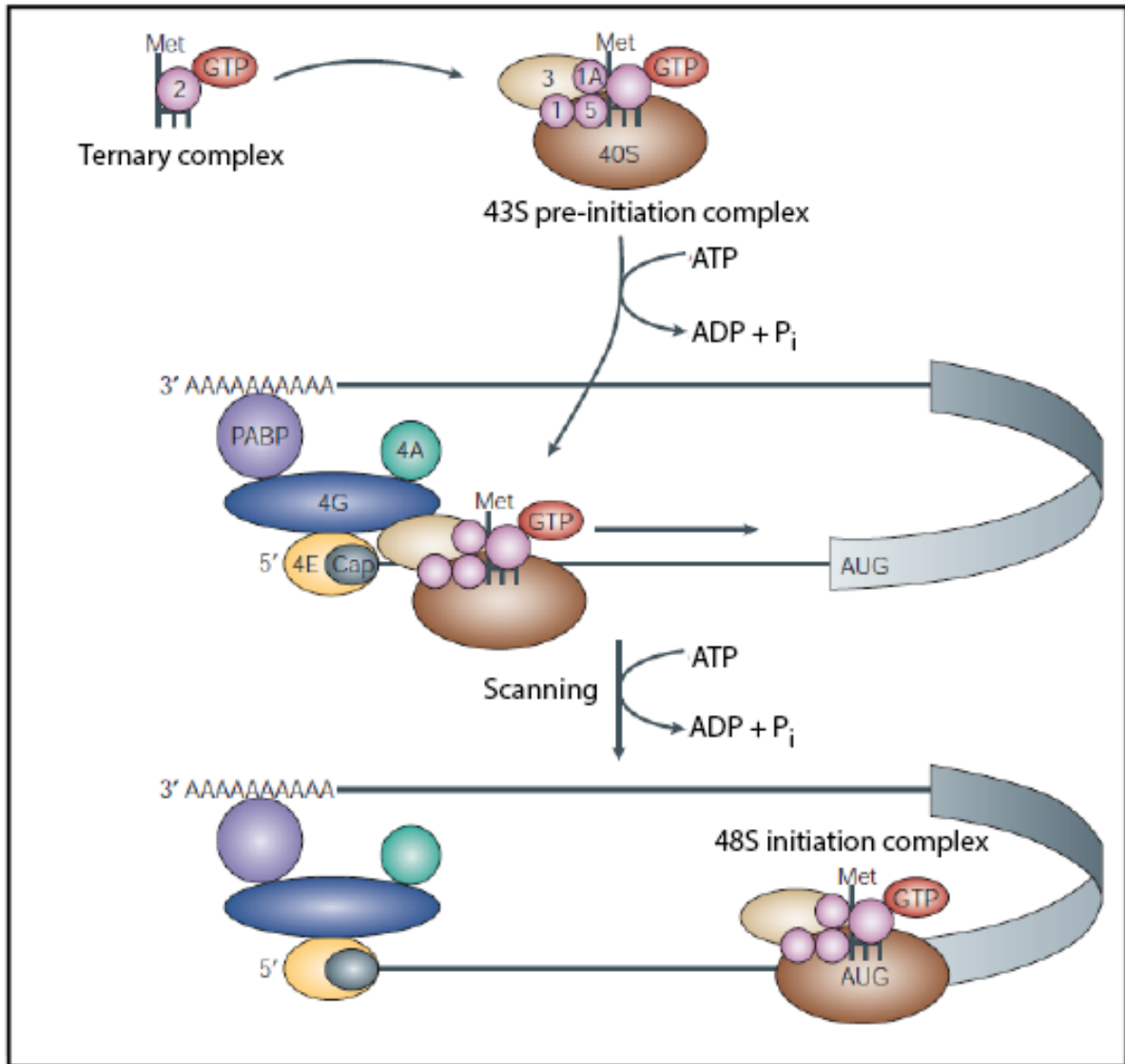


Fig 1.4 Scanning

The so-called 43S pre-initiation complex is made up of the 40S ribosomal subunit, the ternary complex – which contains eIF2, GTP and the initiator methionine tRNA – and eIFs 1, 1A, 3 and 5. This pre-initiation complex binds near the 5' cap of the circularized mRNA and scans in a 5'-3' direction until it reaches the AUG start codon. (Figure modified from Gebauer & Hentze, 2004)

1.2.4 INITIATION

Once the pre-initiation complex has identified the Kozak sequence, it will pause, release several initiation factors, and join with the 60S large ribosomal subunit. Since the initiator tRNA is already a part of the pre-initiation complex, it is able to recognize its match with the start codon. eIF2 hydrolyzes the GTP it is bound with, thereby dissociating eIF3 and eIF4, which allows eIF5B to induce the 60S subunit to join to the 40S subunit (Pestova &

Kolupaeva, 2002). Once the complete 80S monosome is formed, elongation of the polypeptide begins.

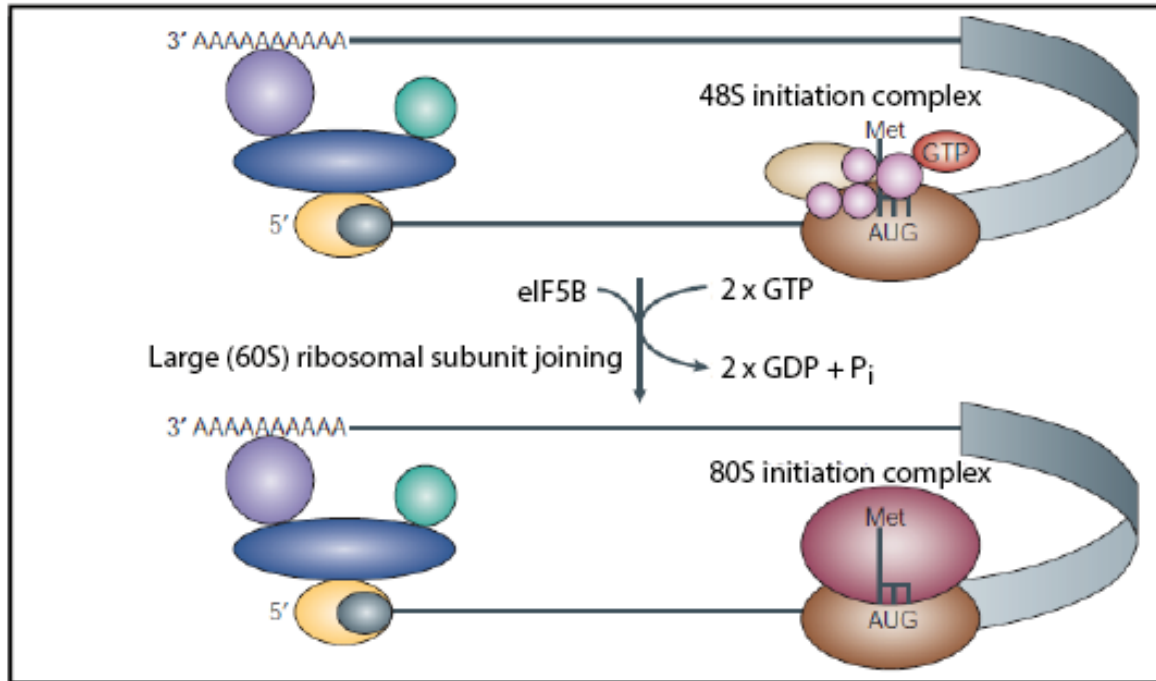


Fig 1.5 Translation Initiation

Once the initiation complex is bound to the AUG start codon of an mRNA, several initiation factors are released, which allows joining of the 60S subunit, creating the 80S initiation complex. (Figure modified from Gebauer & Hentze, 2004)

1.2.5 ELONGATION

At the beginning of elongation, the Met-tRNAⁱ will be in the peptidyl (P) site of the ribosome, with both the E and the aminoacyl (A) sites left open. Eukaryotic elongation factor (eEF) 1A binds to tRNAs, and targets them to the empty A site based on the matching codon sequence. Once the tRNA is in place, the peptidyl transfer complex of the ribosome places the two tRNAs in position, and peptidyl transfer occurs (Keeling & Inagaki, 2004). Next, eEF2 bound with GTP binds next to the tRNA in the A site, and by GTP hydrolysis, releases the bound tRNAs from the ribosome, allowing the ribosomal subunits to ratchet and move along the mRNA. This shifts the tRNAs to the E and P sites, leaving the A site open – a process called translocation (Taylor et al., 2007). The tRNA that is in the E site is released, leaving just the tRNA in the P site connected with the nascent peptide chain. Once the A site is open,

the process continues along the mRNA, extending the peptide chain that is being formed until the ribosome reaches the stop codon.

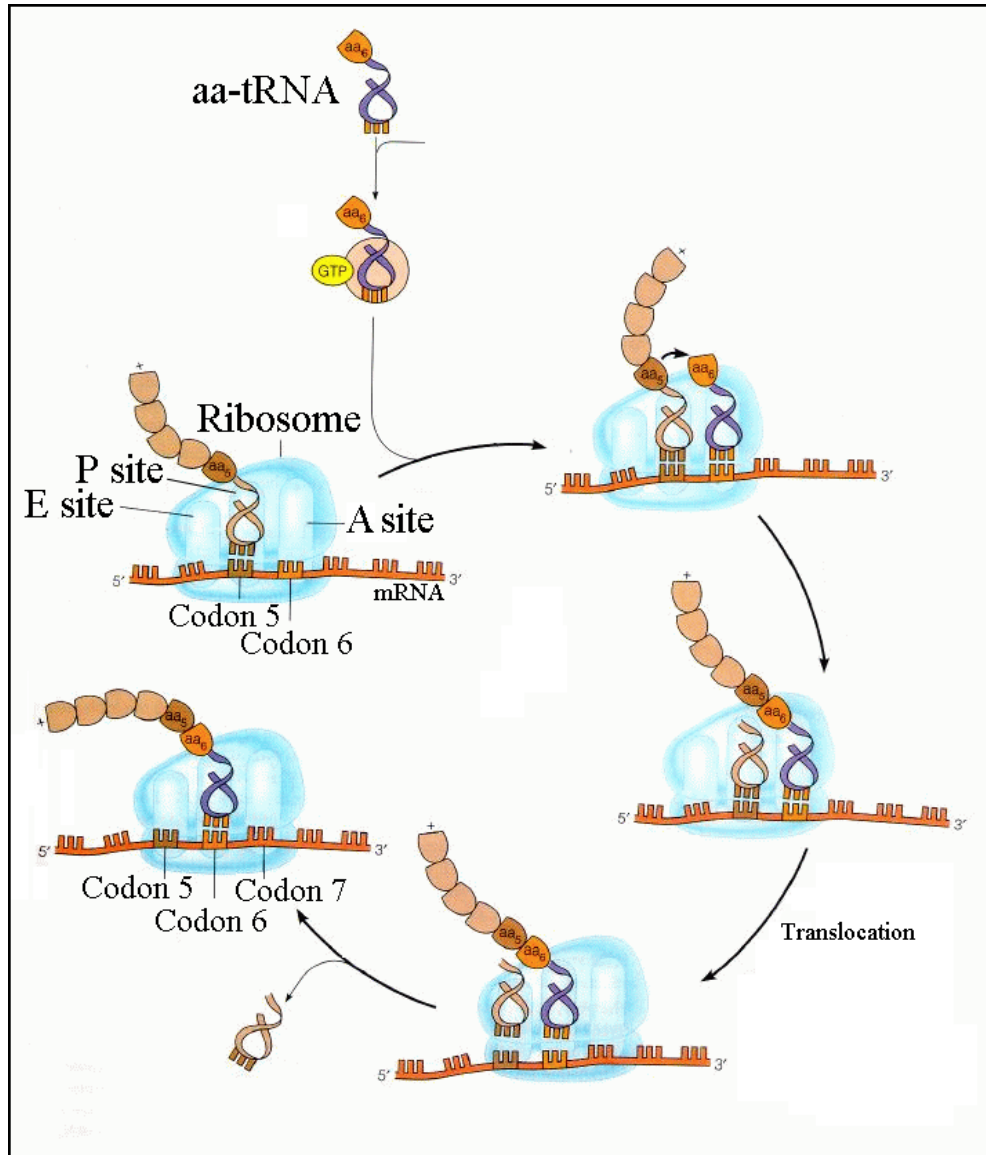


Fig 1.6 Translation Elongation

Elongation occurs when the tRNA containing the amino acid chain is in the P site of the ribosome. The tRNA for the next codon is able to insert itself into the A site of the ribosome. Then through peptidyl transfer, the peptide chain is transferred from the tRNA in the P site to the amino acid attached to the tRNA in the A site. GTP hydrolysis allows translocation to occur, shifting the peptide chain-containing tRNA to the P site, and the now free tRNA to the E site. The tRNA in the E site is released, and the process is able to start again. (Figure modified from Christopher K. Mathews, Kensal E. van Holde, D. R. Appling, 2012)

1.2.6 TERMINATION AND RECYCLING

Translation termination occurs when the translating ribosome reaches one of the stop codons – UAA, UGA or UAG – at the end of the coding sequence on the mRNA (Goldstein, Beaudet, & Caskey, 1970). There are two eukaryotic release factors (eRFs) involved in termination, eRF1 and eRF3. eRF1 is shaped similarly to tRNA, and is involved in stop codon recognition. eRF3 binds to eRF1, and facilitates release of the polypeptide chain through GTP hydrolysis. With the addition of the ABC family ATPase E1 (ABCE1), the ribosomal subunits are separated. In most cases, it seems likely that both ribosomal subunits release the mRNA and are capable of reinitiating on the same or another mRNA (Pisarev et al., 2010).

In some cases, however, the 40S subunit continues scanning, and can promote downstream ORF re-initiation. Whether it can return by continued scanning through the circularized mRNA to the 5'UTR of the original ORF is unclear (For a review, see Jackson, Hellen, & Pestova, 2010).

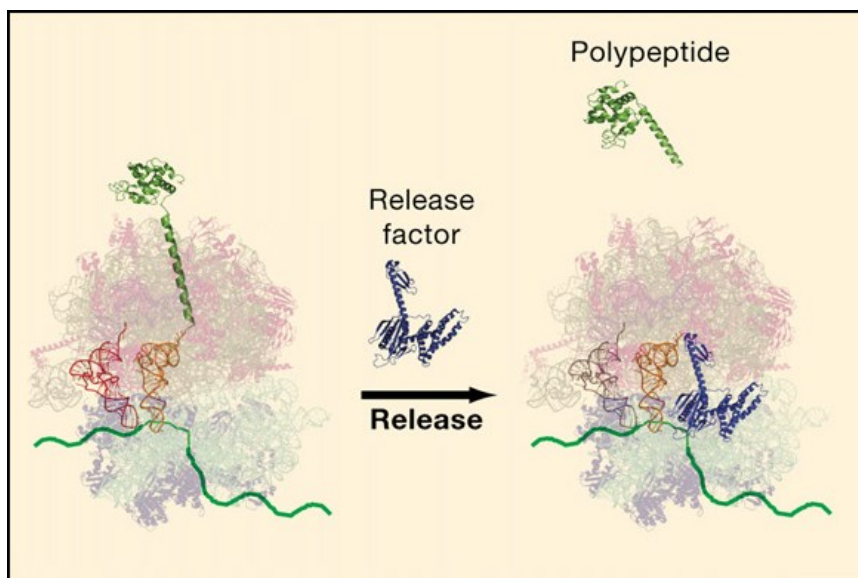


Fig 1.7 Termination

The eukaryotic release factors (eRFs) 1 and 3 bind to each other. When the ribosome reaches the stop codon of the mRNA, these eRFs insert themselves at the A site of the ribosome. This insertion releases the polypeptide chain from the tRNA in the P site. (Figure modified from Zaher & Green, 2009)

1.3 TRANSLATIONAL REGULATION

Canonical translation performs much as is described above, and many RBPs are involved in the normal function of translation. However, translation can also be regulated. There are many different types of regulation, including general translational regulation, and different methods of mRNA-specific translational regulation, including IRESs and RBP binding sites.

1.3.1 GENERAL TRANSLATIONAL CONTROL

Translation can be regulated in several ways, and these methods of control can very broadly be categorized into two groups: methods of general translational control, and methods of mRNA-specific translational control. Though the titles of these categories are not strictly accurate, they provide a working basis for understanding regulation (For a review, see Gebauer & Hentze, 2004).

General translational control can be thought of as a way to alter canonical translation of most or all mRNAs. This type of translational control would affect a large amount of mRNAs, usually by affecting the translational machinery. A clear example of this would be eIF4E-binding protein phosphorylation. eIF4E is strongly implicated in promoting translation of mRNAs. As described above, eIF4E assists in circularizing the mRNA by binding to the 5'UTR of mRNAs as well as to eIF4G, which binds to PABP. While circularization of mRNA is not necessary for translation to occur, it does drastically increase the frequency of translation initiation. eIF4E-binding protein (4E-BP) binds to eIF4E and prevents it from binding to the 5'UTR of mRNAs or to eIF4G. Under normal conditions, this does not occur, since 4E-BP is normally phosphorylated, which alters the 4E-BP conformation, and prevents it from binding to eIF4E. This allows for normal mRNA circularization and translation. However, in altered or disease conditions, phosphorylation of 4E-BP can be prevented, which would prevent circularization of most mRNAs, and thereby drastically reduce canonical translation initiation (Gebauer & Hentze, 2004).

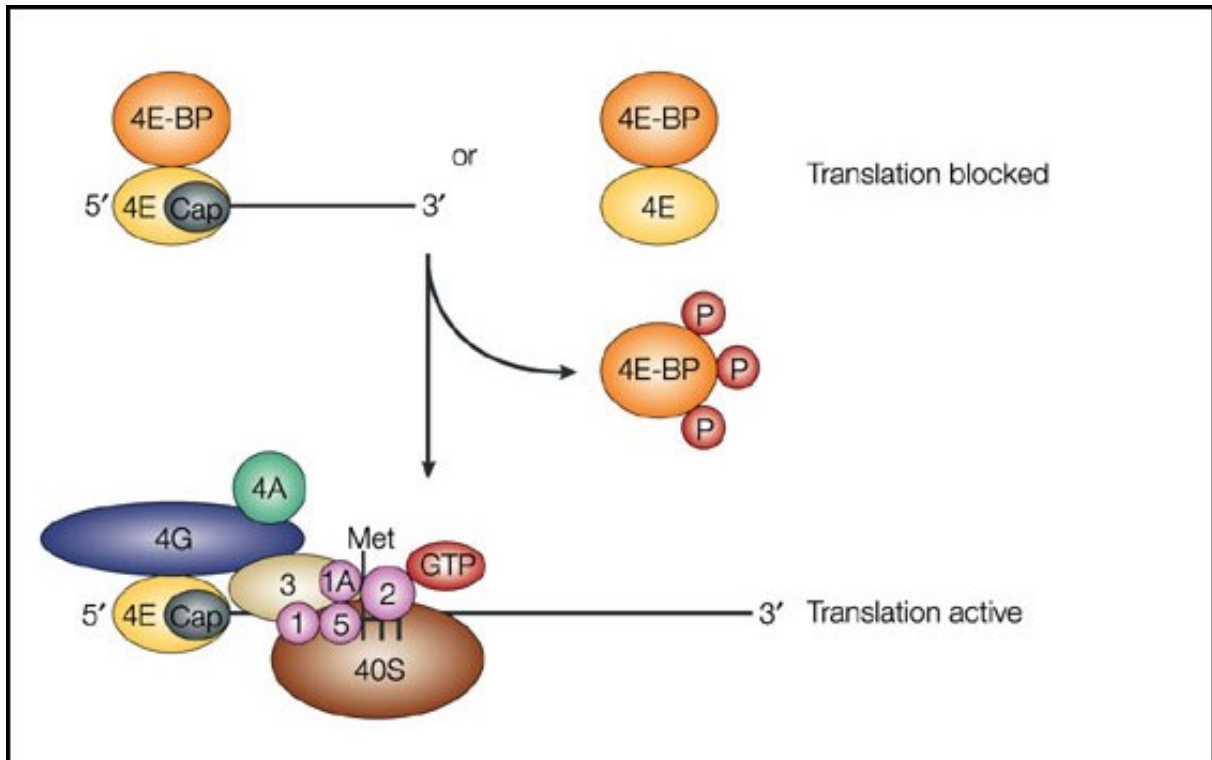


Fig 1.8 4E-BP is involved in general translation

eIF4E-binding protein (4E-BP) has been found to be involved in general translation regulation. Under normal conditions, 4E-BP is phosphorylated. However, under conditions where it isn't phosphorylated, 4E-BP can bind to eIF4E, preventing it from circularizing the mRNA and blocking normal translation from occurring. (Figure modified from Gebauer & Hentze, 2004)

1.3.2 mRNA-SPECIFIC TRANSLATIONAL CONTROL

Unlike general translational control, mRNA-specific translational control tends to affect only one or a few (a small subset) mRNA(s). Often this type of translational regulation occurs by an RBP binding to the 5' or 3' UTR of the mRNAs at a conserved binding site and regulating the translation of these mRNAs. This type of regulation tends to occur only under specific conditions, and can finely regulate the translation of the mRNA binding partner(s).

A clear example of this is the sex lethal (SXL) protein's involvement in regulating the translation of *msl-2* in *Drosophila*. MSL-2 functions to help promote extra transcription of X-linked genes in male *Drosophila*, thereby equalizing the transcription of the male single X-chromosome with the female double X. Therefore, MSL-2 function must be repressed in

females to make sure that this “hypertranscription” does not occur in females as well. This regulation is managed by the SXL protein (Gebauer & Hentze, 2004).

SXL shows clear nuclear and cytoplasmic functions. When in the nucleus, SXL regulates splicing. However, in the cytoplasm, SXL inhibits translation of *msl-2* by binding to its 5' and the 3'UTRs. This binding results in a very specific translational control (Duncan et al., 2006).

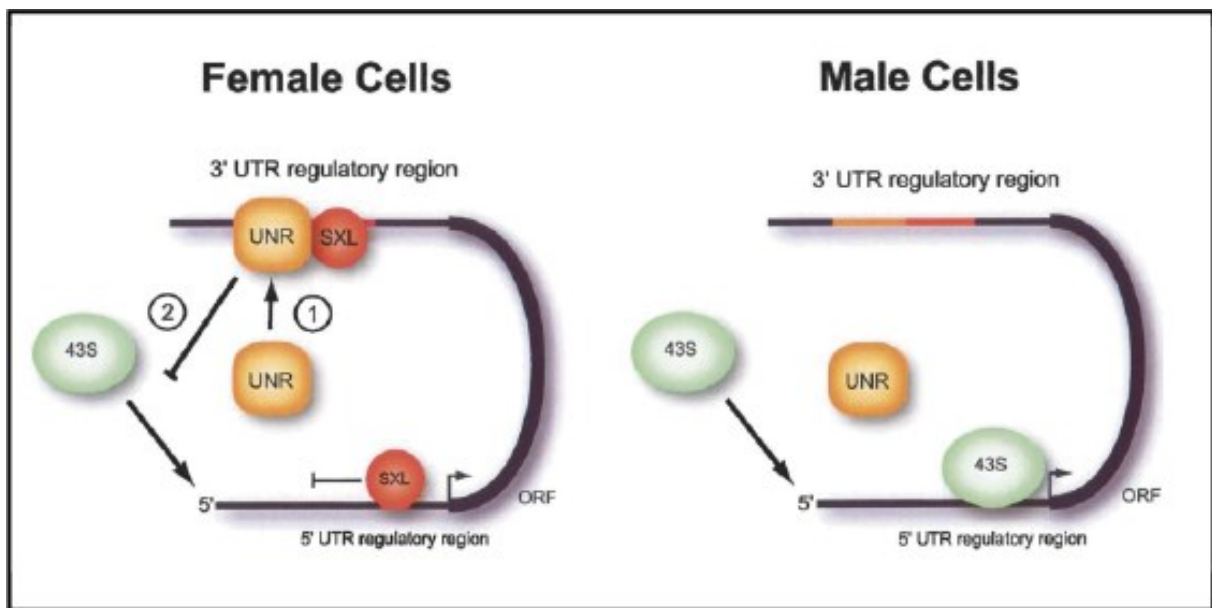


Fig 1.9 Example of specific translational control – Sex lethal

The sex lethal protein (SXL) can specifically prevent translation of the *msl-2* mRNA by binding either to the 5' UTR of the mRNA and preventing the 43S pre-initiation complex from scanning through to the start codon, or by binding to the 3'UTR along with the UNR protein, which helps to prevent translation initiation from occurring. This happens specifically in female *Drosophila* cells, in order to prevent overexpression of the X chromosome linked genes that are transcriptionally regulated by the MSL-2 protein. (Figure modified from Duncan et al., 2006)

1.3.3 INTERNAL RIBOSOME ENTRY SITES

Internal ribosome entry sites (IRESs) were initially identified in viral mRNAs as a way to “hijack” the translational machinery of the infected cells. While cells can shut down canonical translational mechanisms once an infection has been detected, the viral mRNAs are able to proceed through very different methods (Tsukiyama-Kohara, Iizuka, Kohara, & Nomoto, 1992; Wilson, Powell, Hoover, & Sarnow, 2000).

Simply, IRESs are secondary structures found in the 5'UTR of mRNAs that promote ribosome subunit joining and thus translation initiation. There are many different types of viral IRESs, and their level of functioning differs. In some cases, they are cap independent. In others, they do not even need a canonical AUG-start codon.

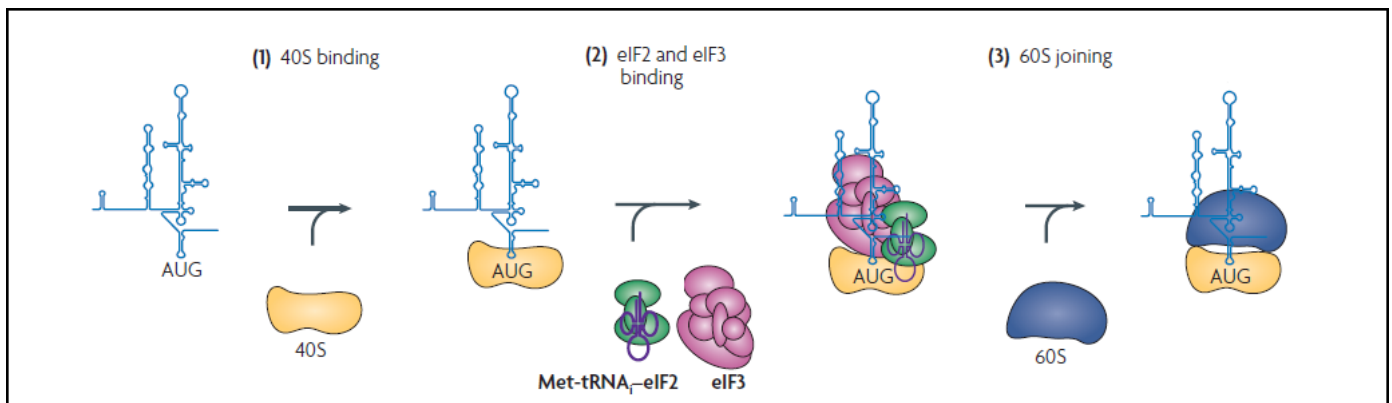


Fig 1.10 Internal Ribosome Entry Sites

Internal ribosome entry sites (IRESs) can regulate translation initiation non-canonically. There are many different types of IRESs, and they can function very differently. One such IRES (shown above) directly promotes ribosomal subunit joining at the IRES structure by recruiting the 40S, ternary complex, and eIF3. This allows the 60S to join, creating a functional monosome that is ready to translate the mRNA. (Figure modified from Fraser & Doudna, 2007)

The case for cellular IRESs has been frequently made, though there are many questions as to its authenticity as of yet (Gilbert, 2010; Johannes & Sarnow, 1998). It is much more difficult to accurately control for the identification of cellular IRESs than it has been for viral IRESs. This is largely because there are many variants of viral IRESs, and their secondary structures

can easily be compared, whereas all cellular IRESs identified as of yet are unique, creating a difficulty in identifying true IRESs. However, it seems likely that cellular IRESs exist, since they very simply and specifically allow for translation of mRNAs under distinctive conditions.

1.4 TAR DNA-BINDING PROTEIN 43 (TDP-43)

TDP-43 was first identified in 1995 as a protein that binds to the HIV transactive response region (TAR) of DNA where it represses transcription of the HIV-1 gene (Ou, Wu, Harrich, García-Martínez, & Gaynor, 1995). Later it was shown to be involved in alternative splicing of the cystic fibrosis transmembrane conductance regulator (CFTR) gene (Buratti et al., 2001). It wasn't until 2006 that TDP-43's role as the main protein found in aggregates of ALS and FTLN was shown by two separate reports (Arai et al., 2006; Neumann et al., 2006). Later, reports of TDP-43 patient mutations found in ALS patients (Kabashi et al., 2008; Sreedharan et al., 2008), TDP-43's important RNA-binding ability (Ayala et al., 2011; Voigt et al., 2010), and its function in splicing regulation in a large subset of mRNAs (Polymenidou et al., 2011; Tollervey et al., 2011) further emphasized the importance of TDP-43's functions.

1.4.1 TDP-43 DOMAINS

TARDBP is the gene that encodes TDP-43. Located on chromosome 1 in humans, it codes for a protein 414 amino acids long. This gene contains several domains of interest, including a nuclear localization sequence (NLS) and nuclear export sequence (NES), integral in shuttling the protein between the nucleus and the cytoplasm. It also contains two RNA recognition motifs (RRM1 and RRM2), which allow TDP-43 to bind to RNA, as well as a so-called "glycine rich" region at the C-terminus of the protein. This glycine-rich region has been identified as the region important for TDP-43's interactions with other proteins. It also is the site for the vast majority of patient mutations that have been identified in ALS (For a review, see Lagier-Tourenne, Polymenidou, & Cleveland, 2010).

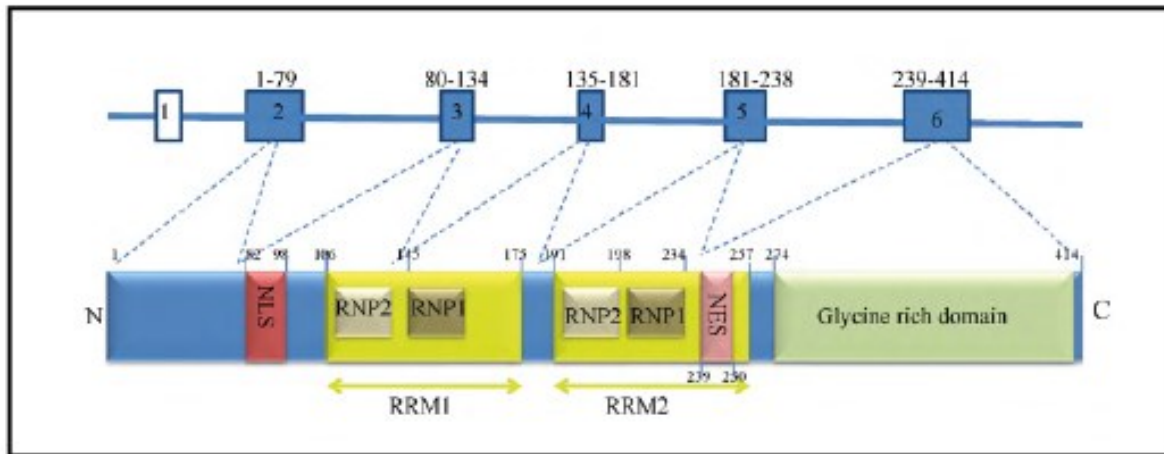


Fig 1.11 TDP-43 Protein Domains

The 414 aa-long TDP-43 protein contains several functional domains, including a nuclear localization sequence (NLS), nuclear export sequence (NES), two RNA recognition motifs (RRM1 and RRM2), as well as a glycine rich domain at its C-terminus. (Figure modified from Warraich, Yang, Nicholson, & Blair, 2010)

1.4.2 NUCLEAR TO CYTOPLASMIC SHUTTLING ABILITY

TDP-43 is a ubiquitously expressed protein, and is normally found largely localized to the nucleus, with a small amount found in the cytoplasm. It has the ability to shuttle back and forth between the nucleus and the cytoplasm due to the presence of both an NLS and NES in the protein sequence. This indicates that while TDP-43 may have a major role in the nucleus, it likely also has a role in the cytoplasm.

TDP-43 is found to shift its localization pattern in affected cells under disease conditions. In these cases, TDP-43 largely localizes to the cytoplasm. Reduced expression in the nucleus has also been reported under these conditions. Cytoplasmic TDP-43 has been found in aggregates in the affected cells of many patients with ALS or FTL, although studies in model organisms question whether aggregation is needed to cause disease (Arai et al., 2006; Neumann et al., 2006).

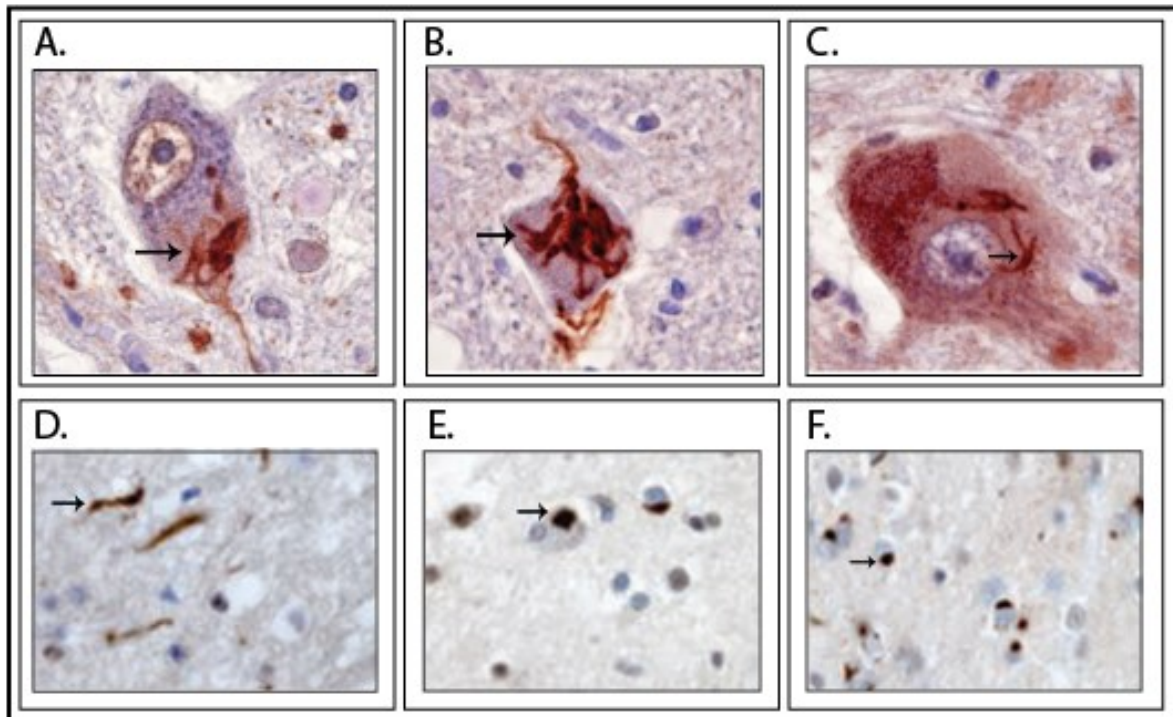


Fig 1.12 TDP-43 positive aggregates in neurodegenerative diseases

TDP-43 was found to be the major protein in aggregates that form in affected cell types in both ALS (A-C) (Arai et al., 2006) and FTLT (D-F) (Neumann et al., 2006). Distinct cytoplasmic aggregates can be identified by immunostaining for ubiquitin (A) or TDP-43 (B-F) and are indicated by the arrows. TDP-43 positive aggregates are identified in approximately 90% of ALS and 50% of FTLT patients. (Figure modified from Arai et al., 2006 (A, B, C) and Neumann et al., 2006 (D, E, F)).

In addition to relocalization under disease conditions, experiments in model systems have shown that TDP-43 expression also shifts to the cytoplasm under stress, injury, or neuronal stimulation. A study performed by Moisse et al. (2009) shows that after neuronal axotomy, TDP-43 relocates to the cytoplasm over a long-term time-course, and later slowly returns to the nucleus. Stress conditions consisting of oxidative stress, heat shock, or certain chemicals have been shown to target TDP-43 to stress granules (Colombrita et al., 2009). Under neuronal stimulation, it has been shown that TDP-43 also relocates to the cytoplasm, and additionally into the dendrites and axons of neurons (Liu-Yesucevitz et al., 2014; Wang, Wu, Chang, & Shen, 2008).

Taken together, it is clear that TDP-43's relocalization from the nucleus to the cytoplasm may have an important role to play in cellular function. Additionally, TDP-43's potential cytoplasmic functions could be different under normal and stress or disease conditions. An

important question regarding TDP-43's altered localization in disease is whether it is causing a nuclear loss of function, a cytoplasmic gain of function, or a combination of the two.

1.4.3 RNA-BINDING ABILITY

Due to the presence of two RRM, TDP-43 has the ability to bind to RNA. By mutational analysis of the RRM, it was shown that largely only RRM1 controls TDP-43's major RNA-binding functions (Voigt et al., 2010). This was only assessed under normal conditions. It seems possible that stress conditions may alter RNA-binding functions, and that RRM2 may have an alternate RNA-binding function that was not identified in these experiments.

In order to identify the RNAs that are bound by TDP-43, high throughput sequencing crosslinking immunoprecipitation (HITS-CLIP) was performed on mouse brains (Polymenidou et al., 2011; Tollervey et al., 2011). This analysis showed that TDP-43 binds to approximately 30% of the mouse transcriptome. 965 alternative splice events were identified after TDP-43 depletion, indicating an important nuclear role for TDP-43 in splicing regulation (Polymenidou et al., 2011). Interestingly, when researchers focused on the mRNAs that TDP-43 binds in the cytoplasm, 34% of the binding sites of TDP-43 were at the 3'UTR, compared with only 3.2% of sites in the nucleus (Tollervey et al., 2011). 3'UTR binding by RBPs in the cytoplasm is often associated with translational regulation, and therefore suggests a possible cytoplasmic function for TDP-43 in translation.

1.4.4 ALTERNATIVE SPLICING REGULATION

While the cytoplasmic function of TDP-43 has not been clearly elucidated, there has been greater focus and progress on the function of TDP-43 in the nucleus. In the same study mentioned above, where it was found that TDP-43 bound to 30% of the mouse transcriptome, it was also shown that much of its RNA-binding function had to do with alternative splicing regulation (Polymenidou et al., 2011). Since TDP-43 was already known to regulate splicing, due to its previous identification as a splice regulator for CFTR, this was not a surprising finding (Buratti et al., 2001). However, it has led researchers to question whether TDP-43's removal from the nucleus and shift to the cytoplasm resulted in a nuclear loss of splicing function in disease conditions.

1.4.5 PROTEIN-BINDING ABILITY

Since TDP-43 contains a large glycine-rich region in the C-terminus that was identified as a protein-binding region, it was of interest to identify the proteins that TDP-43 associates with. The study performed did not delineate between proteins that TDP-43 directly interacted with, and proteins that were indirect partners (Freibaum, Chitta, High, & Taylor, 2010). However, interestingly, the study found that TDP-43 associated strongly with proteins that are involved in RNA metabolism – namely two major clusters: A nuclear/splicing protein cluster and a cytoplasmic/translation protein cluster. This again indicates the possibility that TDP-43 may have multiple, distinct roles to play depending on its cellular localization, and additionally that if it does play a cytoplasmic role, that this role may be an involvement in translational regulation.

1.4.6 PATIENT MUTATIONS

After TDP-43 was identified as one of the major proteins found in the cytoplasmic aggregates of several major diseases, in particular ALS and FTL, patients were screened for mutations in this protein (Kabashi et al., 2008; Sreedharan et al., 2008). More than 30 distinct patient mutations were identified in ALS patients, mostly localized to the glycine-rich region at the C-terminus of the protein. A few FTL patients were found with mutations in TDP-43, but since ALS and FTL are found in a disease continuum, it is possible and even likely that TDP-43 mutations found were actually part of the ALS side of that disease (Benajiba et al., 2009).

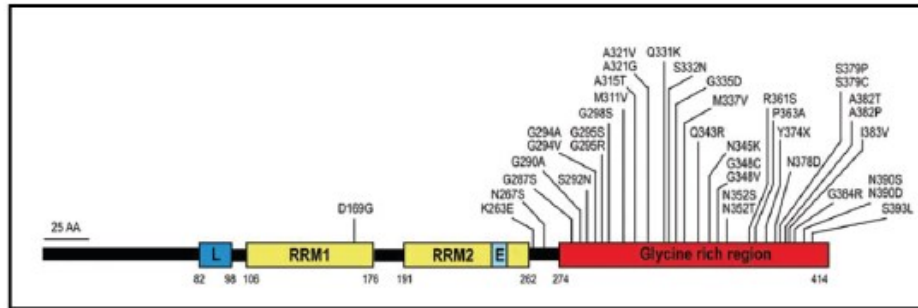


Fig 1.13 TDP-43 patient mutations

More than 30 TDP-43 mutations have been identified in ALS patients, mostly localized to the glycine rich region close to the C-terminus of the protein. A few mutations have been identified in FTLN patients, however due to their scarcity as well as the clinical overlap between ALS and FTLN, it is unclear whether these mutations are actually causing FTLN, or if they are associated still with the ALS disease progression. (Figure modified from Lagier-Tourenne et al., 2010).

It is important to note that patient mutations are not needed to cause TDP-43 pathology in disease. In fact, most ALS patients (more than 90%) show TDP-43 pathology, while only a small percentage have TDP-43 mutations. Nonetheless, TDP-43 mutations in patients indicate that altered TDP-43 function is not just an end result, but rather is likely to be one of the causes of disease.

Much research has been done to identify how these mutations alter TDP-43 function. Disease models expressing patient mutations have presented with motor defects, neuronal degeneration, and neuronal loss (Kabashi et al., 2010; Liachko, Guthrie, & Kraemer, 2010; Ritson et al., 2010; Wegorzewska, Bell, Cairns, Miller, & Baloh, 2009). TDP-43 patient mutations have also been suggested to form more robust aggregates, to more robustly alter TDP-43's localization, and to form altered aggregates in the dendrites of cultured neurons (Liu-Yesucevitz et al., 2014). These studies suggest that while TDP-43 mutations may not be the only way to cause ALS phenotypes, they may alter TDP-43 pathology.

1.4.7 LARGE NUMBER OF NEURODEGENERATIVE DISEASES SHOW TDP-43 PATHOLOGY

TDP-43 was identified as the major protein in aggregates found in ALS and FTLN. Since aggregate formation is an integral phenotype of many different neurodegenerative diseases, many other diseases were screened for altered TDP-43 pathology. AD, PD and CTE were

discussed in previous sections. TDP-43 pathology has also been identified in Huntington's disease, spinal cerebellar ataxia, Lewy body dementia, and hippocampal sclerosis dementia, among others, designating altered TDP-43 localization or aggregation as a common pathological element in many different neurological disorders (Arai et al., 2010; Chen-Plotkin, Lee, & Trojanowski, 2010; Elden et al., 2010; Yokota et al., 2010). It is clearly important to identify how TDP-43 pathology is involved in the progression of neurodegenerative diseases.

1.4.8 RNA-BINDING FUNCTION NEEDED FOR TOXICITY

After RNA-binding was identified as a major role for TDP-43, many tests were made using mutated versions of TDP-43 that removed its RNA-binding ability. Disease models showed that overexpression of TDP-43 caused toxicity, or that patient mutations have damaging effects on the models. Interestingly, when TDP-43's RNA-binding ability was removed in these same model systems, TDP-43 no longer had toxic effects (Fiesel, Schurr, Weber, & Kahle, 2011; Voigt et al., 2010). These studies are extremely important, as they suggest that TDP-43's toxic effect in disease is due to its RNA-binding ability. This indicates that a better understanding of the function behind TDP-43's interaction with its RNA partners would likely be of great interest to the disease research community.

1.5 RNA-BINDING PROTEINS

Since TDP-43's RNA-binding function has been found to be particularly important for its toxicity, it is important to view TDP-43 in the context of other major RNA-binding proteins. Many RNA-binding proteins have been identified and widely described, and understanding how these RBPs function may help to elucidate the function of TDP-43 under disease conditions.

1.5.1 RNA-BINDING PROTEINS INVOLVED IN SPLICING

RNA-binding proteins (RBPs) can have many different functions regarding RNA metabolism, including tasks associated with splicing, mRNA localization, and translation. Many RBPs exhibit functions relating to multiple steps of RNA processing, both in the nucleus and the cytoplasm, or cycling between the two (For a review, see Gebauer & Hentze, 2004).

One such RBP family with multiple cellular functions is the heterogeneous nuclear ribonucleoprotein particle (hnRNP) family. The hnRNPs have functions that fit in with almost every part of mRNA processing, from splicing to localization to translation. They have nuclear/cytoplasmic shuttling abilities, much like TDP-43. In fact, TDP-43 has much in common with the hnRNP family, and in many respects can be considered a member of the hnRNP family (D'Ambrogio et al., 2009).

Many of the hnRNPs have multiple functions. For instance, hnRNPE1 has a function as a regulator of alternative splicing. This hnRNP has been found to associate with different splicing factors such as U1 small nuclear RNP and SC35, and to regulate splicing of the growth hormone receptor. Additionally, hnRNPE1 has been identified to regulate translation. This regulation occurs at many levels of translation, including as an internal ribosome entry site trans-activating factor as well as by binding to the 3'UTR of mRNAs, thus inhibiting their translation (Chaudhury, Chander, & Howe, 2010).

Another RBP involved in splicing is NOVA – a neuron-specific RBP that has been shown to regulate splicing of a subset of mRNAs. Using a method similar to that used to identify TDP-43-bound mRNAs, crosslinking immunoprecipitation (CLIP) found that NOVA binds to around 35 mRNAs, several of which are important for neuronal function (Ule et al., 2003). They also showed that NOVA regulates the splicing of a few of its binding partners (Jensen et al., 2000), and that removal of this function may be involved in diseases such as paraneoplastic opsoclonus myoclonus ataxia (POMA).

1.5.2 RNA-BINDING PROTEINS INVOLVED IN TRANSLATION

As described above, many RBPs can have effects on more than one step of RNA processing. Several have been clearly described in their translational regulatory functions, though they may have other robust functions in RNA processing as well (Duncan et al., 2006; Napoli et al., 2008).

One example of an RBP involved in translation is the fragile X mental retardation protein (FMRP). FMRP is an RBP that causes fragile X mental retardation and other cognitive defects. FMRP associates with polyribosomes and has the ability to repress translation of a large subset of mRNAs. The exact mechanism by which FMRP affects translation of its mRNA targets remains unresolved, but one mechanism appears to be by associating with another protein, CYFIP1, and together binding to eukaryotic initiation factor 4E, preventing it from performing its function in circularizing mRNAs and promoting translation initiation (Napoli et al., 2008). Mutations in FMRP have been shown to inhibit its repression of translation, thus causing disease phenotypes (Feng et al., 1997). It has also been shown that after neuronal stimulation, FMRP levels are decreased and its mRNA partners show increased translation, showing an activity dependent response (Nalavadi, Muddashetty, Gross, & Bassell, 2012).

Another example of an RBP involved in translational regulation is sex lethal (SXL), which is sex-specifically expressed in *Drosophila* (Duncan et al., 2006). The purpose of SXL is to restrict production of the *msl-2* gene. MSL-2 is involved in upregulating X-linked gene production in males, ensuring that similar levels of X-linked genes are produced in males as are in females. Therefore, it is important to make sure that MSL-2 does not function in female *Drosophila*, otherwise it would produce excessive levels of X-linked genes. This restriction of MSL-2 is performed by SXL both at the transcription and the translation levels. SXL inhibits translation of MSL-2 by binding to two different sites on the *msl-2* mRNA – the 5'UTR and the 3'UTR. This binding results in a very specific translational control.

Since it is clear that many RBPs have multiple functions in RNA metabolism, it is possible, and arguably even likely, that TDP-43 could be involved in both splicing in the nucleus and also function as a translational regulator in the cytoplasm.

1.5.3 RNA-BINDING PROTEINS INVOLVED IN NEURODEGENERATIVE DISEASES

Several of the RBPs detailed previously are involved in neurodegenerative diseases. NOVA has been implicated in POMA, while hnRNPs have been found to be involved in Alzheimer's disease and ALS, and FMRP has been implicated in fragile X mental retardation.

With regard to ALS and FTL, TDP-43 is clearly an additional RBP that is involved in neurodegenerative diseases. However, a very similar protein, FUS/TLS, is additionally found to be involved in ALS and FTL (Kwiatkowski et al., 2009). Following many of the same characteristics as TDP-43, FUS/TLS has a similar gene structure, and has been identified as a protein found in aggregates in both ALS and FTL – although a substantially smaller number of patients show aggregates containing FUS/TLS than TDP-43, there is no overlap between the two (Vance et al., 2009). Additionally, FUS/TLS patient mutations have been identified in ALS patients. However, it appears that the mechanisms of how FUS/TLS and TDP-43 function may be highly different.

1.6 THESIS HYPOTHESIS

TDP-43 is an RBP that is implicated in several neurodegenerative diseases. It is normally localized in the nucleus, but shuttles to the cytoplasm. Under disease conditions, TDP-43 largely relocalizes to the cytoplasm, indicating that it likely has a cytoplasmic function. TDP-43 has been shown to bind to 30% of the mouse transcriptome, including to a large percentage of 3'UTRs in the cytoplasmic fraction of bound-mRNAs. Importantly, TDP-43's RNA binding ability is necessary for toxicity in animal and cellular models of disease. Often, RBPs that bind to 3'UTRs in the cytoplasm are involved in translational regulation. Therefore, the hypothesis addressed in this thesis is as follows:

**TDP-43 specifically regulates the translation of protein(s)
important for neuronal health and function.**

2 MATERIALS AND METHODS – TDP-43

2.1 MN1 CELL CULTURE

2.1.1 CHARACTERISTICS OF MN1 CELLS

MN1 cells are a hybridoma cell line of murine motor neurons fused with a neuroblastoma cells line (Fig 2-1). This fusion created an immortalized cell line that can be passaged and expanded with motor neuron-like characteristics. The original creators of the cell line established the motor neuron-like properties by showing that the cells expressed choline acetyltransferase (ChAT), an enzyme frequently used as a cellular marker for motor neuron cells (Salazar-Grueso, Kim, & Kim, 1991). These cells also have the appearance of neurons, to some extent, as they extend neurites toward each other. It is also possible to stimulate further neurite outgrowth through the addition of GDNF and GFR α 1. This cell line was selected because of TDP-43's behavior in the motor neurons of ALS patients, the large amount of starting material needed for polysome profiling experiments, and the ease of manipulating the cell line to produce modified TDP-43 with minimal other changes (e.g. similar expression levels, expressed from the same locus, etc).

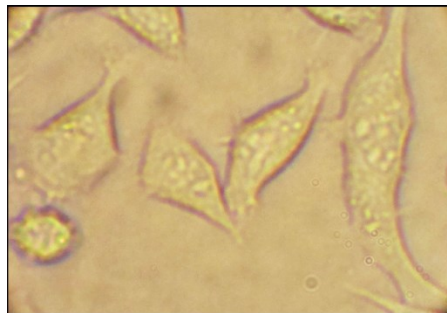


Fig 2-1: Image of MN1 Cells. MN1 cells are a hybridoma of mouse motor neurons and a neuroblastoma cell line.

2.1.2 CELL CULTURE PRACTICES FOR MN1 CELLS

MN1 cell culture practices were similar to those for other mammalian cell lines'. MN1 cells were grown on Sarstedt plates in D-MEM high glucose GlutaMAX culture medium

(Invitrogen, Cat No: 61965), supplemented with 10% Fetal Bovine Serum (Invitrogen) to add growth factors to medium, 1% Penicillin/Streptomycin antibiotics (Invitrogen) to reduce the possibility of bacterial infection, and 2.4% Hepes (Invitrogen, Cat No. 15630056) to buffer the medium at a physiologically optimum pH. Cells containing pFRT/*lacZeo* plasmid insertion were cultured in medium supplemented with 200 ng/ μ l Zeocin (Invitrogen, Cat No: R250-01). Cells containing both pFRT/*lacZeo* and pcDNA6/TR insertion were cultured in medium supplemented with 200 ng/ μ l Zeocin and 5 ng/ μ l blasticidin (Invitrogen, Cat No: R210-01). All cells were incubated at 37°C with 5% CO₂, in a Heraeus HERA cell incubator.

MN1 cells were passaged to a new plate every 2-3 days when they reached 70-90% confluency. Before passing the cells, the old medium was removed and cells were washed once briefly with 0.01 M sterile filtered phosphate buffered saline (PBS) solution. Cells were removed from the plate by adding 10-20% normal growth medium volume of 0.05% Trypsin-EDTA (Invitrogen, Cat No: 25300-054), incubating the plate at room temperature for approximately 2 min, and tapping the sides of the plate to release the cells from the bottom of the plate. Trypsin-EDTA was inactivated by the addition of fresh serum containing medium and 10-20% of volume was moved to a new plate containing pre-warmed medium. The plate was swirled to distribute cells evenly and returned to 37°C, 5% CO₂.

Cells that were deemed important were frozen in 1 ml aliquots and stored in liquid nitrogen. Cells were collected from a near confluent plate, counted, spun down, and resuspended in freezing medium to obtain a concentration of approximately 1x10⁶ cells/ml. Freezing medium was made up of 60% growth medium, 30% FBS, and 10% sterile dimethylsulfoxide (DMSO). Resuspended cells were aliquoted into CryoPure 2.0 ml tubes (Sarstedt, Cat no: 72.379.007), and placed in a Cryo 1°C Freezing container (Nalgene, Cat No: 5100-0001) for 1-3 days at -80°C to freeze cells at a -1°C/min rate. Cells were then transferred to liquid nitrogen for long-term storage.

Frozen cells were thawed when needed by quickly transferring the cryogenic vial to a 37°C water bath, where it was swirled until all but the very last sliver of ice had thawed. The thawed cells were aspirated using a pipette half-full of pre-warmed growth medium. To dilute and remove the DMSO in the freezing medium, cells were transferred to a 15 ml tube containing growth medium to a total volume of 10 ml. Cells were pelleted for 5 min at 1000

rpm at RT and medium was aspirated off. Cells were resuspended in 1 ml of growth medium and plated on a 10 cm dish. The next day, growth medium was exchanged for fresh medium.

2.2 SUBCELLULAR FRACTIONATION

Since TDP-43 is a mostly nuclear protein with shuttling abilities between the nucleus and the cytoplasm, the distribution of endogenous MN1 cell TDP-43 was visualized. This was done by collecting and fractionating cells into their nuclear and cytoplasmic fractions and probing TDP-43 protein levels by immunoblot analysis.

In order to fractionate cells, one 10 cm dish of nearly confluent MN1 cells was harvested and spun down at 200 g for 10 min at 4°C. The cells were then washed twice with ice cold PBS, supernatant was removed, and the cell pellet was resuspended in 1 ml of cold Buffer A (10 mM Hepes (pH 7.6), 1.5 mM MgCl₂, 10 mM KCl, .5 mM Dithiothreitol (DTT), 1x cComplete, Mini, EDTA-free Protease Inhibitor Cocktail (Roche, Cat No: 04693159001)) on ice for 5 min. Cells were then homogenized with 20 strokes from Dounce homogenizer with a type A pestle. Samples were spun at 200 g for 10 min at 4°C to pellet cell membranes and nuclei. At this point, the supernatant contained the cytoplasmic fraction. 750 µl of supernatant and 200 µl of 5x RIPA buffer (250 mM Tris pH 7.5, 7500 mM NaCl, 5% NP-40, 0.25% Deoxycholate, protease inhibitors) were mixed in a new tube. The remaining supernatant from the original tube was discarded, and the pellet was washed twice with ice cold Buffer A. The pellet was then resuspended in 1 ml of Buffer S1 (0.25 M Sucrose, 10 mM MgCl₂, protease inhibitors). 1 ml of Buffer S3 (0.88 M Sucrose, 0.5 mM MgCl₂, protease inhibitors) was added to a 2 ml tube, the resuspended pellet in Buffer S1 was very carefully layered on top, and the tubes were centrifuged at 2800 g for 10 min at 4°C. This sucrose cushion removed the remaining cytoplasmic proteins and cell membrane and pelleted the nuclei. After removing the supernatant, the nuclei were resuspended in 500 µl of 1x RIPA buffer, sonicated on ice 3 x 5 sec at low level to shear genomic DNA, and then centrifuged at 2800 g for 10 min at 4°C. This supernatant was considered the nuclear fraction and was removed to a new tube.

40 µg of protein from each cytoplasmic and nuclear fraction was concentrated by precipitation using trichloroacetic acid (TCA). This was done by adding an equal volume of 20% TCA to each sample, incubating on ice for 30 min, and spinning at top speed for 15 min at 4°C. Supernatant was aspirated, and 300 µl cold acetone was added to the pellet, which

was subsequently spun for 5 min at 4°C. Acetone wash was repeated once, supernatant was removed, and the pellet was allowed to briefly dry.

The pellets were resuspended in SDS loading buffer, and heated to 95°C for 5 min. Protein concentration of samples was measured using Bio-Rad Protein Assay (Bio-Rad, Cat No: 500-0006). Samples were run on a 12% SDS-PAGE gel, wet transferred overnight to a Polyvinylidene Fluoride (PVDF) membrane (Invitrogen), and membrane was blocked for 1 hr at room temperature (RT) using Tris-buffered saline (TBS) with 0.05% Tween (TBS-Tween) containing 5% powdered milk. The membrane was cut and the separate parts were immunoprobed overnight at 4°C shaking with rabbit anti-TDP43 antibody (Epitomics, Cat No: 3769-1) at a 1:1000 dilution or mouse anti-GAPDH antibody (Invitrogen, Cat No: G8795) at 1:20,000 dilution in TBS-Tween containing 5% powdered milk. Since GAPDH is a cytoplasmic protein this staining was used as a control for how clean the nuclear/cytoplasmic separation was. The next day, the blot was washed 3 x 5 min with TBS-Tween before incubation with secondary antibodies for 2 hr at RT with shaking. Peroxidase-Goat Anti-Rabbit IgG (Invitrogen, Cat No: 65-6120) was used as a secondary antibody for TDP-43, and Peroxidase-Goat Anti-Mouse IgM (Invitrogen) was used as a secondary antibody for GAPDH, both at a 1:1000 dilution in TBS-Tween containing 5% powdered milk. The blot was washed 5 x 5 min with TBS-Tween. Bands were chemiluminated using SuperSignal West Dura Extended Duration Substrate (Thermo Scientific, Cat No: 34075), and exposed using a Fujifilm LAS-4000 gel imaging system.

2.3 RNA INTERFERENCE

2.3.1 siRNA TRANSFECTION

RNA interference (RNAi) was performed using the XtremeGene siRNA Transfection Reagent (Roche, Cat No: 04 476 115 001) with a protocol modified from the accompanying user guide. MN1 cells at 80-90% confluency were passed 24 hr prior to transfection in order to obtain 30-50% cell confluency by the time of transfection. For a 24 well plate, this density was around 0.4×10^5 cells per well in 450 μ l of medium. All following measurements are for transfecting a single well of a 24 well plate.

On the day of transfection, 36 μ l of serum free medium was aliquoted into sterile 1.5 ml eppendorf tube ('Tube A') for each well to be transfected. 14 μ l of transfection reagent was pipetted directly into the medium in 'Tube A' and the solution was mixed by pipetting. Quickly, serum free medium was pipetted into a fresh 1.5 ml eppendorf tube ('Tube B') for a final volume of 50 μ l after the addition of siRNA, and 2 μ g of siRNA were added directly into the medium. The solution was mixed by pipetting. One 'Tube A' was mixed with one 'Tube B' by pipetting, and the resulting mixtures were incubated at RT for 20 min. Transfection mixtures were added dropwise to cells, and the plates were swirled gently to distribute the solution. 4-6 hr after transfection reagent was added to cells, cell medium was changed. Cells were allowed to grow for 48 hr before cells were harvested.

siRNAs were ordered from Ambion, Life Sciences. GAPDH was used as a positive control for the protocol, and scrambled siRNA was used as the negative control.

<u>siRNA</u>	<u>Sense Sequence</u>	<u>Antisense Sequence</u>	<u>Cat. No.</u>
TARDBP (mus musculus)	GGAGAGGAUUUGAUCUUAtt	UAAUGAUCAAAUCCUCUCCAC	S106687
GAPDH (mus musculus)	--	--	4390849
Scrambled Negative Control	--	--	4390843

Fig 2-2: siRNAs used for RNAi. All three siRNAs used were Silencer Select siRNAs and were purchased from Ambion, Life Sciences

2.3.2 siRNA IMMUNOBLOT

Efficiency of siRNA transfection was checked by immunoblot. Cells treated with each type of siRNA were collected 48 hr after transfection and spun down at 1,000 g for 10 min. Supernatant was removed and cell pellets were lysed on ice for 30 min using 100 μ l RIPA buffer. Cell lysate was sonicated briefly to shear genomic DNA and centrifuged at 4°C for 10 min at 3,000g. Supernatant was removed to a new tube, and protein content was measured using the Bio-Rad Protein Assay.

5 μ g of protein from each sample was separated on a 12% SDS-PAGE gel. The gel was wet transferred overnight to a PVDF membrane (Invitrogen). The PVDF membrane was blocked for 1 hr at RT using TBS-Tween containing 5% powdered milk, then overnight at 4°C,

shaking, with rabbit anti-TDP43 antibody (Epitomics, Cat No: 3769-1) or mouse anti-GAPDH antibody (Invitrogen, Cat No: G8795) at a dilution of 1:1000 or 1:20,000, respectively, in TBS-Tween containing 0.02% sodium azide. The next day, membranes were washed 3 x 5 min in TBS-Tween. Membranes were incubated for 2 hr at RT with secondary antibody anti-mouse HRP (Invitrogen) for GAPDH and Peroxidase-Goat Anti-Rabbit IgG (Invitrogen, Cat No: 65-6120) for TDP-43 in TBS-Tween. Membranes were washed 5 x 5 min with TBS-Tween. Bands were chemiluminated using SuperSignal West Dura Extended Duration Substrate (Thermo Scientific, Cat No: 34075), and exposed using a Fujifilm LAS-4000 gel imaging system.

2.4 Flp-In T-REx STABLE CELL

2.4.1 TRANSFECTION AND STABILIZATION OF MN1 CELLS

The Flp-In T-REx cell line method was established by Invitrogen (Cat No: K6500-01). Cell lines that have been modified using this technique stably express the gene of interest (GOI) from a single integration site in the cell genome in a tetracycline inducible manner. The plasmids used for this technique were from Invitrogen (Fig 3).

<u>Plasmid Name</u>	<u>Purpose</u>	<u>Cat No</u>
pFRT/ <i>lacZeo</i>	Integrates FRT site and <i>lacZ-Zeocin</i> fusion gene into cellular genome	V6015-20
pcDNA6/TR	Integrates <i>TetR</i> for tetracycline production and confers blasticidin resistance	V1025-20
pcDNA5/FRT/TO	Can be modified to carry gene of interest downstream of tetracycline regulated promoter and FRT site, confers hygromycin resistance	V6520-20
pOG44	Expresses Flp recombinase	V6005-20

Figure 2-3: Plasmids used to create Flp-In T-REx Cell Line. Plasmids from Invitrogen with their purposes for creating the Flp-In T-REx cell line.

MN1 cells were transfected with pFRT/*lacZeo* plasmid marked both by LacZ production as well as Zeocin resistance. This transfection was performed using Effectene Transfection Reagent (Qiagen; Cat No: 301425) in a procedure modified from the manufacturers

specifications. One third of a 70-90% confluent 10 cm dish of MN1 cells was passed to a new 10 cm dish 24 hr prior to transfection so that cells would be 40-80% confluent by the time of transfection.

The day of transfection, 2 µg of DNA were diluted in Buffer EC to a final volume of 300 µl in a 1.5 ml eppendorf tube. 16 µl of Enhancer were added to the solution to condense the DNA and the tube was vortexed for one second. The tube was then incubated at room temperature for 5 min. 60 µl of Effectene Transfection Reagent, which forms micelles around the DNA to transmit it into cells, was added to the DNA-Enhancer mixture, the tube was vortexed for 10 sec, and incubated at RT for 10 min. During the incubation of the DNA-Enhancer mixture, cells were prepared for transfection. Growth medium was removed a plate of cells, cells were washed once with PBS, and 7 ml of fresh growth medium was added back to the cells. 3 ml of growth medium and, after incubation, the transfection reagent were added to a 15 ml tube and mixed by pipetting. This solution was added dropwise to cells, cells were gently swirled to distribute transfection reagent and the plate was returned to the 37°C incubator for 24 hr. This transfection protocol was used for all transfections performed for the creation of the Flp-In T-REx cell line.

MN1 cells transfected with pFRT/*lacZeo* plasmid were split to 8 x 10 cm dishes 24 hr after transfection. 24 hr after this split, the medium was exchanged for these 8 dishes as well as for one 10 cm dish containing untransfected MN1 cells and replaced with growth medium containing 200 ng/µl of Zeocin. After two weeks, no cells remained on the untransfected MN1 cell dish under selection. Transfected cells that survived Zeocin treatment were further split into 96 well plates so that there was only 1 cell per well. Clones were expanded from single cells and were further tested for integration of pFRT/*lacZeo* plasmid.

MN1 clones containing pFRT/*lacZeo* were transfected with the pcDNA6/TR plasmid to confer cells with the ability to produce tetracycline repressors and blasticidin resistance. This transfection was performed using Effectene Transfection Reagent with the protocol described above.

MN1 cells transfected with both pFRT/*lacZeo* and pcDNA6/TR plasmids were split to 2 x 10 cm dishes 24 hr after transfection. 24 hr after this split, the medium was exchanged for these dishes as well as for one untransfected MN1 cell 10 cm dish and replaced with growth

medium containing 200 ng/μl of Zeocin and 5 ng/μl blasticidin. After two weeks, no cells remained on the untransfected MN1 cell dish under selection. Transfected cells that survived Zeocin and blasticidin treatment were further split into 96 well plates so that there was only one cell per well. Clones were expanded from single cells and stored for future use.

MN1 clones containing both pFRT/*lacZeo* and pcDNA6/TR were co-transfected with the pcDNA5/FRT/TO plasmid containing an FRT site with the gene of interest and hygromycin resistance along with the pOG44 plasmid that expressed the flip recombinase protein. This co-transfection allows the flip recombinase to homologously recombine the luciferase gene into the FRT single integration site. This transfection was performed using Effectene Transfection Reagent with the protocol described above.

MN1 cells transfected were then split to 2 x 10 cm dishes 24 hr after transfection. 24 hr after this split, the medium was exchanged for these dishes as well as for one untransfected MN1 cell 10 cm dish and replaced with growth medium containing 5 ng/μl blasticidin and 10 ng/μl hygromycin. No Zeocin was added, as Zeocin resistance is removed once the gene of interest is “flipped in”. After two weeks, no cells remained on the untransfected MN1 cell dish under selection. Transfected cells that survived blasticidin and hygromycin treatment were further split into 96 well plates so that there was only one cell per well. Clones were expanded from single cells and stored for future use. These were the final stable cell lines.

Stable cell lines were induced to express the genes of interest that had been “flipped in” by the addition of tetracycline at a concentration of 0.5, 1, or 5 μg/ml to the cell culture media. Cells were incubated at 37 °C for 24 or 48 hr before cells were collected and protein was isolated.

2.4.2 X-GAL TEST OF LacZ EXPRESSION

Clones that were expanded from the pFRT/*lacZeo* transfection in Zeocin containing medium were additionally screened for β-galactosidase expression from the LacZ gene. This was done through the addition of the chemical X-β-gal (Carl Roth, Cat No: 2315.3). Cells were grown in a plate containing a glass coverslip. Once the cells had adhered to the coverslip, the coverslip was moved to a 6 well plate and washed 2-3 times with RT PBS, and fixed for 10 min in 3.7% formaldehyde in PBS. Formaldehyde solution was removed at the end of 10

min, and coverslips were briefly rinsed twice with PBS before the addition of X-gal staining solution (3.3 mM $\text{K}_4\text{Fe}(\text{CN})_6 \cdot 3\text{H}_2\text{O}$, 3.3 mM $\text{K}_3\text{Fe}(\text{CN})_6$, 1 mM MgCl_2). X-gal dissolved in DMSO was added to this solution to a final concentration of 0.1%. Cells were incubated overnight at 37°C in order to visualize X-gal.

2.4.3 GALACTO STAR SYSTEM FOR DETECTION OF β -GALACTOSIDASE

Cells were prepared according to the Galacto Star System (Applied Biosystems) manual. 48 hr prior to experiment, MN1 clones were passed 1:5 to 6 cm plates. 0.5 mM DTT was added to the lysis solution. Cells were washed 2x with RT PBS. Cells were covered with a thin layer of lysis solution (250 μl per 6 cm plate). Cells were collected by scraping, and centrifuged for 2 min to pellet. Supernatant was transferred to a fresh tube. The Galacto-Star substrate was diluted 1:50 with Reaction Buffer Diluent and kept at RT. 5 μl of supernatant was transferred to a microplate, and 100 μl reaction buffer were added. Samples were mixed by pipetting and incubated at RT for 30 min. Signal was measured using the Victor3 (TM) 1420 Multilabel counter luminometer (Perkin Elmer).

2.4.4 SOUTHERN BLOT

Clones were screened for single integration of pFRT/*lacZeo* plasmids through Southern blot analysis. Genomic DNA from the clones was isolated using the AppliChem DNA Isolation Reagent for Genomic DNA (Cat No: A3418,0050). Cells were collected from a 10 cm dish with 1 ml of DNA isolation reagent, and incubated at RT for 5 min. Lysate was centrifuged for 10 min at 10,000 g to remove cellular debris. Lysate was moved to a new tube, and 1 ml of 100% ethanol (EtOH) was added. Tubes were inverted several times to mix and incubated at RT for 3 min. Tubes were centrifuged for 5 min at 5,000 g to pellet DNA. DNA pellet was washed twice with 1 ml 95% EtOH, and centrifuged at 1,000 g for 1 min to re-pellet. Pellet was air dried for 5 min, and DNA was dissolved in 100-500 μl Low TE buffer, and incubated at 37°C overnight.

Genomic DNA was digested using HindIII (Fermentas). 20 μl of genomic DNA was added to an eppendorf tube along with 5 μl of HindIII, 5 μl of 10x Sample buffer and 20 μl of $\text{NF-H}_2\text{O}$. These tubes were incubated at 37°C overnight to fully digest genomic DNA.

Digested genomic DNA samples were mixed with bromophenol blue and were run on a 0.8% agarose gel. The gel was washed in 0.25 M HCl until the bromophenol blue turned slightly yellow. The gel was then washed briefly with H₂O followed by a 15 min wash with 0.4 M NaOH. The gel was transferred to a nylon membrane overnight using the NaOH transfer method. The next day, the membrane was washed with 2x SSC (0.3 M NaCl, 0.03 M Na₃C₆H₅O₇·2H₂O) for less than 10 min, dried briefly on filter paper and baked for 2 hr at 80°C to crosslink the DNA to the membrane.

To create a DNA probe specific for pFRT/*lacZeo*, a 425 nucleotide fragment was cut from the pFRT/*lacZeo* plasmid using MluI restriction enzyme (New England Biolabs). This fragment was gel purified using the QIAquick Gel Extraction Kit (Qiagen, Cat No: 28706). To label this probe, Megaprime DNA Labeling System was used (Amersham, Cat No: RPN1604). The method was taken from the protocol provided with the kit. In an eppendorf tube, 25 ng of DNA and 5 µl of random primer were combined and heated to 95°C for 5 min, then cooled on ice. 4 µl of dGTP, dTTP, and dCTP were added, plus 5 µl reaction buffer and H₂O up to 43 µl. In the radioactivity room, 5 µl of P³² labeled dATP and 2 µl of polymerase enzyme were added to the tube, and the tube was incubated at 37°C for 15 min. After incubation, 50 µl TE Buffer were added to the probe, and then the entire solution was applied to a column for purification, and centrifuged for 5 min.

The baked membrane was placed inside a hybridization bottle along with hybridization buffer (7% SDS, 1.5x SSPE (0.225 M NaCl, 150 mM NaH₂PO₄·H_xO, 15 mM EDTA, pH 7.4), 10% Polyethylene glycol 6000) and denatured herring sperm DNA. The blot was pre-hybridized, rolling, for 1 hr at 60°C. Labeled probe was heated to 95°C for 5 min and added to fresh hybridization buffer to a 2.5 x 10⁵ cpm/ml dilution. Pre-hybridization solution was removed, and the hybridization solution containing the labeled probe was added to the hybridization bottle and rotated overnight at 65°C.

The next day, hybridization mix was discarded, and the bottle was half filled with prewarmed 2x SSC, shaken, and solution was discarded. New warm 2x SSC was added to the top of the bottle, and the bottle was rotated for 15 min at 65°C. Buffer was discarded. Wash step was repeated until no radioactivity could be detected by the hand Geiger counter. Membrane was placed between saran wrap and exposed.

2.4.5 LUCIFERASE ASSAY

MN1 cells with luciferase vector flipped in were trypsinized and cells were counted. 200,000 cells were used for each clone. Cells were spun down at 1,000 g for 2 min at 4°C, and washed twice with cold 1x PBS. Cells were lysed with 100 µl 1x Passive Lysis Buffer (Promega, Cat No: E1910), and lysate was kept on ice for 10-15 min. Lysate was spun down at 10,000g for 10 min at 4°C. 5 µl of supernatant for each sample was loaded in duplicate to a well of a 96 well luminometer plate, leaving space inbetween to reduce background readings. The plate was measured in the Victor3 (TM) 1420 Multilabel counter luminometer (Perkin Elmer), which was set to dispense 100 µl of Luciferase Assay Substrate (Promega, Cat No: E1910) to each well prior to reading.

2.5 PLASMID CLONING

Cloning and manipulation of TDP-43 to form constructs of interest was performed both for use in the Flp-In T-REx Stable Cell Lines and for transient transfection of cells. A human TDP-43 (hTDP-43) clone was ordered from Open Biosystems (Clone IDs 30389805). This clone contains partial 5' and 3'UTRs, and the full ORF of the gene.

hTDP-43 was provided in pCMV Sport 6.1 vector containing ampicillin resistance. The clone was provided as a glycerol stock of *Escherichia coli* containing the vector, and was streaked onto LB plates containing Ampicillin, and grown at 37°C overnight. Clones were picked from these plates and cultured in LB liquid containing Ampicillin overnight at 37°C, shaking at 225 rpm. Plasmids were isolated from these cultures using the QIAprep Spin Miniprep Kit (Qiagen, Cat No: 27106) or the QIAGEN Plasmid *Plus* Maxi Kit (Cat No: 12963), depending on the starting culture volume. The plasmid isolation procedure followed the instructions provided by the kits.

For small scale DNA preparation, the QIAprep Spin Miniprep Kit (Qiagen, Cat No: 27106) was used. *E. Coli* was cultured overnight in 5 ml of LB broth. The next day, cells were pelleted at 3,000 g for 20 min, liquid was removed, and the cells were resuspended in 250 µl of cold resuspension buffer P1. This solution was transferred to an eppendorf tube, and 200 µl of buffer P2 lysis buffer was added, and mixed by inverting several times. 350 µl of

buffer N3 neutralization buffer were added and tubes were mixed by inverting several times. Samples were centrifuged for 10 min at 17,900 g. The supernatants after this spin were applied to a QIAprep spin column containing a silica membrane that binds to DNA, and centrifuged for 1 min at 17,900 g. Liquid was removed from the bottom tube. Columns were washed with 500 ml of buffer PB wash buffer and centrifuged for 1 min at 17,900 g. Liquid was removed from the bottom tube. Columns were washed with 750 ml of buffer PE wash buffer and centrifuged for 1 min at 17,900 g. Liquid was removed from the bottom tube. Columns were centrifuged for an additional 1 min at 17,900 g to remove residual liquid, and the columns were moved to a fresh eppendorf tube. 50 μ l of buffer EB elution buffer was added to the center of the column, and incubated at RT for 1 min. Columns were then spun for 1 min at 17,900 g to remove the DNA from the silica membrane of the column.

A similar protocol was used for large scale DNA preparation, but using the Plasmid *Plus* Maxiprep Kit (Qiagen, Cat No: 12963). Cells were cultured in 100 ml of LB broth overnight at 37°C with shaking at 225 rpm. The next day, cells were pelleted by centrifugation at 3000 g for 20 min. Supernatant was removed, and the pellet was resuspended in 8 ml of cold Buffer P1 resuspension buffer. 8 ml of Buffer P2 lysis buffer was added to this solution, the tube was mixed by inverting, and solution was incubated for 3 min at room temperature. After incubation, 8 ml of Buffer S3 neutralization buffer was added to the lysate and the tube was mixed by inversion. The solution was applied to a QIAfilter cartridge, where it was allowed to separate during 10 min incubation at RT. The liquid from the cartridge was then filtered into a new tube, and 5 ml of Buffer BB was added, and the tube was inverted to mix the solution. This solution was poured into a QIAGEN Plasmid *Plus* Maxi Spin Column with tube extender that was connected to the vacuum manifold. After liquid was drawn through the column, 700 μ l of Buffer ETR was added to the column. Once the liquid was drawn through the column, 700 μ l of Buffer PE wash buffer was applied to the column. The column was moved to a new eppendorf tube and was centrifuged for 1 min at 10,000 g to remove residual wash buffer. The column was moved to a new eppendorf tube and 400 μ l of Buffer EB elution buffer was applied to the center of the column to elute the DNA. The column was incubated at room temperature for 1 min and then centrifuged at 10,000 g.

The full-length ORF of TDP-43 was amplified from the plasmids by polymerase chain reaction (PCR). The primers used for this contained 5' overhang that contained a Sall enzyme cut site and a 3' overhang containing a NotI enzyme cut site. This allowed ligation of the

PCR product with a plasmid cut with the same enzymes. hTDP-43 was amplified in two different PCR reactions: once with a reverse primer containing the stop codon, and once with a reverse primer without a stop codon. The second amplification allows for the addition of 3'-tags to the protein product.

<u>Primer Name</u>	<u>Primer Sequence</u>	<u>Primer Function</u>
mhTDP43 S(SalI) For	CGGCGGTCGACATGTCTGAATATATTCGGGTAAC	Forward primer
mhTDP43 Stop(NotI)Rev	CATAGCGGCCGCCTACATTCCCCAGCCAGAAG	Reverse primer with stop codon
mhTDP43 NoStop(NotI)Rev	CTAAGCGGCCGCCATTCCCCAGCCAGAAGACTTAG	Reverse primer no stop codon

Fig 2-4: Human TDP-43 primers. These primers were used to clone human TDP-43 containing specific enzyme digestion sites at the 5' and 3' ends, to allow easy ligation into the pcMV Sport6 plasmid.

The PCR reactions were run with GoTaq Polymerase (Promega), and contained 10 µl 5x Buffer provided with the polymerase, 1 µl dNTP mixture, 1 µl upstream primer, 1 µl downstream primer, 0.25 µl GoTaq Polymerase, 500 ng DNA and H₂O up to 50 µl. The reactions were cycled under the following parameters: 1 cycle of 95°C for 2 min; 28 cycles of 95°C for 1 min, 58°C for 1 min, and 72°C for 2 min; 1 cycle of 72°C for 5 min and then left at 4°C for infinity.

After cycling, PCR reactions were purified using the QIAquick PCR Purification Kit (Qiagen, Cat No: 28104). The protocol used was taken from the manual provided by the kit. 5x the volume of the PCR reaction of Buffer PB was added to the PCR mixture and pipetted to mix. This mixture was applied to a QIAquick spin column over a 2 ml collection tube to bind the DNA to the column matrix. The tube was centrifuged for 1 min at 17,900 g, and flow-through was discarded. 750 µl of Buffer PE wash buffer was added to the column, the column was centrifuged for 1 min at 17,900 g, and flow-through was discarded. The tubes were centrifuged for an additional 1 min at 17,900 g to remove residual buffer, and the columns were moved to a new eppendorf tube. To elute the DNA, 50 µl of Buffer EB elution buffer was applied to the center of the column, incubated at RT for 1 min, and centrifuged for 1 min at 17,900 g.

Purified PCR reactions and plasmid pCMV Sport 6 were each cut with both SalI and NotI enzymes to prepare them for ligation. Enzyme digestions consisted of 2000 ng DNA, 5 µl

10x Buffer #4 from NEB, 5 μ l BSA from NEB, 2.5 μ l each Sall and NotI enzymes from NEB, and H₂O up to 50 μ l. Solutions were then incubated at 37°C for 2 hr and run on a 1% agarose gel. Bands corresponding to the appropriate size were excised and gel purified using the QIAquick Gel Extraction Kit (Qiagen, Cat No: 28706).

The protocol used was taken from the manual provided by the kit. 3 gel volumes of buffer QG were added to the gel in an eppendorf tube. The tube was incubated at 50°C for 10 min, vortexing briefly every 2 min to dissolve the gel. 1 gel volume of isopropanol was added to the tube, and sample was inverted to mix. The sample was applied to a QIAquick spin column in a 2 ml collection tube in order to bind the DNA to the column matrix. The column was centrifuged for 1 min at 17,900 g. Flow through was discarded, and 500 μ l of Buffer QG was added to wash the column. The tube was centrifuged for 1 min at 17,900 g and flow through was discarded. 750 μ l of Buffer PE wash buffer was added to the column, tube was centrifuged for 1 min at 17,900 g, and flow through was discarded. The tube was centrifuged once more to remove residual wash buffer, and the column was moved to a new eppendorf tube. To remove the DNA from the column matrix, 30 μ l of Buffer EB elution buffer was added to the center of the column, and incubated at RT for 1 min. Column was then centrifuged at 17,900 g for 1 min.

Gel purified enzyme digestions of the plasmid and the PCR fragments were then ligated together to form a full plasmid. This was done using T4 DNA ligase (New England Biolabs). The insert PCR fragments and the linearized plasmid were combined together in a 1:3 molar ratio. 1 μ l of T4 DNA ligase and 2 μ l of 10x T4 DNA Ligase Buffer were added. H₂O was added up to 20 μ l. Solution was mixed by pipetting and incubated overnight at 16°C.

The ligations were transformed into XL1 Blue Competent Cells (Stratagene). XL1 Blue cells, which were stored at -80°C, were thawed on ice for 30 min. 2.5 μ l of ligation was added to one tube of 100 μ l of cells. The tubes were quickly flicked to mix, then incubated on ice for 30 min. Tubes were heat pulsed for 45 sec at 42°C to allow the DNA to enter the cells, and then returned to ice for 2 min. 10 μ l of cells were plated on LB plates containing ampicillin, and plates were incubated overnight at 37°C. Plasmids were isolated from these ligations using the QIAprep Spin Miniprep Kit or QIAGEN Plasmid *Plus* Maxi Kit DNA isolation methods described earlier.

To better monitor the proteins when they are produced *in vitro*, a FLAG-tag for the 5' end of the sequences and a V5-tag for the 3' end of the sequences were designed. By a similar method, a nuclear export sequence was also designed to be added to the 5' end of the sequences in order to target the protein to the cytoplasm. These additional modifications were made by creating the forward and reverse sequences as oligos with 5' and 3' overhangs that match with KpnI and Sall restriction enzymes for the 5' end of the sequence and XbaI and HindIII restriction enzymes for the 3' end of the sequence. The oligos were ordered from Invitrogen, and reconstituted to approximately 1.5 µg/µl. The forward and reverse oligos were mixed together in a 1:1 ratio (5 µl to 5 µl), and incubated at 70°C for 10 min.

The plasmids containing human or mouse TDP-43 with stop or no stop codons were digested with restriction enzymes depending on the tags that would be added. Plasmids were digested with KpnI and Sall for 5' FLAG, FLAG-NES, or FLAG-mutated NES addition and with XbaI and HindIII enzymes for 3' V5 addition. These plasmids could then be ligated with the tagged inserts using T4 DNA Ligase and the method described earlier.

<u>Oligo Name</u>	<u>Oligo Sequence</u>	<u>Oligo Description</u>
FLAG KS A	CACCATGGACTACAAAGACGATGACGACAAGG	Forward sequence for FLAG-tag insertion via KpnI and Sall
FLAG KS B	TCGACCTTGTCGTCATCGTCTTTGTAGTCCATGGTGGTAC	Reverse sequence for FLAG-tag insertion via KpnI and Sall
FLAG-NES KS A	CACCATGGACTACAAAGACGATGACGACAAGAATGAATTAGC CTTGAAATTAGCAGGTCTTGATATCAACAAGACAG	Forward sequence for FLAG-Nuclear Export Signal insertion via KpnI and Sall
FLAG-NES KS B	TCGACTGTCTTGTGATATCAAGACCTGCTAATTTCAAGGCTA ATTCATTCTTGTCGTCATCGTCTTTGTAGTCCATGGTGGTAC	Reverse sequence for FLAG-Nuclear Export Signal insertion via KpnI and Sall
FLAG-NESMut KS A	CACCATGGACTACAAAGACGATGACGACAAGAATGAATTAGC CTTGAAATTAGCAGGTGCTGATATCAACAAGACAG	Forward sequence for FLAG-Mutant Nuclear Export Signal insertion via KpnI and Sall
FLAG-NESMut KS B	TCGACTGTCTTGTGATATCAGCACCTGCTAATTTCAAGGCTA ATTCATTCTTGTCGTCATCGTCTTTGTAGTCCATGGTGGTAC	Reverse sequence for FLAG-Mutant Nuclear Export Signal insertion via KpnI and Sall
V5 Xba HindIII A	CTAGATGGTAAGCCTATCCCTAACCTCTCCTCGGTCTCGATT CTACGTGAGGATCCA	Forward sequence for V5-tag insertion via XbaI and HindIII
V5 Xba HindIII B	AGCTTGATCCTCACGTAGAATCGAGACCGAGGAGAGGGTTA GGGATAGGCTTACCAI	Reverse sequence for V5-tag insertion via XbaI and HindIII

Fig 2-5: FLAG, NES and V5 Oligos. Oligos were used to create short DNA sequences to ligate into cut plasmids. These allowed the addition of FLAG, FLAG-NES, FLAG-mutant NES and V5 containing specific enzyme overhangs at both their 5' and 3' ends.

Mutations were introduced into the human TDP-43 containing plasmids using the QuikChange Site-Directed Mutagenesis Kit (Agilent Technologies, Cat No: 200519). Sample reactions consisted of 5 µl of 10X reaction buffer, 25 ng of dsDNA template, 125 ng of forward primer, 125 ng of reverse primer, 1 µl of dNTP mix, 1 µl *PfuTurbo* DNA polymerase and ddH₂O up to 50 µl. Samples were cycled in a PCR machine in the following order: 1 cycle 95°C for 30 sec; 12 cycles of 95°C for 30 sec, 55°C for 1 min and 68°C for 6 min. Samples were then cooled on ice for 2 min, and 1 µl *DpnI* restriction enzyme was added to each sample. Samples were gently mixed by pipetting, centrifuged for 1 min and incubated at 37°C for 1 hr for parental DNA strand digestion.

<u>Primer Name</u>	<u>Primer Sequence</u>	<u>Primer Function</u>
A315Tmut TDP43 Forward (PAGE Purified)	GGTGGGATGAACTTTGGTACGTTTCAGCATTAAATCCAGCC	Changing nucleotide 315 from A to T
A315Tmut TDP43 Reverse (PAGE Purified)	GGCTGGATTAATGCTGAACGTACCAAAGTTCATCCCACC	Changing nucleotide 315 from A to T
G348Cmut TDP43 Forward (PAGE Purified)	GCCAGCCAGCAGAACCAGTCATGCCCATCGGGTAATAACC	Changing nucleotide 348 from G to C
G348Cmut TDP43 Reverse (PAGE Purified)	GGTTATTACCCGATGGGCATGACTGGTTCTGCTGGCTGGC	Changing nucleotide 348 from G to C
A382Tmut TDP43 Forward (PAGE Purified)	GGCTCTAATTCTGGTGCAACAATTGGTTGGGGATCAGC	Changing nucleotide 382 from A to T
A382Tmut TDP43 Reverse (PAGE Purified)	GCTGATCCCCAACCAATTGTTGCACCAGAATTAGAGCC	Changing nucleotide 382 from A to T

Fig 2-6: Mutagenesis Primers. Primers containing one of three patient mutations to be used with the QuikChange Site-Directed Mutagenesis Kit.

Mutated DNA was transformed into XL1 Blue Supercompetent Cells (provided with the QuikChange Site-Directed Mutagenesis Kit). 1 µl of *DpnI* treated DNA was added to 50 µl of XL1 Blue Supercompetent Cells. Reactions were flicked to mix, and incubated on ice for 30 min. Cells were heat pulsed at 42°C for 45 sec, then returned to ice for two min. 500 µl of prewarmed LB broth was added to transformation reactions, and the reactions were incubated at 37°C for 1 hr with shaking at 225 rpm. The entire transformation reaction was plated on

LB plates with ampicillin, and plates were incubated overnight at 37°C. Single colonies were selected from the plate, cultured, and DNA was isolated using the QIAprep Spin Miniprep Kit or QIAGEN Plasmid *Plus* Maxi Kit methods as described earlier in this section.

<u>Plasmid Name</u>	<u>Plasmid Function</u>
hTDP43 FLAG + V5 in pCMV Sport6	Human TDP-43 with 5' FLAG-tag and 3' V5-tag in pCMV Sport6 vector
hTDP43 FLAG NES + V5 in pCMV Sport6	Human TDP-43 with 5' FLAG-tag + nuclear export signal and 3' V5-tag in pCMV Sport6 vector
hTDP43 FLAG mut NES + V5 in pCMV Sport6	Human TDP-43 with 5' FLAG-tag + mutated nuclear export signal and 3' V5-tag in pCMV Sport6 vector
hTDP43 A315T FLAG + V5 in pCMV Sport6	Human TDP-43 containing A315T mutation with 5' FLAG-tag and 3' V5-tag in pCMV Sport6 vector
hTDP43 A315T FLAG NES + V5 in pCMV Sport6	Human TDP-43 containing A315T mutation with 5' FLAG-tag + nuclear export signal and 3' V5-tag in pCMV Sport6 vector
hTDP43 A315T FLAG mut NES + V5 in pCMV Sport6	Human TDP-43 containing A315T mutation with 5' FLAG-tag + mutated nuclear export signal and 3' V5-tag in pCMV Sport6 vector
hTDP43 G348C FLAG + V5 in pCMV Sport6	Human TDP-43 containing G348C mutation with 5' FLAG-tag and 3' V5-tag in pCMV Sport6 vector
hTDP43 G348C FLAG NES + V5 in pCMV Sport6	Human TDP-43 containing G348C mutation with 5' FLAG-tag + nuclear export signal and 3' V5-tag in pCMV Sport6 vector
hTDP43 G348C FLAG mut NES + V5 in pCMV Sport6	Human TDP-43 containing G348C mutation with 5' FLAG-tag + mutated nuclear export signal and 3' V5-tag in pCMV Sport6 vector
hTDP43 A382T FLAG + V5 in pCMV Sport6	Human TDP-43 containing A382T mutation with 5' FLAG-tag and 3' V5-tag in pCMV Sport6 vector
hTDP43 A382T FLAG NES + V5 in pCMV Sport6	Human TDP-43 containing A382T mutation with 5' FLAG-tag + nuclear export signal and 3' V5-tag in pCMV Sport6 vector
hTDP43 A382T FLAG mut NES + V5 in pCMV Sport6	Human TDP-43 containing A382T mutation with 5' FLAG-tag + mutated nuclear export signal and 3' V5-tag in pCMV Sport6 vector

Fig 2-7: Plasmids. A list of all plasmids containing different tags and mutations that will be used to look at altered expression of TDP-43 in the Flp-In T-REx stable MN1 cell line.

2.6 TRANSIENT TRANSFECTION

MN1 cells were transiently transfected with plasmids using Qiagen's Effectene Transfection Reagent. Most cells were transfected in 10 cm dishes. When smaller dishes were used, the same protocol was utilized, but converted to the smaller dish's surface area. The basic protocol was based on the Qiagen protocol.

24 hr prior to transfection, cells were passed to approximately 30% confluency. On the day of transfection, cells were around 60-80% confluent. In an eppendorf tube, 2 µg of plasmid DNA was diluted in Buffer EC up to a total volume of 300 µl. 16 µl of Enhancer were added to the tube, and the tube was vortexed for 1 sec. The tube was then incubated at RT for 5 min, and 60 µl of Effectene Transfection Reagent was added to the DNA-Enhancer mix. The mixture was vortexed for 10 sec and then incubated at RT for 10 min. During this incubation, the growth media was removed from the cells, the cells were washed once with pre-warmed PBS, and 7 ml of fresh, pre-warmed growth media was added to the dish. After the 10 min incubation, 3 ml of growth media were added to the DNA-Enhancer, the mixture was pipetted to mix, and then added on top of the cells, dropwise. The dish was gently swirled to mix the growth media, and returned to the incubator. Cells were ready 24 hr later.

2.7 WESTERN BLOT ANALYSIS

Cells and samples were checked for protein expression. Cells were collected and spun down at 1,000 g for 10 min. Supernatant was removed and cell pellets were lysed on ice for 30 min using 100 µl RIPA buffer. Cell lysate was sonicated briefly to shear genomic DNA and centrifuged at 4°C for 10 min at 3,000 g. Supernatant was removed to a new tube, and protein content was measured using the Bio-Rad Protein Assay.

Equal amounts of protein from each sample – typically 5-10 µg – were loaded on and separated across a 12% SDS-PAGE gel in 1x running buffer. The gel was wet transferred to a PVDF membrane overnight. The PVDF membrane was blocked for 1 hr at RT using TBS-Tween containing 5% powdered milk, then overnight at 4°C, shaking, with primary antibody. The next day, membranes were washed 3 x 5 min in TBS-Tween. Membranes were incubated for 2 hr at RT with secondary antibody anti-mouse HRP (Invitrogen) or Peroxidase-Goat Anti-

Rabbit IgG (Invitrogen, Cat No: 65-6120) for TDP in TBS-Tween. Membranes were washed 5 x 5 min with TBS-Tween. Bands were chemiluminated using SuperSignal West Dura Extended Duration Substrate (Thermo Scientific, Cat No: 34075), and exposed using a Fujifilm LAS-4000 gel imaging system.

RIPA buffer for cells

1 M Tris pH 7.4	2.5 ml (final concentration: 50 mM)
NaCl	0.438 g
SDS	0.05 g
Sodium Deoxycholate	0.25 g
Triton X 100	0.5 ml
-Roche Tablet according to manufacturer's guide	
H ₂ O	50 ml

10x Running Buffer

Tris base	30 g
Glycine	144 g
SDS	10 g
H ₂ O	up to 1000 ml

1x Wet Transfer Buffer

Glycine	28.8 g
Tris base	6.04 g
Methanol	200 ml
H ₂ O	1.6 L

2.8 POLYSOME PROFILING FROM MN1 CELLS

To separate the mRNAs bound to polysomes from the total mRNA pool, MN1 cells were run through a gradient profiling system. 48 hr post seeding, cells were treated with 50 µg/ml cycloheximide added dropwise to growth medium, and swirled to distribute. Cells were returned to the 37°C incubator for 30 min to allow cycloheximide to inhibit translocation. For cells treated with puromycin, 200 µg/ml puromycin was added to cells for 20 min prior to cycloheximide addition. All other experimental procedures were the same.

During the incubation, sucrose gradients were formed and cooled. Fresh 50 ml sucrose solutions with 50% and 17.5% sucrose were made in gradient buffer containing 1.875 ml 2M KCl, 75 µl of 1M MgCl₂, and 500 µl of 1M Tris-HCl, and filter sterilized through a 0.22 micron filter.

Using a cannula, the bottom half of an Open-Top Polyclear Centrifuge Tube (Seton, Cat No: 7031) was filled with the light, 17.5%, sucrose solution. Using a second cannula, the heavy, 50%, sucrose solution was layered, slowly, below the light solution up to the halfway mark. Tubes were capped and formed into a gradient using the SHORT Sucr 17-50% wv setting on the Gradient Master gradient former (BioComp, Model No 108). After rotating, tubes were stored at 4°C for 30 min to prechill.

After forming gradients, the plates containing the treated cells were removed from the 37°C incubator and immediately placed on ice. Growth medium was aspirated off and cells were washed twice with ice-cold PBS containing 50 µg/ml of cycloheximide. Cells were collected in polysome lysis buffer (20 mM Tris, 10 mM MgCl₂, 100 mM NaCl, 0.4% NP-40, Roche Complete Protease Inhibitor, 100 U/ml RNasin, cycloheximide 50 µg/ml in cycloheximide treated samples). Tubes were incubated on ice for 10 min, and then centrifuged for 10 sec to pellet the nuclei. The supernatant was transferred to a new eppendorf tube, and centrifuged for 10 min at 10,000 g at 4°C to pellet any residual debris. After the spin, lysate was transferred to a new tube. For EDTA treated lysate, 30 µl of 250 mM EDTA was added to 470 µl lysate.

Lysate was normalized as it was loaded onto sucrose gradients. The protein concentrations of all samples were measured by the BioRad Protein Assay, and were normalized across the

protein concentrations. The samples were very carefully loaded onto the sucrose gradients on a balance, in order to carefully monitor the amount loaded. Gradients were ultracentrifuged in an SW40Ti rotor at 35,000 rpm for 2.5 hr at 4°C. Gradients were kept in 4°C room until fractionated.

Gradients were fractionated using a Piston Gradient Fractionator (BioComp, Model No: 152) (Fig 2-8). Samples were collected from top to bottom of the tubes. The piston was set to move at 0.3 mm/sec, with a distance of 3.00 per sample, with 27 samples total collected. This results in approximately 500 µl per fraction. As samples were removed from the top, they were passed through a Model EM-1 Econo UV Monitor (Bio-Rad, Cat No: 731-8160), which is set at 254 absorbance in order to measure RNA absorbance. Absorbance readouts were transmitted to and processed into graph form using the UV gradient profile program (BioComp, version 6.10).

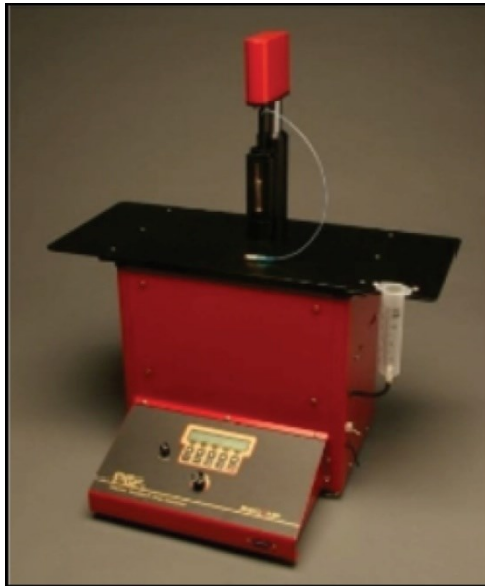


Fig 2-8: BioComp Piston Gradient Fractionator. The BioComp Piston Gradient Fractionator allows consistent fractionation of gradients (in the case of this project, sucrose), which are passed through a UV monitor to determine the RNA levels of each fraction. (Figure modified from Bor et al., 2006).

2.9 POLYSOME PROFILING FROM MOUSE BRAINSTEMS

In addition to MN1 cells, polysome profiles were generated from mouse brainstems. Mouse brainstems were dissected in MN1 media containing 50 µg/ml cycloheximide, a chemical that freezes ribosomes at the translocation step of translation. This allows purification of mRNA with the ribosomes still attached. The tissue was then transferred to Hanks Buffered Saline Solution containing trypsin (500 ml HBSS-Ca²⁺-Mg²⁺ with 500 ml Trypsin EDTA 0.25%) and 50 µg/ml cycloheximide. Tissue was then incubated at 37°C for 45 min. Liquid was removed, and 1 ml of MN1 media containing 50 µg/ml cycloheximide, and tubes were spun at 1500 rpm for 5 min. Tissue was washed 2x with PBS + 50 µg/ml cycloheximide, with spins at 1500 rpm for 5 min. PBS + 50 µg/ml cycloheximide was added to tissue, and tissue was incubated on ice for 10 min. Tubes were spun again at 1500 rpm for 5 min and liquid was removed. Tissue was moved to a 2 ml Dounce homogenizer, and 1 ml of lysis buffer was added on top, before douncing with an A pestle. Lysate was removed back to an eppendorf tube and incubated on ice for 30 min, vortexing every 10 min. Tubes were then spun at 10,000 rpm for 5 min at 4°C. Sample-containing liquid was moved to a new tube. Samples were measured for protein concentration using the BioRad Protein Assay, and equal amounts of protein content were loaded on each sucrose gradient.

Gradient formation, ultracentrifugation, and fractionation were performed as described above in section 2.8.

2.10 POLYSOME TO MONOSOME RATIO CALCULATION

Polysome to monosome ratios (P/M ratios) are calculated to provide information about how translation is being regulated. A standard P/M for a control sample must be taken for every experiment, since polysome profiles can be changed by very small alterations in cell and lysate preparation. All other runs from within the same experiment can be compared to this standard in order to verify whether the P/M ratio has increased (higher polysomes, lower monosome, or both) or decreased (lower polysomes, higher monosome, or both). An increased P/M ratio implies that there is a translation elongation defect and there are more ribosomes attached to the mRNAs as a result, whereas a decreased P/M ratio implies a translation initiation defect with more single ribosomes stuck at the start codon.

P/M ratios were calculated by drawing a line below the monosome peak across the polysome profile. A vertical line was drawn at the lowest point between the monosome and disome peaks. The area below the monosome curve (Fig 2-9, M) and the area below the polysomes (Fig 2-9, P) were measured using ImageJ to count the pixels. A ratio was taken of these two numbers and P/M ratios were compared.

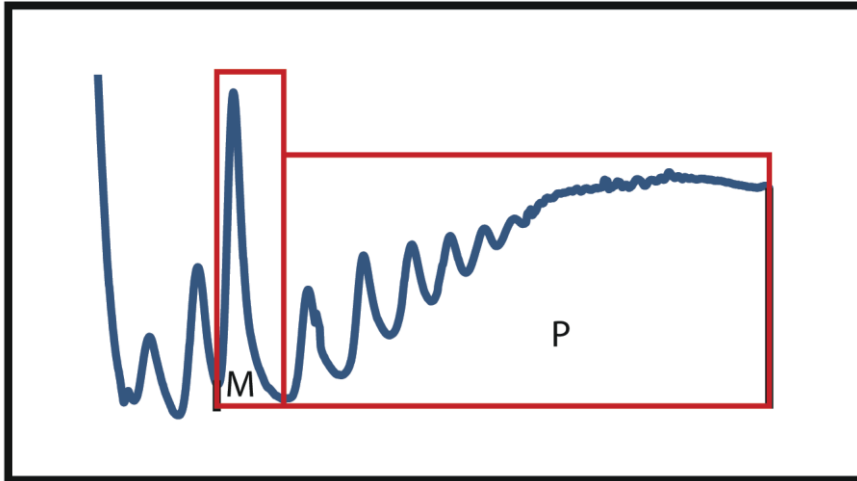


Fig 2-9: P/M ratio calculations. A representative polysome profile shown with sectioning of the monosome (M) and the polysomes (P) as done for P/M ratio calculations. The area of M and the area of P were measured by ImageJ in order to create a P/M ratio.

For statistical analysis of P/M ratios, multiple runs were done for each polysome profile. Excel was used to calculate statistical significance using one-tailed type 3 t-tests. Data are presented as mean \pm SEM. * indicates a p-value of $p < 0.05$.

2.11 PROTEIN ISOLATION FROM POLYSOME FRACTIONS

The protein contents of the fractions collected were isolated using a TCA precipitation. 500 μ l of 20% TCA was added to each sample, samples were mixed, and incubated on ice. Tubes were then centrifuged at maximum speed for 15 min at 4°C, and supernatant was discarded. 400 μ l of acetone was added to each sample, samples were centrifuged at maximum speed for 5 min at RT, and supernatant was discarded. Pellet was air dried for 10 min at 50°C. Pellets were resuspended in 26 μ l of NuPAGE lithium dodecyl sulfate (LDS) Sample Buffer

(Invitrogen, Cat No NP0008). LDS Sample Buffer was used as an optimal denaturing and reducing sample buffer for samples run on 4-12% NuPAGE Bis-Tris Gels.

12 μ l of sample in loading buffer was loaded into each lane of a 17 well, 4-12% NuPAGE Bis-Tris Gel (Invitrogen, Cat No: NP0327Box). Gels were run using 2-(N-morpholino)ethanesulfonic acid (MES) Buffer, containing 50 mM MES, 50 mM Tris Base, 0.1% SDS, 1 mM EDTA with pH adjusted to 7.3. Gels were wet transferred overnight to a PVDF membrane (Invitrogen). Membranes were blocked with TBS-Tween with 5% powdered milk for 1 hour, and were probed overnight, shaking at 4°C using primary antibodies in TBS-Tween (Tween-20 added to TBS until a final concentration of 0.05%) containing 0.02% sodium azide. Primary antibodies used were Ribosomal Protein L26 rabbit polyclonal (Cell Signaling Technology, Cat No: 2065) for staining of the large ribosomal subunit 26 protein and S6 Ribosomal Protein (54D2) mouse monoclonal antibody (Cell Signaling Technology, Cat No: 2317) for staining of the small ribosomal subunit 6 protein. The next day, blots were washed 3x5 min in TBS-Tween. Blots were incubated for 2 hr with secondary antibody anti-mouse HRP for S6 and anti-rabbit HRP for L26 in TBS-Tween with 1% sodium azide at room temperature shaking. Blots were washed 5x5 min with TBS-Tween. Bands were chemiluminated using SuperSignal West Dura Extended Duration Substrate (Thermo Scientific, Cat No: 34075), and exposed using a Fujifilm LAS-4000 gel imaging system.

If western blot band intensity was quantified, this was done using ImageJ (NIH). Files were opened in ImageJ, and bands were outlined with the “Rectangular Selection” tool, which kept the same area for multiple lanes in the same blot. Under Analyze>Gels, “Plot Lanes” was selected, which generates a profile plot for the intensity of each band. By drawing a straight line under the peak for the band intensity, selecting the “wand” tool, and clicking inside the area of the peak, ImageJ generated a relative area calculation under Analyze>Gels>Label Peaks. This allowed for quantitative comparison of band intensities.

2.12 RNA PURIFICATION AND cDNA SYNTHESIS FROM POLYSOME FRACTIONS

Trizol reagent (Life Technologies) was added to samples in a 3:1 ratio (250 μ l of fractions were taken to a new tube and 750 μ l of trizol reagent was added). 200 μ l of chloroform was added to each sample, and tubes were mixed by vigorous shaking for 30 sec. Tubes were centrifuged at 12000 g at 4°C for 15 min. The upper phase was transferred to a new tube and RNA was precipitated overnight at -80°C with a sodium acetate precipitation (30 μ l sodium acetate final concentration of 0.3M, 300 μ l Isopropanol, 5 μ l GlycoBlue). Sample was spun directly from the -80°C freezer at 13000g at 4°C for 15 min. The sample was then rinsed twice with 70% ethanol, spinning down in between at 13,000 g at 4°C for 5 min. The pellet was air dried for 15 min under the cell culture hood, and then resuspended in 100 μ l water.

RNA was then further purified using the Qiagen RNeasy kit. The protocol for purification was followed exactly as described in the protocol provided by the kit. 350 μ l of Buffer RLT was added to the sample, and mixed. Then 250 μ l 100% ethanol was added to the RNA, and mixed again. Sample was then transferred to the spin column over a 2 ml tube and centrifuged for 15 sec at 8000 g. Flow through was discarded, and 500 μ l Buffer RPE was added to the RNeasy spin column. The column was centrifuged for 15 sec at 8000 g and flow through was discarded. Again, 500 μ l Buffer RPE was added to the column, and the column was centrifuged for 2 min at 8000g. The column was spun at 8000 g for an additional 1 min to remove any residual liquid. After moving the column to a new tube, 30 μ l of RNase free water was added to the membrane, and the column was centrifuged for 1 min at 8000 g.

DNA was digested by the addition of DNase I (Roche). Samples were concentrated by an overnight Sodium Acetate precipitation at -80°C (30 μ l Sodium Acetate, 300 μ l Isopropanol, 5 μ l GlycoBlue). The next day, samples were spun directly from the -80°C freezer at 13000 g at 4°C for 15 min. Samples were washed twice with 70% EtOH, spinning between at 13000 g at 4°C for 5 min. Pellet was dried for 15 min under the cell culture hood, and pellet was resuspended in 20 μ l H₂O.

cDNA was reverse transcribed using SuperscriptII (Invitrogen). 1 μ l of 50 ng random primers, 7 μ l of RNA, and 4 μ l of dNTP mix were added to an eppendorf tube. The mixture was heated to 65°C for 5 min and the quickly chilled on ice. Then 4 μ l of first strand buffer, 2

μl of 0.1 DTT and 1 μl of RNasin plus were added to the sample, and the sample was mixed gently. Sample was incubated at 25°C for 2 min, 1 μl of SuperScript II RT was added, and sample was gently pipetted. Sample was incubated at 25°C for 10 min, and then at 42°C for 50 min. The enzyme was inactivated by heating the sample to 70°C for 15 min.

Parental strand RNA was digested with 1 μl RNAse H (NEB) for 20 min at 37°C, and RNAse H was inactivated by an incubation at 70°C.

2.13 REAL-TIME PCR

Real-time PCR primers were selected from pre-designed primers in the Harvard PrimerBank. Primers were diluted to 100 pmol/μl stock. Using the diluted primers, a pool was created depending on the number of samples being run using that primer. From 1x, that pool contained 0.06 μl forward primer, 0.06 μl reverse primer and 4.88 μl H₂O. cDNA was diluted 10 μl of cDNA into 240 μl of H₂O. 10 μl of FastStart Universal SYBR Green Master ROX (Roche: 04 913 914 001) was added to each sample well. 2x dilutions of cDNA were made, and 5 μl of cDNA samples were pipetted to each well. 5 μl of the primer mix pool was then added. The plate was spun down and sealed, and real-time PCR was performed on the 7900HT Fast Real-Time PCR machine (Life Technologies).

<u>Gene</u>	<u>Forward Primer</u>	<u>Reverse Primer</u>
Tardbp	5'-CGTGTCTCAGTGTATGAGAGGAGTC-3'	5'-CTGCAGAGGAAGCATCTGTCTCATCC-3'
Fus/Tls	5'- GCTTCAAACGACTATAACCAACA-3'	5'- GGCCATAACCACTGTA ACTCTGT-3'
Grn	5'-ATGTGGGTCCTGATGAGCTG-3'	5'-GCTCGTTATTCTAGGCCATGTG-3'
Nefl	5'-GACCTCAAGTCTATCCGCACA-3'	5'-GCTTCTCGTTAGTGGCGTCTT-3'
Gria2	5'-TTCTCCTGTTTTATGGGGACTGA-3'	5'-CCCTACCCGAAATGCACTGTA-3'

2.14 Click-iT NASCENT PROTEIN SYNTHESIS MEASUREMENT

10cm dishes of MN1 cells were washed 1x with PBS. PBS was removed and cells were incubated for 1 hr at 37°C in 4 ml of methionine- and cysteine-free medium. 50 μg/ml

cycloheximide was added to a negative control dish of cells, as cycloheximide should prevent nascent protein synthesis from occurring. 100 μ M Click-iT AHA (Invitrogen) was added to the cells, and cells were returned to the 37°C incubator for an additional 2 hr. After the incubation, cells were collected on ice by removing 3 ml of medium, and scraping cells into the remaining 1 ml of medium. Cells were washed 3x with ice-cold PBS, spinning down at 1000 g inbetween. PBS was removed, and cells were lysed in 25 μ l ice-cold lysis buffer with protease inhibitors and phosphatase inhibitors to preserve the proteins for quantification. 5 μ l H₂O, 50 μ l Click-iT Reaction Buffer, 5 μ l Component C (CuSO₄) and 5 μ l fresh Click-iT Reaction Buffer Additive 1 were added and samples were incubated at RT for 3 min. 10 μ l Click-iT Reaction Buffer Additive 2 were added to samples and samples were incubated at RT for 20 min. Proteins were precipitated by sodium acetate precipitation and pellets were air-dried for 15 min. 25 μ l LDS NuPAGE loading buffer were added to each sample, and samples were incubated for 10 min at 70°C. Proteins were run on a NuPAGE Novex 4-12% BisTris-Acrylamide gel. The gel was stained with SYPRO Ruby (Life Technologies) and TAMRA signal assayed with a Fujifilm Fluorescent Image Analyzer FLA-9000. Protein quantity was measured from the resulting image using the FLA-9000 accompanying software.

2.15 BacTRAP IMMUNOPRECIPITATIONS FROM MN1 CELLS AND MOUSE BRAINSTEM

BacTRAP immunoprecipitation was performed using two systems: MN1 cells and mouse brainstem. Preparation of material will be described first and then the method for immunoprecipitation after, as the immunoprecipitation method is the same for both systems. Method was developed from the original paper (Heiman et al., 2008), personal communication with Prof. Myriam Heiman, and from our own experiences.

MN1 cells were transfected with pEGFP-C2 plasmid (Clontech) or pEGFP-C2 plasmid containing the sequence for L10a (kindly provided by Dr. Froylan Calderon de Anda). In some cases, cells were co-transfected with FLAG-hTDP43-V5. Transfection was performed as described above. 24 hr after transfection, cells were collected, and spun down at 1000 g for 10 min at 4°C. Cells were then lysed.

Brain lysate was prepared as for the polysome profiles.

Beads were then prepared as follows. Monoclonal antibodies were thawed on ice, then spun at max speed for 10 min at 4°C. Antibodies were moved to a new tube, and 0.02% sodium azide was added. Streptavidin MyOne T1 Dynabeads were resuspended by hand mixing, and 300 µl beads were transferred to an eppendorf tube. The tube was placed in the provided magnet for 1 min, and supernatant was removed. Beads were resuspended in 1 ml PBS. Beads were then incubated in 120 µl of Biotinylated Protein L for 35 min at RT using gentle end over end rotation. The coated beads were then washed 5x with PBS containing 3% IgG, Protease-free BSA. 100 µg of anti GFP in 1 ml 0.15 M KCl buffer was added (50 µg of HtZ-GFP 19C8 and 50 µg of HtZ-GFP 19F7). Beads were incubated at RT for 1 hr, rotating slowly. Tubes were placed on the magnet for 1 min, and supernatant was removed. Beads were washed 3x in 1 ml 0.15 M KCl, resuspended in 200 µl 0.15 M KCl, and stored on ice.

Sample was added to beads, and beads were incubated overnight at 4°C with end over end rotation. Beads were collected on the magnet on ice, and supernatant was removed. Beads were washed 4x in 1 ml 0.35 M KCl.

If beads were being used for real-time PCR, the RNA purification protocol described in section 2.11 was used. If beads were being used for western blot, 1x loading buffer was added directly to the beads, and beads were boiled at 95°C for 5 min.

2.16 RIBOSOME FOOTPRINTING

Ribosome footprinting protocol was developed from Ingolia, Ghaemmaghami, Newman, & Weissman, (2009). 10 cm plates containing MN1 cells to be used were removed from the 37°C incubator and immediately placed on ice. Growth medium was aspirated off and cells were washed twice with ice-cold PBS containing 50 µg/ml of cycloheximide. Cells were collected by scraping in 1 ml of ice-cold PBS containing 50 µg/ml of cycloheximide, and centrifuged at 2000 g for 5 min. Supernatant was removed, and the cell pellet was either saved, if it was going to be used for total RNA library, or resuspended in 300 µl lysis buffer if it was going to be used for the footprinting library. Tubes were incubated on ice for 10 min, and then centrifuged for 10 sec to pellet the nuclei. The supernatant was transferred to a new eppendorf tube, and centrifuged for 10 min at 10,000 g at 4°C to pellet any residual debris. After the spin, lysate was transferred to a new tube.

0.02 μ l of RNase I was added to 300 μ l of lysate. Samples were incubated at 25°C in a shaking thermomixer for 45 min. 1.5 μ l SUPERaseIN (RNase inhibitor) (Life Technologies #AM2694) was added to each aliquot. Samples were then loaded onto sucrose gradients, ultracentrifuged, and fractionated as described above. The fractions containing the monosomal peak were selected.

RNA was extracted from the fractions by adding 40 μ l of 20% SDS and 650 μ l acid phenol per 600 μ l of pooled fractions. The samples were then incubated for 10 min in a 65°C water bath, vortexing every minute. Samples were immediately transferred to ice for 5 min. Then 650 μ l of chloroform was added, and samples were vortexed. Tubes were spun at top speed for 5 min and the aqueous supernatant was removed to a new tube. 650 μ l PCI were added per 600 μ l of diluted extract, and tubes were vortexed, and then spun at top speed for 5 min. The aqueous supernatant was again moved to a new tube, and 1/9 volume of 3 M sodium acetate (NaOAc) was added, plus 1 volume Isopropanol and 3 μ l of GlycoBlue. Samples were chilled between 30 min and overnight at -80°C. Samples were spun at top speed at 4°C for 30 min, and pellet was washed in 750 μ l 80% EtOH. Pellet was then air-dried and resuspended in 5 μ l 10 mM Tris, pH 8.0. This generated the footprinting RNA starting material.

For the total RNA library generation, the cell pellet taken above had RNA extracted by addition of 400 μ l Trizol. Cells were lysed by pipetting up and down. Sample was then incubated at RT for 5 min. 80 μ l chloroform was added to samples and the tubes were shaken vigorously by hand, and then incubated at RT for 3 min. Samples were then centrifuged for 15 min at 12000 g at 4°C. The aqueous supernatant was transferred to a new tube, and 2 μ l of GlycoBlue and 200 μ l of Isopropanol were added. Samples were incubated for 10 min -80°C, then centrifuged for 15 min at 12000 g at 4°C. The pellet was washed in 750 μ l 80% EtOH and air dried, and then resuspended in 100 μ l 10 mM Tris pH 7.5.

Total RNA was Poly(A) selected. This was done by adding 100 μ l binding buffer to the sample and incubating for 2 min at 65°C in a shaking thermomixer. Sample was then placed on ice and 0.5 μ l RNAsin was added. Dynabeads Oligo(dT)₂₅ (Life Technologies #610-02) were resuspended by vortexing. 200 μ l beads were pipetted into an eppendorf tube and placed on the magnet. Storage buffer was removed and beads were washed 1x with 100 μ l binding buffer. 100 μ l binding buffer was added to resuspended beads as well as the

denatured RNA. Sample was incubated 5 min inverted by hand, and then tube was placed on magnet and supernatant was removed. Beads were washed 2x with 200 μ l wash buffer B. Then 18 μ l 10 mM Tris, pH 7.5 was added to beads, and they were incubated for 2 min at 80°C in a shaking thermomixer. Elute was transferred to a PCR tube and placed ice.

Total RNA was then fragmented. This was done by adding 2 μ l 10x RNA fragmentation buffer (Life Technologies # AM8740). Reactions were incubated in a PCR machine for 5 min at 94°C. The sample was immediately placed on ice, and 2 μ l 10x stop solution (Life Technologies # AM8740) was added, and sample was mixed. 80ML H₂O, 11 μ l 3M NaOAc, 2 μ l GlycoBlue and 100 μ l isopropanol were added to the sample, and the sample was chilled for 30 min to overnight at -80°C. Sample was spun at top speed at 4°C for 30 min to pellet RNA. Pellet was washed in 750 μ l 80% EtOH, air dried, and resuspended in 5 μ l 10 mM Tris pH8.0. This generated the “Total RNA” starting material.

The total RNA and the footprinting RNA starting material were used in parallel from here on out. 5 μ l 2x Novex TBE-Urea Sample Buffer (Life Technologies #LC6876) was added to each sample. 10bp DNA ladder was prepared (Life Technologies #10821-015) and control RNA was prepared using a 28mer RNA and a 34mer RNA as markers. Samples were denatured for 90s at 80°C, then kept on ice until loaded. The precast 15% TBE/Urea/polyacrylamide gel (Life Technologies #EC68855BOX) was pre run for 20 min at 200 V. The gel was then loaded, and run for an additional 65 min at 200V. Gel was stained for 60 min in SYBR Gold (1:10000) in TBE. The gel was photographed using the FLA9000 machine (Fujifilm). The region of the sample corresponding to the region marked by the control oligos was excised. A 0.5 ml tube was pierced with an 18.5 gauge needle and placed inside a microcentrifuge tube. The excited gel piece was placed into the smaller tube, and nested tubes were spun for 3 min at top speed to force the gel through the needle hole. 360 μ l H₂O was added to the gel, and gel was soaked for 10 min at 70°C on a shaking thermomixer. The gel elution was added to a Spin X Zentrifugen Filtersystem CA 2.2 ml 0.22 μ m column (Fisher Scientific #10104101) and spun for 3 min at top speed. 40 μ l 3M NaOAc, 1.5 μ l GlycoBlue and 500 μ l Isopropanol were added to the sample, and the sample was incubated from 30 min to overnight at -80°C. Sample was then spun at top speed at 4°C for 30 min to pellet the RNA, pellet was washed in 750 μ l 80% EtOH, air dried, and resuspended in 10 μ l 10 mM Tris, pH 8.0.

Next, samples were dephosphorylated. First, 33 μ l H₂O were added, and samples were denatured for 90s at 80°C. Samples were then placed on ice, and 7 μ l of dephosphorylation mix were added (5 μ l T4 PNK buffer, 1 μ l SUPERaseIn (RNase inhibitor), 1 μ l T4 PNK (NEB #M0201)). Samples were incubated for 1 hr at 37°C, and then for 10 min at 70°C. 39 μ l H₂O, 1 μ l GlycoBlue, 10 μ l 3M NaOAc, and 150 μ l isopropanol were added to samples, and samples were incubated from 30 min to overnight at -80°C. Samples were spun at 4°C for 30 min to pellet the RNA. Pellets were washed in 740 μ l 80% EtOH, air dried, and resuspended in 8.5 μ l 10 mM Tris, pH 8.0.

Linkers were then ligated to the samples. 1.5 μ l of preadenylated Universal miRNA Cloning Linker (NEB #S1315) were added to the samples, and samples were denatured for 90 sec at 80°C, then cooled to RT. A ligation reaction was set up (RNA-linker, 2 μ l 10x T4 Rnl2 buffer, 6 μ l 50% PEG 8000, 1 μ l SUPERaseIn (RNase inhibitor), 1 μ l T4 Rnl2 (Neb #M0242)), and incubated for 2.5 hr at RT. 338 μ l H₂O, 1.5 μ l GlycoBlue, 40 μ l 3 M NaOAc, and 500 μ l Isopropanol were added to samples, and samples were incubated from 30 min to overnight at -80°C. Samples were then spun at 4°C for 30 min to pellet the RNA. Pellet was washed in 750 μ l 80% EtOH, air dried, and resuspended in 5 μ l 10 mM Tris, pH 8.0.

5 μ l 2x Novex TBE-Urea Sample Buffer (Life Technologies #LC6876) was added to each sample. 10bp DNA ladder was prepared (Life Technologies #10821-015) and control RNA was prepared using a 28mer RNA and a 34mer RNA as markers. Samples were denatured for 90s at 80°C, then kept on ice until loaded. The precast 15% TBE/Urea/polyacrylamide gel (Life Technologies #EC68855BOX) was pre run for 20 min at 200 V. The gel was then loaded, and run for an additional 65 min at 200 V. Gel was stained for 60 min in SYBR Gold (1:10000) in TBE. The gel was photographed using the FLA9000 machine (Fujifilm). The region of the sample corresponding to the region marked by the control oligos was excised. A 0.5 ml tube was pierced with an 18.5 gauge needle and placed inside a microcentrifuge tube. The excised gel piece was placed into the smaller tube, and nested tubes were spun for 3 min at top speed to force the gel through the needle hole. 360 μ l H₂O was added to the gel, and gel was soaked for 10 min at 70°C on a shaking thermomixer. The gel elution was added to a Spin X Zentrifugen Filtersystem CA 2.2 ml 0.22 μ m column (Fisher Scientific #10104101) and spun for 3 min at top speed. 40 μ l 3M NaOAc, 1.5 μ l GlycoBlue and 500 μ l Isopropanol were added to the sample, and the sample was incubated from 30 min to overnight at -80°C.

Sample was then spun at top speed at 4°C for 30 min to pellet the RNA, pellet was washed in 750 µl 80% EtOH, air dried, and resuspended in 7 µl 10 mM Tris, pH 8.0.

Samples were then reverse transcribed. 2 µl of reverse transcription primers were added to a PCR tube and denatured for 90s at 80°C in a PCR machine. The tube was then placed in ice, and the PCR machine was cooled to 48°C. A reverse transcription reaction was then set up (Ligation + primer, 4 µl first strand buffer, 4 µl 2.5 mM dNTPs, 1 µl 100 mM DTT, 1 µl SUPERaseIn (RNase inhibitor), 1 µl SuperScript III (Life Technologies #18080-093). and incubated for 30 min at 48°C in the PCR machine. The reaction was then hydrolyzed by adding 2.2 µl 1 N NaOH, and samples were incubated for 20 min at 90°C. 156 µl H₂O, 2.0 µl GlycoBlue, 20 µl 3M NaOAc, and 300 µl isopropanol were added to samples, and samples were incubated from 30 min to overnight at -80°C. Samples were then spun at 4°C for 30 min to pellet the RNA. Pellet was washed in 740 µl 8-% EtOH, air dried, and resuspended in 5 µl 10 mM Tris pH 8.0.

5 µl 2x Novex TBE-Urea Sample Buffer (Life Technologies #LC6876) was added to each sample. 10bp DNA ladder was prepared (Life Technologies #10821-015) and control RNA was prepared using a 28mer RNA and a 34mer RNA as markers. Samples were denatured for 90 sec at 80°C, then kept on ice until loaded. The precast 15% TBE/Urea/polyacrylamide gel (Life Technologies #EC68855BOX) was pre-run for 20 min at 200 V. The gel was then loaded, and run for an additional 75 min at 200 V. Gel was stained for 60 min in SYBR Gold (1:10000) in TBE. The gel was photographed using the FLA9000 machine (Fujifilm). The region of the sample corresponding to the region marked by the control oligos was excised. A 0.5 ml tube was pierced with an 18.5 gauge needle and placed inside a microcentrifuge tube. The excised gel piece was placed into the smaller tube, and nested tubes were spun for 3 min at top speed to force the gel through the needle hole. 360 µl H₂O was added to the gel, and gel was soaked for 10 min at 70°C on a shaking thermomixer. The gel elution was added to a Spin X Zentrifugen Filtersystem CA 2.2 ml 0.22 µm column (Fisher Scientific #10104101) and spun for 3 min at top speed. 40 µl 3M NaOAc, 1.5 µl GlycoBlue and 500 µl Isopropanol were added to the sample, and the sample was incubated from 30 min to overnight at -80°C. Sample was then spun at top speed at 4°C for 30 min to pellet the RNA, pellet was washed in 750 µl 80% EtOH, air dried, and resuspended in 15 µl 10 mM Tris, pH 8.0.

Samples were then circularized. This was done by setting up a circularization reaction (First strand cDNA, 2 μ l 10x CircLigase buffer, 1 μ l 1mM ATP, 1 μ l MnCl₂, 1 μ l CircLigase (Biozym #131405)) and incubated for 1 hr at 60°C in a PCR machine. The reaction was inactivated for 10 min at 80°C. 156 μ l H₂O, 2 μ l GlycoBlue, 20 μ l 3 M NaOAc, and 300 μ l Isopropanol were added to the sample. Sample was incubated for 30 min to overnight at -80°C. Samples were then spun at 4°C for 30 min to pellet the RNA. Pellet was washed in 750 μ l 80% EtOH, air dried, and resuspended in 5 μ l 10 mM Tris, pH 8.0.

Samples were then PCR amplified. A PCR mixture was created with a different indexed reverse primer for each sample (20 μ l 5x Phusion HF buffer, 8 μ l 2.5 mM dNTPs, 0.5 μ l 100 μ M Forward library primer, 0.5 μ l 100 μ M Reverse indexed library primer, 65 μ l H₂O, 5 μ l circularized DNA template, 1 μ l Phusion polymerase (NEB #M0530). 16 μ l aliquots of each sample were placed into 5 tubes. Tubes were thermocycled (1 cycle: 30 sec 98°C; 10-18 cycles: 10 sec 98°C, 10 sec 65°C, 5 sec 72°C). Tubes were removed after 10, 12, 14, 16, and 18 extension cycles.

4 μ l of 5x Novex High Density TBE Sample Buffer (Life Technologies #LC6678) was added to each sample. 10 bp DNA ladder was prepared. A 10% polyacrylamide non-denaturing gel was loaded, and run for 50 min at 180V. Gel was stained for 60 min in SYBR Gold (1:10000 in TBE). Gel was photographed. Prominent product band at 176 nt was excised and placed into a 2 ml tube. 400 μ l of DNA Gel Extraction Buffer was added (3 ml 5 M NaCl, 1 M Tris pH8.0, 100 μ l 0.5 M EDTA, 46.4 ml H₂O). Samples were rotated on a shaker overnight.

1.5 ml GlycoBlue and 500 μ l Isopropanol were added to the samples, and samples were incubated for 30 min to overnight at -80°C. Samples were then spun at top speed at 4°C for 30 min to pellet the RNA. Pellet was washed in 750 μ l 80% EtOH, air dried, and resuspended in 15 μ l 10 mM Tris, pH 8.0

2.17 ANTIBODIES

Antibody Name	Company	Catalogue Number
TARDBP EPR5810	Epitomics	3769-1
HtzGFP_04	Monoclonal Antibody Core Facility (MACF) Sloan Kettering Institute for Cancer Research	clone19F7
HtzGFP_02	Monoclonal Antibody Core Facility (MACF) Sloan Kettering Institute for Cancer Research	clone 19C8
GAPDH	Invitrogen	G8795
Ribosomal Protein L26 Antibody	Cell Signaling Technologies	2065
S6 Ribosomal Protein (54D2)	Cell Signaling Technologies	2317
V5	Invitrogen	46-1157
Ribosomal Protein L7a (E109)	Cell Signaling Technologies	2415
GFP Antibody	Cell Signaling Technologies	2555

3 RESULTS – TDP-43

3.1 KNOCKDOWN OF TDP-43 IN MN1 CELLS DOES NOT SIGNIFICANTLY ALTER GLOBAL TRANSLATION

3.1.1 MOTOR NEURON-LIKE MN1 CELLS EXPRESS ENDOGENOUS TDP-43 MOSTLY IN THE NUCLEUS

As ALS – a disease that largely affects motor neurons – is one of the major TDP-43 proteinopathies, we selected the MN1 cell line for many of our cell culture experiments. This cell line was generated by fusing mouse motor neurons with neuroblastoma cells in order to generate a motor neuron-like immortalized cell line. These cells have previously been shown to express choline acetyltransferase (ChAT) similar to motor neurons, and to produce minor neurites (Salazar-Gruesso et al., 1991).

Under normal cellular conditions, TDP-43 protein is found mostly in the nucleus with a small amount found in the cytoplasm (For a review, see Lagier-Tourenne et al., 2010). As we planned to use the MN1 cells for numerous experiments, it was important to first check that endogenously expressed TDP-43 in MN1 cells was localized in a similar manner to what is found normally in human cells. If MN1 endogenous TDP-43 did not behave in a characteristic manner, it is likely that these cells would not be a good model for our experiments to assay how altered expression of TDP-43 functions in relation to translation.

After fractionating MN1 cells into their nuclear and cytoplasmic components, the cells were probed by western blot analysis to identify the location of TDP-43 protein. Consistent with previous studies, TDP-43 was mostly found in the nuclear fraction, with a small amount found in the cytoplasmic fraction (Fig 3.1). GAPDH, a protein found in the cytoplasm, was used as a positive control for our cellular fractionation. As GAPDH was found mostly in the cytoplasmic fraction, and TDP-43 expression was found to be mostly nuclear with a small amount in the cytoplasm, we concluded that these cells would function properly for our experimental purposes.

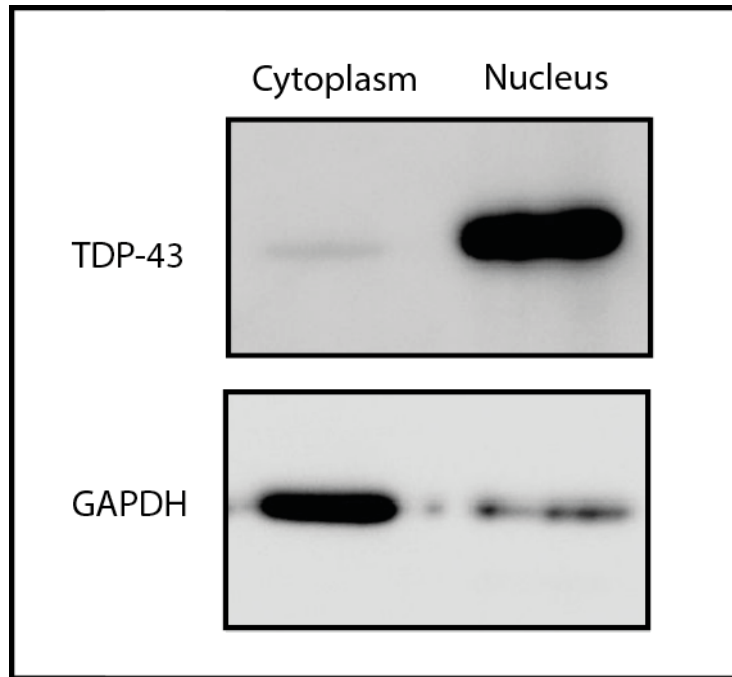


Figure 3.1 Cellular distribution of endogenous TDP-43

MN1 cells were fractionated into nuclear and cytoplasmic fractions, and probed by western blot. TDP-43 was found to be expressed mostly in the nucleus, with a small fraction found in the cytoplasm, as is expected for TDP-43 expression in most cell types. GAPDH, as a cytoplasmic protein, was used as a control for the fractionation.

3.1.2 ROBUST POLYSOME PROFILING FROM MN1 CELL EXTRACTS

Polysome profile generation is a powerful method used to analyze translation in cells or tissues. The protocol will briefly be outlined here (more detail can be found in section 2.8). Ribosomes can be frozen in the translocation stage of translation by a chemical called cycloheximide. This chemical allows downstream processing of cell lysate while maintaining the ribosomes bound to the mRNA. Cells were treated with cycloheximide, lysate was obtained from cells or tissues, loaded on top of a sucrose gradient, and ultracentrifuged to separate the lysate components by sedimentation rate – of particular interest are the 40S and 60S ribosomal subunits, the 80S/monosome, and polysomes. After ultracentrifugation, the gradient was fractionated, and fractions were passed through a UV monitor set to absorb at a wavelength of 254, which allowed visualization of the nucleic acid concentration in each fraction. The resulting graph resolved peaks for the 40S and 60S ribosomal subunits, the monosome, disome, trisome etc (Fig 3.2 A). General alterations in the graph indicate large-

scale, general changes in translation. For instance, a large increase in the 80S monosome peak would indicate a likely initiation defect, whereas a decrease in the 80S monosome peak along with an increase in the polysome peaks would indicate an elongation defect.

In addition to general translation visualization, by isolating RNA or protein from individual fractions and subsequently measuring the concentration of specific RNAs or proteins of interest, it is possible to see changes in localization of these species across the fractions of the gradient. mRNAs that move from so-called “light fractions” – the lighter densities of sucrose – to heavier fractions under altered conditions usually indicate an increased overall translation of these mRNAs. Conversely, movement of mRNA species to lighter fractions typically indicates a decrease in their translation.

Proteins that bind to cytoplasmic mRNAs, to ribosomal proteins, or to fully assembled ribosomes are good candidates to have a functional role in regulating translation. These can be identified by purifying protein from individual fractions produced by polysome profiling and probing the fractions by western blot to determine the localization of specific proteins across the gradient.

At the beginning of this thesis research, this method was not yet running in the Duncan laboratory. Therefore, the polysome profiling method had to be fully established using the BioComp Gradient Fractionator system and the BioComp Gradient Master. The Gradient Master allows for consistent generation of sucrose gradients in an expedited manner, compared with the step freeze method that was commonly used in the past. Stepwise gradients are made by layering solutions of decreasing sucrose density and freezing them at -80°C between each addition. After all layers have been added, the gradients are placed at 4°C overnight so that the sucrose solutions may thaw and mix. The Gradient Master, on the other hand, allows the production of a gradual gradient from just two sucrose density solutions, and mixes them by rotating the tube at a preset angle. This allows gradients to be produced freshly the day of use, and also creates a more consistently reproducible sucrose gradient.

Polysome profiles can be produced by ultracentrifuging lysate-loaded sucrose gradients and subsequently poking a hole in the bottom of the tube. By counting a determined number of drops per sample, the fractions can then be measured for nucleic acid concentration, and the

concentrations can be plotted. This plot is called the polysome profile. This method is time consuming and labor intensive, and the graph generated is not high resolution, as the drops from the bottom of the tube may cause the sucrose, and therefore the centrifuge-separated RNA, to mix. We therefore chose to establish polysome profiling in our laboratory using a Gradient Fractionator, a machine that automatically fractionates gradients from top to bottom using a trumpet-ended tip. This tip removes a uniform layer of sucrose from the top of the gradient without disturbing the sucrose below. It then automatically passes these fractions through a UV monitor, which measures the concentration of nucleic acid constantly, producing a graphical readout while collecting the fractions with an automatic fraction collector (Fig 3.2 A). This machinery allows consistent fractionation without disturbing lower sucrose in the process, producing more precise and higher-resolution polysome profiles, and automatic alignment of the graphs with the fractions produced. It is both more efficient, and more accurate than alternatives.

In order to establish polysome profiling in our laboratory, we produced lysate from MN1 cells. This lysate was either used under normal conditions or after being treated with EDTA – a cation chelator. EDTA chelates magnesium, which is important for the stability of RNA structure thereby allowing ribosomal subunits to stay bound. Upon addition of EDTA, it has been shown previously that polysomes and monosomes dissociate, leaving just the 40S and 60S subunits detectable by polysome profiling. This is a method frequently used to assure that the polysome profile graph output from the UV monitor is, in fact, polysomes. Our untreated MN1 cell lysate produced graphs that were highly consistent with what has been shown for polysome profiles produced in other laboratories. The 40S and 60S subunits are visible, as well as a larger monosome peak, followed by several polysome peaks. As expected, in the presence of EDTA, all polysomes as well as the 80S monosome are dissociated into their 40S and 60S subunits (Fig 3.2 B). This indicates that our polysome profiling method is robustly working with MN1 cells.

We additionally confirmed that the peaks contained the expected ribosomal subunit protein components. This was done by isolating the protein from each fraction generated by the polysome fractionator and then probing by western blot for either a large ribosomal subunit protein (L26) or a small ribosomal subunit protein (S6). These proteins migrated in a pattern similar to where they should be based on the peak locations of the polysome profile graphs

(Fig 3.2 B). This further confirms that the peaks visualized using our polysome profile method are indeed the 40S, 60S, 80S, and polysome peaks expected.

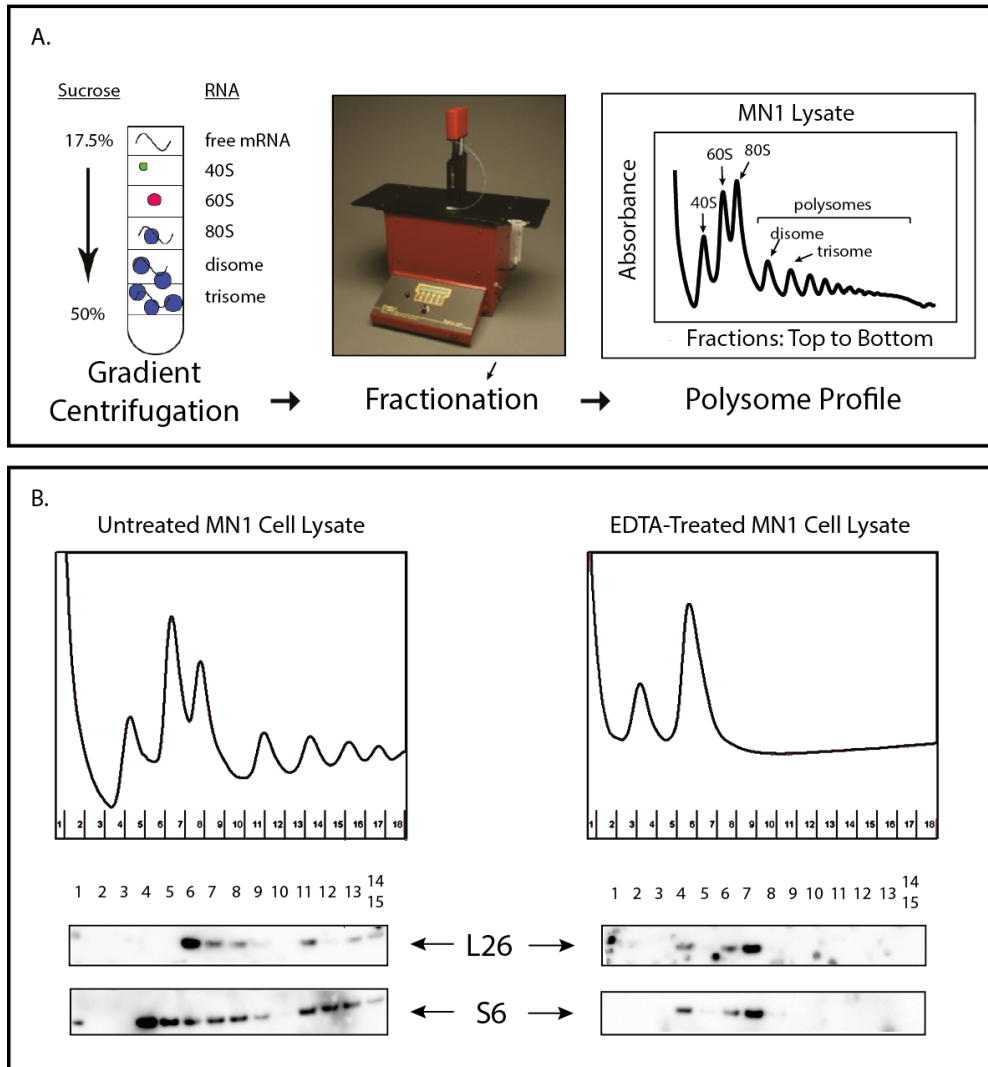


Figure 3.2 Polysome profiling was established in the laboratory for MN1 cells

- A. Overview of the polysome profiling assay. Cellular lysate is loaded on top of a sucrose gradient (all gradients used in the following sections are 17.5-50% sucrose gradients) and ultracentrifuged to distribute the lysate through the different densities. The gradients are then fractionated from top to bottom, and fractions are passed through a UV Monitor set at wavelength 254 to identify nucleic acids present in the fractions. These quantities are graphed, forming a profile (the one shown is an actual profile generated with our MN1 cells) that can resolve the 40S and 60S subunits, the 80S monosome, and the individual polysome peaks (disome, trisome, etc).
- B. MN1 cell profiles either untreated, or treated with EDTA to dissociate the ribosomes into their individual subunits. Protein was isolated from fractions and probed by western blot for either large ribosomal subunit protein L26 or small ribosomal subunit protein S6. This shows the altered distribution of the subunits in two different analyses.

3.1.3 TDP-43 IS EFFICIENTLY KNOCKED DOWN BY siRNA IN MN1 CELLS

In order to investigate TDP-43 function, it is essential to be able to manipulate TDP-43's expression levels. One such way to assay TDP-43's effect on translation is to significantly reduce expression levels of TDP-43. Using MN1 cells, we knocked down TDP-43 using XtremeGene siRNA Transfection Reagent (Roche) and Silencer Select siRNAs (Ambion). TDP-43 was highly efficiently and consistently knocked down using these reagents (Fig 3.3). Protein levels were reduced by more than 80%. GAPDH siRNA was used as a positive control, and showed a significant reduction of GAPDH protein. Scrambled negative control siRNAs showed no reduction of either GAPDH or TDP-43 proteins, as expected. Taken together, our knockdown method provides us with a specific, reproducible, and efficient knockdown of TDP-43.

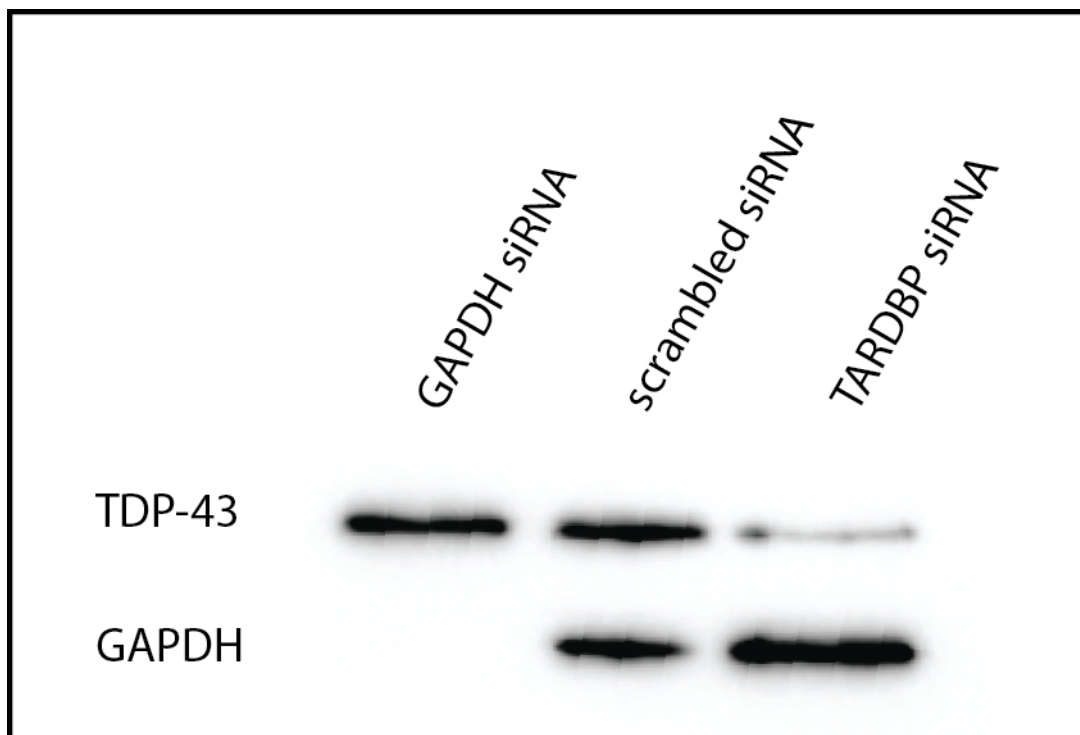


Figure 3.3 Knockdown of TDP-43 is efficient

MN1 cells were treated with TARDBP siRNA to reduce TDP-43 levels, GAPDH siRNA as a positive control, or a scrambled negative control siRNA. TARDBP siRNA efficiently knocked down TDP-43 protein levels, and GAPDH siRNA also reduced GAPDH levels as expected, while the scrambled negative control siRNA showed no effect on either TDP-43 or GAPDH protein levels.

3.1.4 TDP-43 REDUCTION DOES NOT AFFECT GLOBAL TRANSLATION IN MN1 CELLS

Since TDP-43 binds to a large portion of the transcriptome (Polymenidou et al., 2011) and shuttles between the nucleus and cytoplasm, we believe that TDP-43 may have an effect on translational regulation – a cytoplasmic event that involves RBPs bound to mRNAs. In particular, we were interested in assessing whether knockdown of endogenous TDP-43 or transient expression of specific TDP-43 variants would show any effect on translation. In principle, the translational regulatory effects generated by manipulating TDP-43 expression could be general translation effects or mRNA-specific effects. Importantly, polysome profiling can be used to assess both possibilities.

Since we established an efficient knockdown of TDP-43, we first checked whether reduction of TDP-43 in MN1 cells showed general alterations in translation. After efficient knockdown (Fig 3.4 A), MN1 cell lysate was loaded on top of a sucrose gradient, ultracentrifuged, and fractionated. No visible change in polysome profiles was found when comparing MN1 cells treated with TARDBP siRNA against MN1 cells treated with scrambled negative control siRNA (Fig 3.4 B).

Polysome to monosome ratios (P/M ratios) were calculated to provide information about how translation was being regulated. A standard P/M for a control sample must be taken for every experiment, since polysome profiles can be changed by very small alterations in cell and lysate preparation. All other runs from within the same experiment can be compared to this standard in order to verify whether the P/M ratio has increased (higher polysomes, lower monosome, or both) or decreased (lower polysomes, higher monosome, or both). An increased P/M ratio implies that there is likely a translation elongation defect and that there are more ribosomes attached to the mRNAs as a result, whereas a decreased P/M ratio implies a likely translation initiation defect with more single ribosomes stuck at the start codon.

P/M ratios were calculated by drawing a line below the monosome peak across the polysome profile. The area below the monosome curve and the area below the polysomes were measured using ImageJ, a ratio was taken of these two numbers, and P/M ratios were compared. No statistically significant difference was found after calculating the polysome to monosome (P/M) ratios of these graphs (Fig 3.4 C; see Materials and Methods 2.10). This

suggests that a reduction in TDP-43 protein levels does not significantly affect general translation.

To further clarify if knockdown of TDP-43 had any translational regulatory effects, we measured nascent protein synthesis with the non-radioactive Click-iT AHA Protein Synthesis kit (see Materials and Methods 2.14). We assessed nascent protein synthesis levels in TARDBP siRNA-treated MN1 cells, scrambled negative control siRNA-treated MN1 cells, or cells treated with cycloheximide (a translation inhibitor and positive control to show reduced nascent protein synthesis). Consistent with our profiling data, we observed no statistically significant alteration in the amount of nascent protein produced after TDP-43 depletion (Fig 3.4 D). We concluded that knockdown of TDP-43 in MN1 cells does not have a significant effect on general translation.

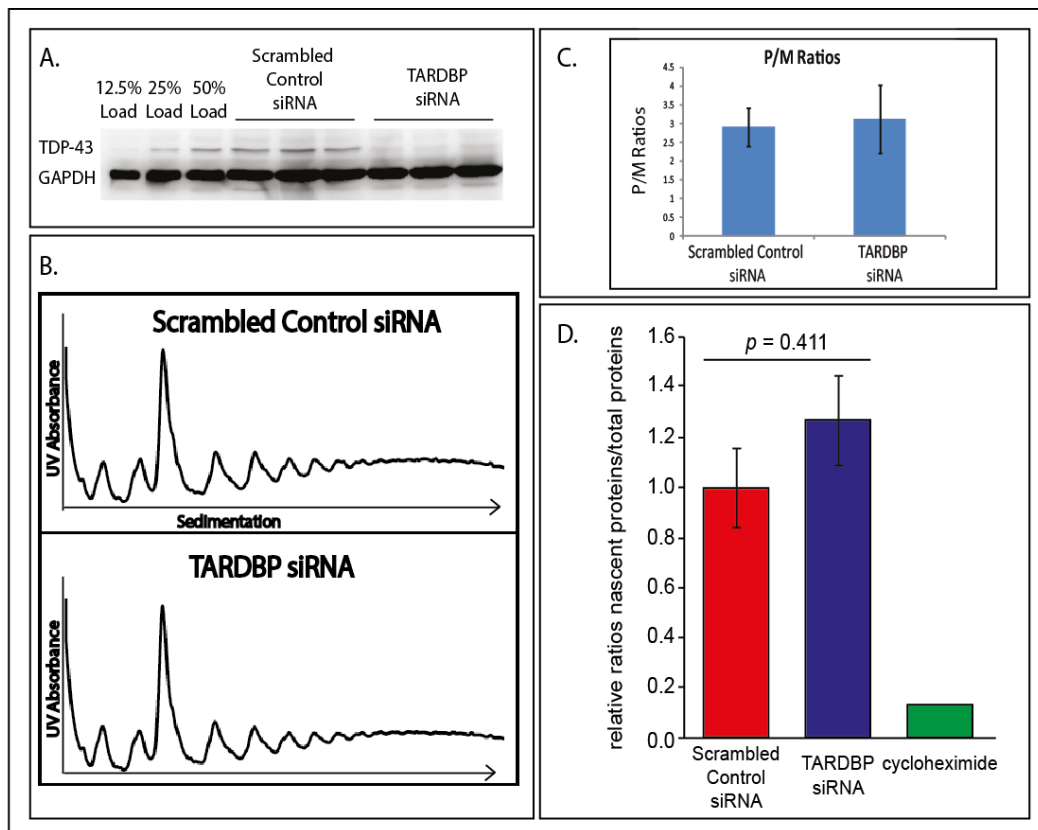


Figure 3.4 Knockdown of TDP-43 does not affect general translation in MN1 cells

A. Knockdown of TDP-43 in all three individual samples used for polysome profiling showed reduction of TDP-43 by more than 80%. Scrambled control siRNA showed no reduction of TDP-43. GAPDH was probed as a loading control. Additional loading controls are protein percentages of untreated MN1 cells lysate.

B. Representative polysome profiles for MN1 cells treated with either TARDBP or scrambled negative control siRNA. Profiles showed no obvious differences.

C. Polysome to monosome ratios calculated from the polysomes generated with knockdown using TARDBP or scrambled negative control siRNAs. No significant difference was found between these polysome to monosome ratios. (P-value scrambled control to TARDBP: $p=0.310$: one-tailed, type 3 t-test). Biological-replicate data ($n = 6$) are presented as mean \pm SEM.

D. Nascent protein synthesis was measured in MN1 cells treated with either TARDBP or scrambled negative control siRNAs, or treated with cycloheximide as a positive control for translation inhibition. No significant difference in nascent protein synthesis was found between the TDP-43 knockdown and the negative control cells (P-value scrambled control to TARDBP: $p=0.411$: one-tailed, type 3 t-test). Biological-triplicate data ($n = 3$) are presented as mean \pm SEM.

3.2 TRANSIENT EXPRESSION OF TDP-43 VARIANTS IN MN1 CELLS DOES NOT ALTER GLOBAL TRANSLATION

3.2.1 STABLE-INDUCIBLE “Flp-In T-REx” MN1 CELL LINE EXPRESSED TDP-43 VARIANTS AT VERY LOW LEVELS

Altered TDP-43 expression and localization are associated with ALS pathology, though how exactly this causes disease is not yet clear. Altered expression levels (Xu et al., 2010), protein localization (Barmada et al., 2010), or TDP-43 containing a patient mutation (Sreedharan et al., 2008) could all contribute to disease etiology. Thus, in addition to knockdown of TDP-43 in MN1 cells, we felt that it was very important to be able to easily, robustly, and consistently express TDP-43 variants in mammalian cells. For this purpose, we generated a stable-inducible MN1 cell line using the Flp-In T-Rex (Invitrogen) method. This complex and multi-step method would allow us to inducibly express different protein variants at similar levels from the same locus integration site (Fig 3.5).

The need to express TDP-43 variants at similar levels was very important in our consideration of methods, as it has been shown that reduction or over-expression of TDP-43 levels can cause disease-like responses in several different model systems (Fiesel et al., 2011; Xu et al., 2010). We hoped to circumvent the possibility that any changes we saw in translation after expression of TDP-43 variants were due to minor differences in protein expression levels. Since by using the Flp-In T-REx core kit all variants would be expressed from the same integration locus, the chance of achieving highly similar expression levels was greatly increased.

Having the ability to induce TDP-43 expression could be useful in two different ways. First of all, if expression levels were slightly different, it might enable us to regulate expression levels by altering the amount or timing of tetracycline added to the cells to induce expression. Secondly, having the ability to selectively induce TDP-43 would allow us to regulate the timing of TDP-43 expression. This could be an interesting factor to study with regards to stress events, but also would be very useful if overexpression of TDP-43 in certain cases proved to be toxic over an extended period of time.

We generated several TDP-43 variants to express in the MN1 cell line. Although MN1 cells are mouse cells, we wanted to express human TDP-43 (hTDP-43), since it is hTDP-43 that causes neurodegenerative diseases as we know them in humans. The constructs we created contained both a FLAG-tag at the N-terminus and a V5-tag at the C-terminus of the hTDP-43 protein in order to increase our chances of identifying the protein expression.

Both mouse and human TDP-43 are normally localized to the cell nucleus, and have the ability to shuttle to the cytoplasm under normal conditions. Interestingly, in disease-affected cells, TDP-43 shows a strong increase in cytoplasmic localization, and is sometimes completely cleared from the nucleus. We therefore generated in addition to wildtype FLAG-hTDP43-V5, a FLAG-hTDP43-V5 variant that also contained an extra nuclear export sequence (NES) at the C-terminus in order to target the protein preferentially to the cytoplasm. This would allow us to better understand whether TDP-43's localization in particular has an effect on disease progression.

Many different mutations have been identified in ALS and a few FTLN patients. This indicates that the mutations in TDP-43 may in some way be involved in the disease progression. We therefore generated a FLAG-hTDP43-V5 variant that contains the relatively frequently occurring TDP-43 mutation, A315T.

The Flp-In T-REx method for generating stable inducible cell lines is comprised of several steps of plasmid integration and antibiotic selection of resistant clones in order to generate the final cell line that genes of interest (GOIs) can be “flipped in” to (Fig 3.5; a more detailed description of this method can be found in section 2.4). The cell line must contain the following:

- 1) A single integration site under the SV40 promoter containing an FRT site that will allow GOIs to be “flipped in” at this site. This DNA sequence also expresses lacZ and has a Zeocin resistance gene.
- 2) A tetracycline repressor (TetR) gene under CMV promotion. This sequence also contains a blasticidin resistance gene.

The GOI is placed in a plasmid containing a further FRT site and is downstream of two tetracycline operator (TetO2) sites that can be bound by TetR, and the plasmid additionally contains a hygromycin resistance gene. By co-transfecting this plasmid along with a plasmid expressing the Flp recombinase, homologous recombination of the GOI into the FRT site

already established in the cell line will occur. This way, many different genes can be recombined into the same integration site, which helps to keep the amount of protein produced relatively comparable. It also reduces off-target effects, since no new genes will be interrupted due to GOI integration.

TetR is expressed under basal conditions of the cell line once it has been integrated. When TetR is expressed, it binds upstream of the GOI at the TetO2 sites under normal conditions, preventing transcription of that particular gene. In the event that tetracycline is added to the cells, the TetR binds preferentially to the tetracycline, which blocks the TetR from binding the TetO2 sites upstream of the GOI. This allows production of the GOI.

In order to generate our Flp-In T-REx cell line, we first transfected our MN1 cells with the pFRTlacZeo plasmid. This plasmid contains the FRT site that GOIs will be “flipped in” to at a later time point, as well as the genes for lacZ and for Zeocin resistance. We selected single clone colonies of MN1 cells that were resistant to Zeocin. We then checked for lacZ expression by staining with X-gal, and also quantitatively monitored β -galactosidase enzymatic activity using a luminescent substrate assay. Clones that showed blue X-gal staining and high levels of β -galactosidase activity in quantitative assays were then checked by Southern blot to look for single integration sites. Single integration sites are important for several reasons. First, when the GOI is integrated at a later step, it is important to know that all GOIs are integrated the same number of times. If one integrates only once, and another multiple times, this would partially defeat the regulation of how much protein is made. Second, the more integration sites, the higher the chance that an integration site might disrupt production of a gene necessary for cellular health. Finally, the TetR expression levels must be high enough to completely repress the expression of the GOI until addition of tetracycline. If there are multiples integration sites for the FRT site, it may be much more difficult for the TetR protein to efficiently turn off the GOI production.

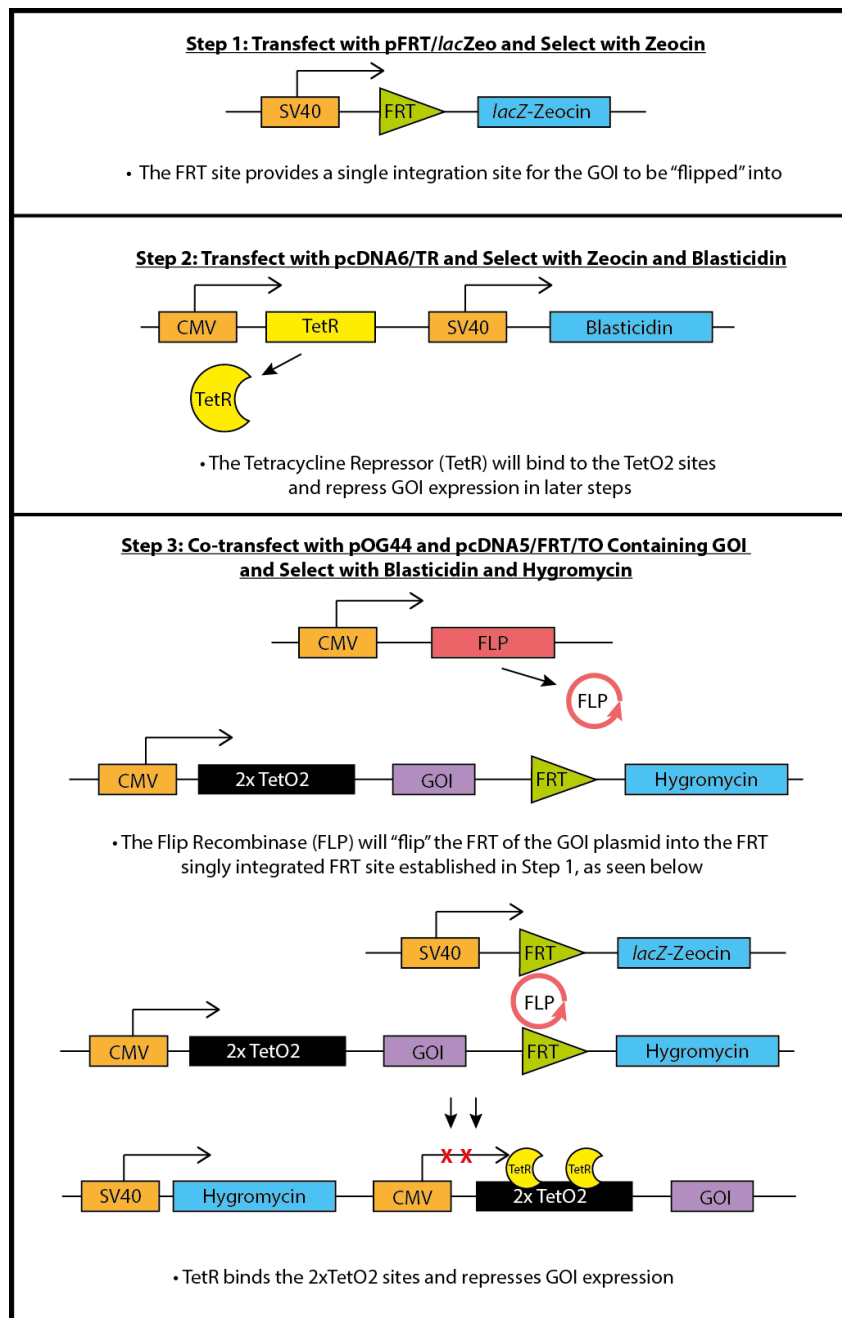


Figure 3.5 Flp-In T-REx Core Kit cell line generation overview

Step 1: Cells are transfected with the pFRT/lacZeo plasmid containing an FRT site and with a lacZ/Zeocin cassette. The FRT site allows the flip recombinase to insert genes of interest into the FRT site. Cells are selected for Zeocin resistance and tested for lacZ expression. Cells are additionally checked for single integration sites to ensure that only one FRT site is available to be “flipped into”. Step 2: Zeocin-resistant, single integrant clones are transfected with the pcDNA6/TR plasmid containing the tetracycline repressor gene and blasticidin resistance. Clones are selected for both Zeocin and blasticidin resistance. Step 3: Zeocin- and blasticidin-resistant clones from step 2 are co-transfected with the pOG44 plasmid, which expresses the flip recombinase, and pcDNA/FRT/TO plasmid that contains the gene of interest downstream of a tetracycline operon, and alongside an FRT site and hygromycin resistance. The Flip Recombinase will “flip” the gene of interest into the single FRT integration site. The TetR will bind to the TetO2 sites and repress transcription of the gene of interest until addition of tetracycline. Clones are selected for Hygromycin and blasticidin resistance.

Many of our clones showed both blue X-gal staining as well as high levels of β -galactosidase in a quantitative microplate-based assay (Fig 3.6 A,B). Southern blot analysis revealed several clones with apparent single integration sites, in particular clones 2, 12, and 17 (Fig 3. C). Since expression levels will be difficult to monitor until later steps, several clones were selected to be processed in parallel for the next steps.

After single integrant clones were identified and selected, these cells were next transfected with the pcDNA6/TR plasmid containing the TetR gene along with blasticidin resistance gene. Again, single clone colonies were selected for their blasticidin resistance, in addition to Zeocin resistance. From each of the single integrant clones, multiple blasticidin resistant clones were selected, in hopes that production of TetR protein in one of these clones would be at a high enough level to shut down GOI expression once the GOIs were “flipped in”.

After blasticidin selection, we needed to test the levels of protein production from the different clones. This was done by co-transfecting the FRT/TR cells with a pcDNA5/FRT/TO plasmid containing an FRT site with a luciferase gene and hygromycin resistance along with the pOG44 plasmid that expresses the flip recombinase protein. This co-transfection allows the flip recombinase to homologously recombine the luciferase gene into the FRT single integration site. Clones were selected for their hygromycin resistance, along with blasticidin resistance (Zeocin resistance has been removed at this step). After adding tetracycline to the clones, we measured the luciferase levels of these clones in order to select the best candidates to “flip” our GOIs into (Fig 3.6 D). Clones 17 and 2 expressed luciferase at the highest levels, and were therefore selected for future experiments.

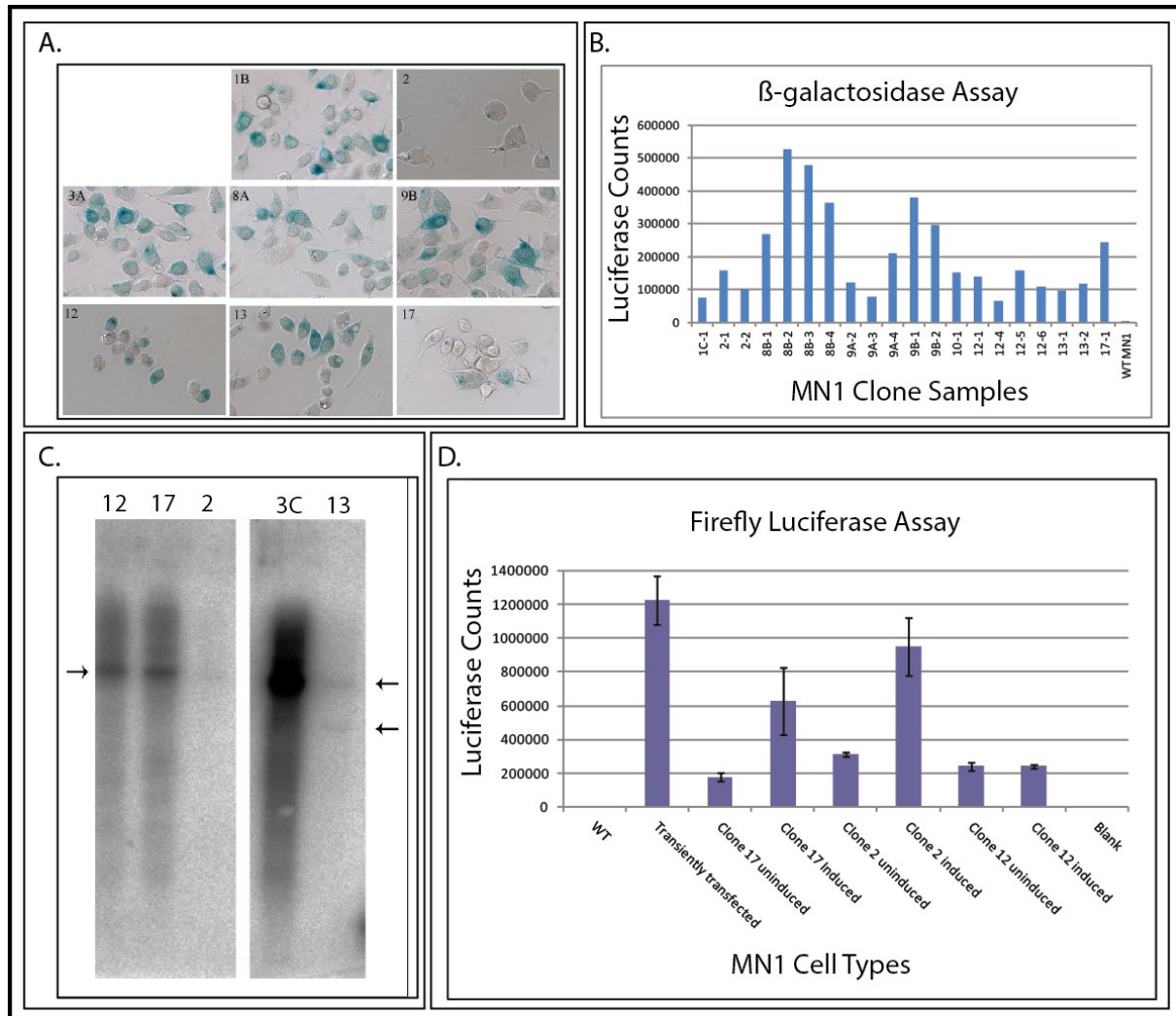


Figure 3.6 Clone selection and validation

A. Cells were stained using X-gal. Clones that express β -galactosidase will hydrolyze the X-gal, producing a blue compound. B. β -galactosidase activity can also be measured through a quantitative luciferase assay. Different clones produced varying levels of β -gal activity. No error bars were generated, as this was a singular experiment meant to give a rough idea of general expression levels. C. Southern blot assay to identify clones with single integration sites. Three clones (12,17,2) were identified as having a single band, indicating a single integration site. Other clones (3C, 13) had visibly multiple integration sites. D. Firefly luciferase was flipped in to the single integrant clones. A luciferase assay indicated that clone 17 and clone 2 showed a marked increase in protein expression when induced. Clone 12, however, did not show an increase in expression. WT MN1 cells were used as a negative control, and MN1 cells transiently transfected with luciferase were used as a positive control. Biological-triplicate data ($n = 3$) are presented as mean \pm SEM.

We flipped in several GOIs in parallel to these clones and selected single clone colonies that were resistant to hygromycin and blasticidin (Fig 3.7 A-C). When probed by western blot using a V5 antibody, it was clear that several of these clones clearly expressed the GOIs at a detectable level (Fig 3.7 D). Some clones appeared to express GOIs without the addition of

tetracycline, indicating that perhaps integration of TetR plasmid was not successful, or is expressed at much too low a level to reliably shut off the expression of the GOI.

Unfortunately, when we assayed the same clones that showed increased V5 expression level by immunoblotting with several different TDP-43 antibodies, the levels of integrated TDP-43 were not high enough to be detected by western blot analysis (Fig 3.7 D). The only band that was visible in these western blots was the endogenous TDP-43 band. Both the endogenous and the exogenously expressed TDP-43 should be visible, due to the addition of the FLAG- and V5-tag (an example can be seen from cells transiently transfected with the same plasmids that were “flipped in” in Fig 3.8 C). This indicates that the “flipped in” TDP-43 variants, while expressing at low levels, do not come close to reaching the expression levels of endogenous TDP-43. Because of the significantly higher expression level of endogenous TDP-43, we believe that it is likely that we would not be able to detect any translational regulation effects produced by expression of these protein variants.

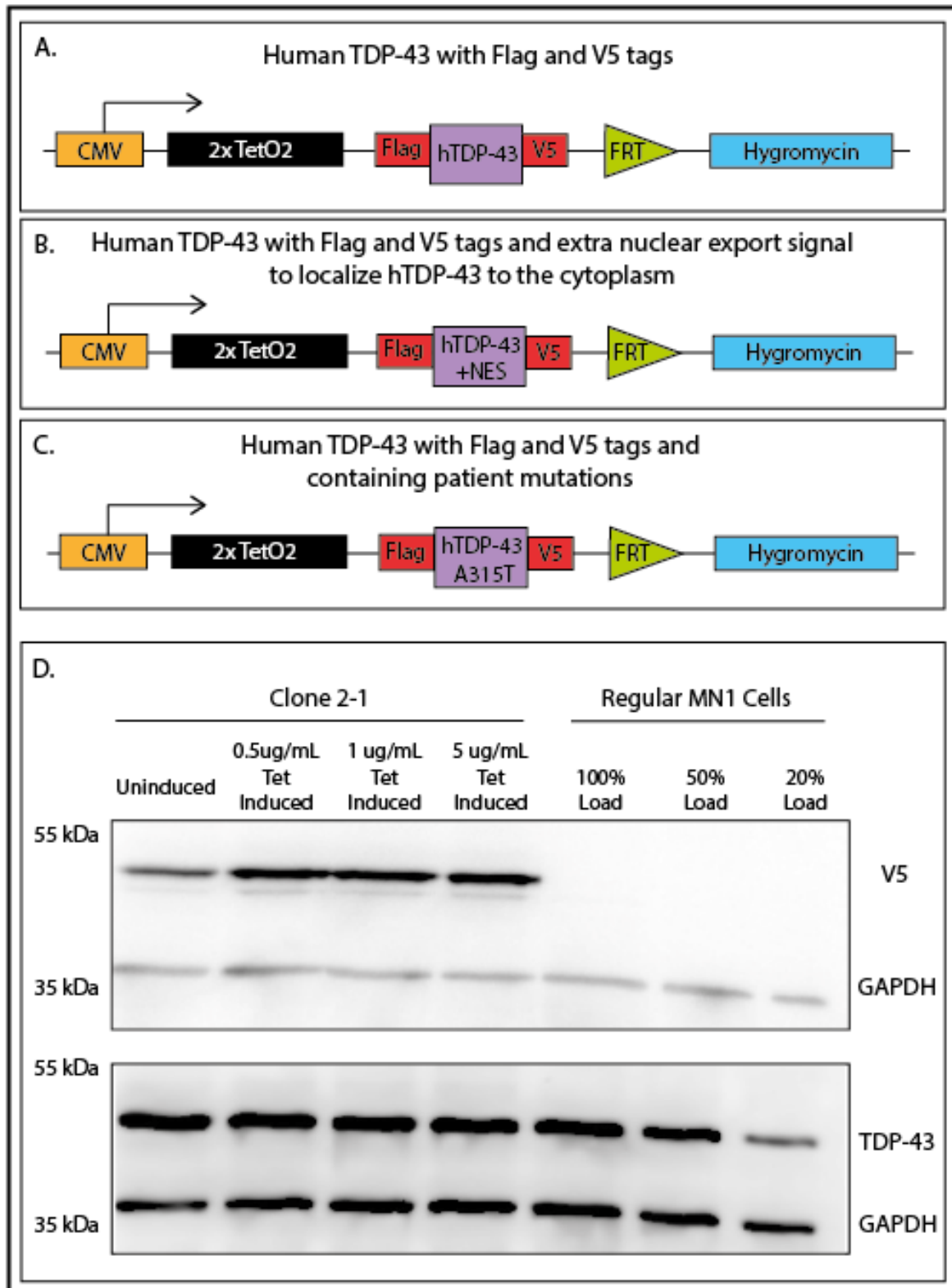


Figure 3.7 Induced expression levels of TDP-43 variants are low

A-C. Schematic of sequences “flipped in” to the single integrant FRT site clones. Sequences were cloned to include either hTDP-43 with a FLAG- and V5-tag (A), FLAG-hTDP43-V5 with an extra NES to target it to the cytoplasm (B), or FLAG-hTDP43-V5 with the A315T patient mutation (C). D. Induction of TDP-43 expression using different concentrations of tetracycline showed a clear induction when probed for V5. However, when probing using TDP-43 antibody, only the endogenous TDP-43 band was visible.

In normal MN1 cells, we checked if the low expression level of TDP-43 was due to a problem with the plasmids, and whether TDP-43 could be produced when transiently transfected into MN1 cells. The transiently transfected MN1 cells were able to produce the protein to a much higher level than the induced cell lines did, to a level quite similar to endogenous TDP-43 levels (Fig 3.8 C). There could be a number of reasons for this; in fact, the Flp-In T-REx manual itself suggests that 3T3 cells and BHK cells both show down-regulation of protein production and loss of gene expression, indicating that some cell lines do not respond well to this protocol. It is very well possible that MN1 cells fall into that category. Conversely, it might be that we did not manage to select clones that had the initial FRT integration at sites that are conducive to high protein level production. In either case, it is clear while the method for generating Flp-In T-REx MN1 cells worked in our hands, the product generated was not useful for the purposes of our future experiments due to the low expression levels of TDP-43 protein.

Since the stable cell line method worked, but not in the correct way for our purposes, we decided to move forward with our experiments using transiently transfected cells.

3.2.2 GENERAL TRANSLATION IS NOT ALTERED IN MN1 CELLS TRANSIENTLY TRANSFECTED WITH TDP-43 VARIANTS

In order to check our TDP-43 variants in MN1 cells, we first needed to show that transient transfection of these cells resulted in a robust expression at very similar levels across the different variants. We transiently transfected the cells with FLAG-hTDP43-V5, FLAG-hTDP43-NES-V5 and FLAG-A315T-hTDP43-V5. We probed for TDP-43 by western blot analysis. In this case, we were able to see a strong production of all three TDP-43 species, near the level of endogenous TDP-43 production (Fig 3.8 C). Importantly, all three exogenous TDP-43 variants were expressed at very similar levels. This suggests that this method of transient transfection could enable systematic comparison of TDP-43 variants.

Having established that our transient transfection method was working robustly, we next checked whether MN1 cells transiently transfected with hTDP-43, hTDP-43-NES, or hTDP-43-A315T showed altered general translation. We did this using the same polysome profiling method used to check for general translation in the TDP-43 knockdown MN1 cells (see

section 3.1.4) – by running polysome profiles and calculating P/M ratios. Similar to our MN1 cells with TDP-43 depletion by RNAi, we did not see any alterations in general translation when comparing MN1 cells transiently transfected with hTDP-43, hTDP-43 with an extra NES, or hTDP-43 with the A315T patient mutation (Fig 3.8 A). Additionally, when we calculated P/M ratios, it was clear that there was no change between the different transfections (Fig 3.8 B; see Materials and Methods 2.10 for a description of P/M ratio calculation).

Taken together with our TDP-43 knockdown results, these results strongly indicate that in MN1 cells, there is no detectable effect of TDP-43 on general translation under standard growth conditions. However, these results do not preclude an effect of TDP-43 on translation of a specific subset of mRNAs. We therefore concentrated our future efforts on this possibility.

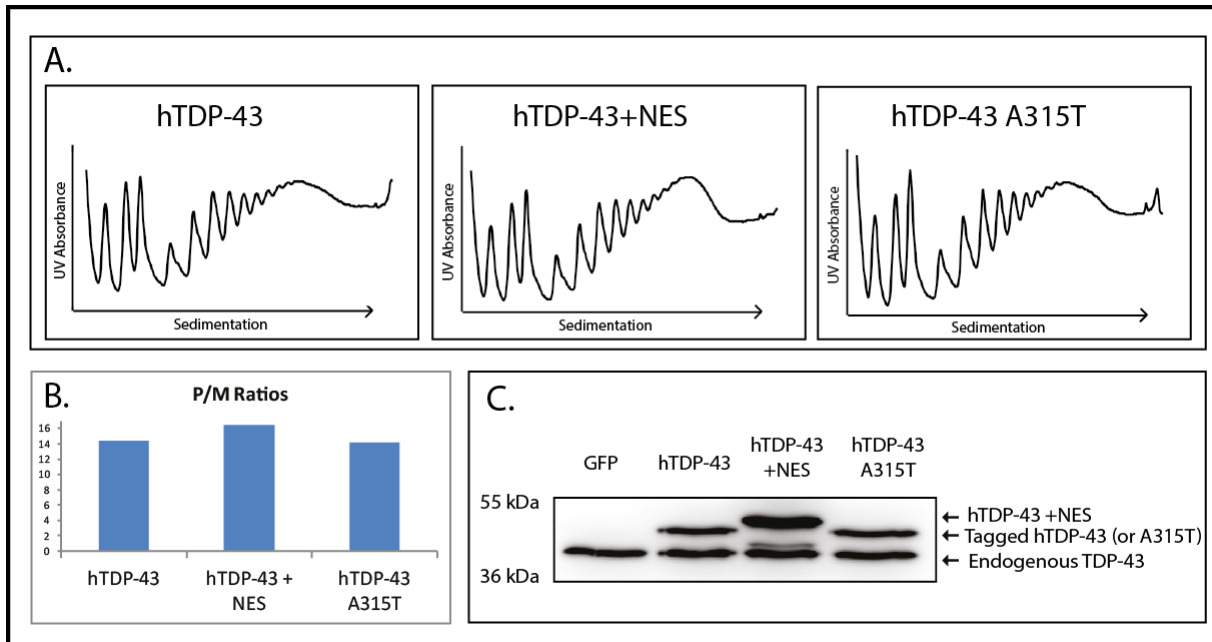


Figure 3.8 No general translational alterations after transfection with hTDP-43 variants

A. Polysome profiles generated from MN1 cells transiently transfected with hTDP-43, hTDP-43-NES or hTDP-43-A315T. The polysome profiles look strikingly similar. Repeat profiles were not run, as results looked similar to TDP-43 knockdown. B. Calculation of polysome to monosome ratios revealed minimal differences between the P/M ratios of each graph. (n=1) C. Expression levels of hTDP-43 variants are highly similar, as seen when probed by western blot with TDP-43 antibody. Since endogenous TDP-43 is also visible in these blots, it is possible to identify whether exogenously expressed TDP-43 regulates endogenous TDP-43 protein expression levels.

3.3 TRANSLATIONAL EFFICIENCY OF SELECTED CANDIDATE mRNAs WAS NOT AFFECTED BY TDP-43 KNOCKDOWN

No general translational changes were seen either after knockdown of TDP-43 or exogenous expression of hTDP-43 variants in MN1 cells. This might be because TDP-43 does not have a general translational effect, but rather an effect only on a small subset – perhaps only one or two – mRNAs. To address this possibility, we selected a set of candidate mRNAs to check whether they displayed altered localization within polysome fractions.

If translation is up- or down-regulated without any changes in the amount of mRNA entering translation, it therefore follows that the changes in translation must occur at the level of the number of ribosomes translating the same amount of mRNA. For example, if an mRNA is normally translated by two ribosomes, but cellular conditions shift it to being translated by 10 ribosomes, it is safe to say that translation has increased and more protein will be produced without a change in the amount of starting mRNA material. Conversely, if an mRNA starts out being translated by 10 ribosomes, and is shifted to being translated by two ribosomes, translation is reduced.

This shift in translation can be visualized in many different ways. One could look globally to see shifts in translation of many different mRNAs at the same time. However, it is also possible to easily look for shifts in translation of specific mRNAs by quantifying the concentration of these mRNAs in polysome fractions under different conditions.

We selected a subset of mRNAs that we thought might be translationally regulated under altered TDP-43 conditions. These mRNAs were selected from a list of mRNAs bound by TDP-43 that was generated using the HITS-CLIP (high throughput sequencing crosslinked immunoprecipitation) method (Polymenidou et al., 2011; Tollervey et al., 2011). The laboratories that produced this list found that TDP-43 binds to approximately 30% of the mouse transcriptome. Interestingly, several of the cytoplasmically localized TDP-43-bound mRNAs were enriched for TDP-43 binding sites in their 3' UTRs. This is of particular interest, as proteins that bind at the 3' UTRs of mRNAs have been previously shown to frequently act as translational regulators. Of these mRNAs that are bound by TDP-43 in their

3'UTRs, several are associated with TDP-43 proteinopathies in other ways. The mRNAs that we selected are:

- 1) TAR DNA Binding Protein 43 (TARDBP) – TDP-43's mRNA was found to contain 5 binding sites for TDP-43 in the 3' UTR. This suggests that TDP-43 could be involved in auto-regulating translation of its own mRNA. This could explain why TDP-43 expression levels are so important. TDP-43 is involved in many neurodegenerative diseases, so altered self-regulation would be of major interest.
- 2) Fused in Sarcoma/Translocated in Sarcoma (FUS/TLS) – FUS is the second major RBP found in ALS and FTLN aggregates. There is no overlap between TDP-43 and FUS in aggregates. One TDP-43 binding site was identified in the FUS mRNA 3'UTR.
- 3) Progranulin (Grn) – Grn mutations have been identified in FTLN patients. One TDP-43 binding site was identified in the progranulin 3'UTR.
- 4) Neurofilament light chain (Nefl) – Nefl has been shown to be involved in ALS pathogenesis. One TDP-43 binding site was identified in the Nefl 3'UTR 1.
- 5) Ionotropic glutamate receptor, AMPA 2 (Gria2) – Gria2 is of interest as it is involved in neuronal signal processing. With three TDP-43 binding sites in its 3'UTR, it is also the mRNA on our list with the highest number of 3'UTR binding sites after TARDBP.

Real-time PCR primers for each of these mRNAs were selected from the Harvard PrimerBank. RNA was isolated from fractions across polysome profiles generated from MN1 cells either treated with TARDBP siRNA or with scrambled negative control siRNA (Fig 3.9 A). Real-time PCR was then run in triplicate for each fraction for each of these genes to control for pipetting error and normalized to luciferase spike in controls.

The real-time PCR for TARDBP showed a definite shift in the localization of TARDBP mRNA in fractions from heavy fractions to light fractions, consistent with an average decrease in the number of ribosomes associated with this mRNA after knockdown (Fig 3.9 B). However, since TARDBP mRNA itself was being knocked down in these cells, the simplest explanation for this shift is that it reflects TARDBP being cleaved by DICER. This should result in an increase in the level of shorter mRNA decay intermediates that would no longer

be ribosome engaged or can only be translated by a reduced number of ribosomes due to the decreased mRNA length. In other words, this shift could reflect the effects of RNAi itself, rather than altered auto-regulation of translation by TDP-43. Alternatively, it may be that the reduced amount of TDP-43 protein indeed leads to a specifically altered translational state of intact TARDBP mRNA, but this would need to be verified using other methods.

Real-time PCR for FUS/TLS, Grn, Nefl, and Gria2 did not show any shifts in polysome association when comparing TARDBP knockdown cells to negative control cells (Fig 3.9 C-F). This is perhaps not surprising, as there are a large number of mRNAs that TDP-43 could potentially be regulating. If it is indeed regulating only one or two, or a small subset of mRNAs, it may be difficult to identify which of these mRNAs are regulated by a candidate approach, and we would therefore need to move forward with the search for genes regulated by TDP-43 in a larger, genome-wide approach.

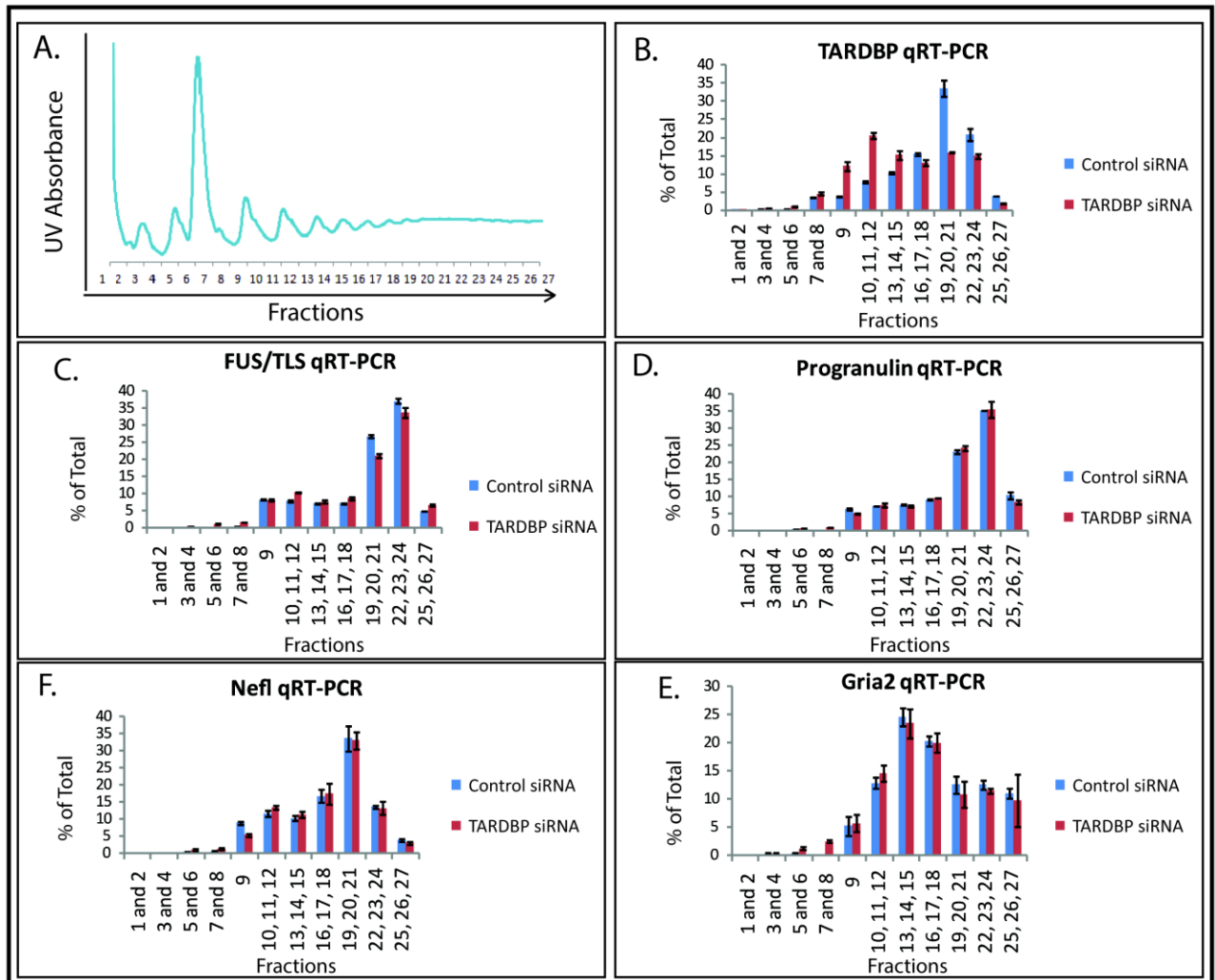


Figure 3.9 No altered polysome association found for candidate gene set

A. Polysome profiles were generated from MN1 cells that were treated with either TARDBP or scrambled negative control siRNA. RNA was isolated from each fraction, and real-time PCR was run using candidate gene primers in each fraction to see the distribution of the mRNAs. B. After treatment with TARDBP siRNA, TARDBP's distribution pattern shifted from heavy polysomes to lighter fractions. C-F. The other four candidate genes that were tested (FUS/TLS, Grn, Nefl, Gria2) showed no change in fraction distribution. Experimental-triplicate data ($n = 3$) are presented as mean \pm SEM.

3.4 TDP-43 IS ASSOCIATED WITH RIBOSOMES AND POLYSOMES

3.4.1 TRANSIENTLY TRANSFECTED TDP-43 PROTEIN ASSOCIATES WITH POLYSOMES

Proteins that regulate translation can do so through many different mechanisms (For a review, see Gebauer & Hentze, 2004). For example, translation can be regulated if a protein prevents the translational machinery from performing its normal function or if it increases the translational machinery's ability to function. Proteins involved in translation can also bring mRNAs to the translational machinery so that the mRNAs can be translated, or they can prevent mRNAs from being translated. Frequently, proteins involved in translational regulation are associated, either directly or indirectly, with the polysomes. If TDP-43 is involved in translation, it is possible that it would be found associated with the translational machinery.

In order to assess whether TDP-43 is associated with polysomes, we ran polysome profiles using lysate from MN1 cells transiently transfected with FLAG-hTDP-43-V5-tag (Fig 3.10). The protein found in each fraction of the polysomes was isolated via TCA precipitation, and western blot analysis was performed. Since the level of protein isolated from each fraction was quite low, detection of TDP-43 protein was contingent on having a very sensitive antibody. We therefore probed for TDP-43 using a commercially available V5 antibody, as previous experience indicated that this antibody is extremely sensitive for protein detection in western blots. We also probed for the large ribosomal subunit protein L7a, which allowed us to verify the distribution of the large subunit of the ribosome across the gradient. Very importantly, and of high interest, we found TDP43-V5 signal in all of the polysome fractions, strongly suggesting that TDP-43 associates with polysomes (Fig 3.11). This strongly suggests that TDP-43 may have a function in translational regulation. This association is particularly interesting, since TDP-43 has only previously been shown to associate with polysomes after the addition of sodium arsenite, an oxidative stress inducer (Higashi et al., 2013). This is the first time that TDP-43 has been shown to associate with polysomes independent of that type of stress induction.

In order to assess whether TDP-43 is associated with polysomes or if it is merely co-migrating with polysomes due to association with some other large cellular complex, we ran control polysome profiles where the lysate was treated with EDTA (Fig 3.10). EDTA dissociates polysomes by chelating magnesium, which alters RNA tertiary structures and dissociates ribosomes into their subunits. If TDP-43 is in fact associated with the translational machinery, TDP-43 should also shift to the lighter sucrose density fractions along with the dissociated subunits. After isolating the protein, and probing by western blot, we were able to see that V5-tagged TDP-43 shifted to the same fractions of the 40S and 60S peaks of the polysome (Fig 3.11). L7a also shifted to the lighter fractions, suggesting that the ribosome was indeed dissociated.

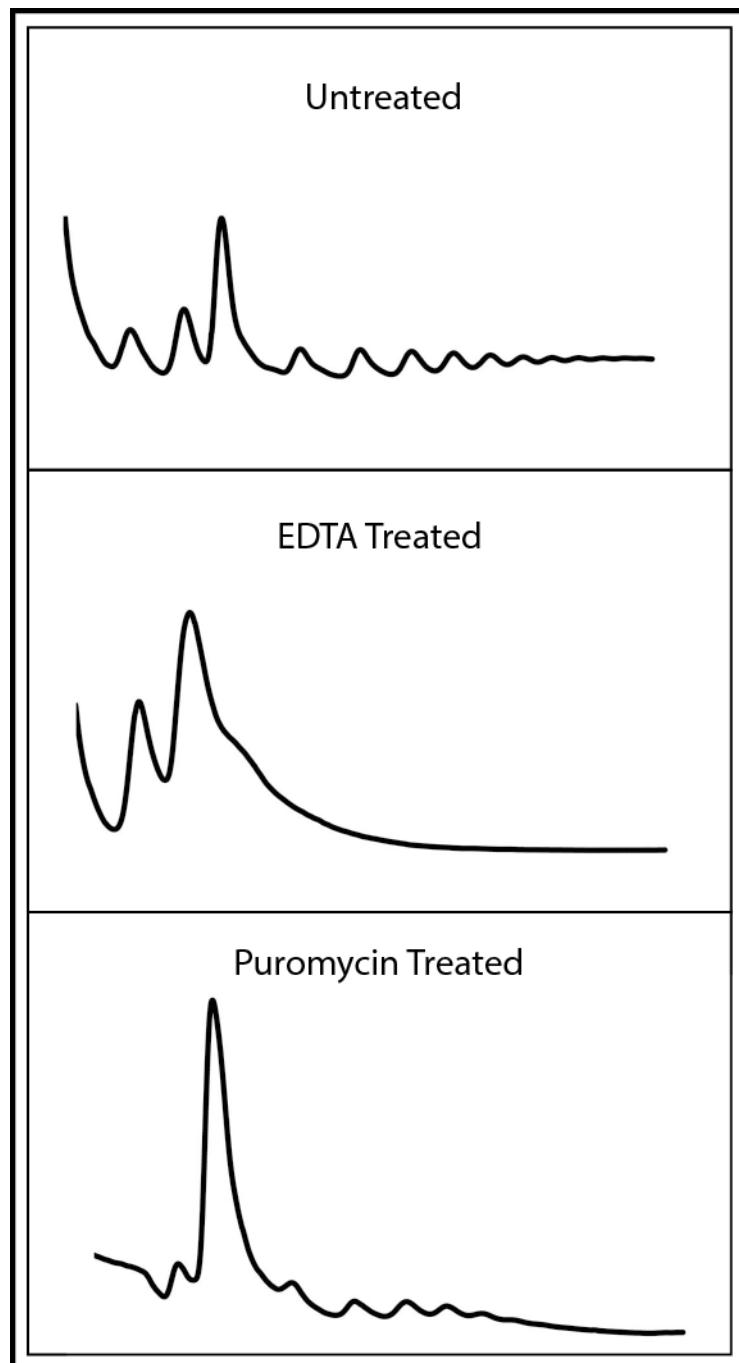


Figure 3.10 Polysome profiles are altered as expected after EDTA or Puromycin treatment

Polysome profiles were generated to check TDP-43's association with polysome fractions. EDTA should dissociate ribosomes into their subunits, which it does, as seen by the two lone peaks in the light fractions of the polysomes. Puromycin is a translation inhibitor, which acts on ribosomes to promote dissociation. As expected, puromycin also reduces the polysome fractions.

Since cation chelators such as EDTA can affect many different cellular processes, we also checked whether a more specific translation inhibition could show a similar effect. We did this by treating the MN1 cells with a low level dosage of a translation inhibitor, puromycin.

Puromycin inhibits translation by entering the A site of the ribosome, binding to the elongating polypeptide chain, and causing premature release (Blobel & Sabatini, 1971). Importantly for our purposes, puromycin is known to cause polysome dissociation, but does so by a much more specific mechanism than EDTA. Thus, we would expect that by adding puromycin to the MN1 cells before processing, we would see a decrease in translation, as evidenced by reduced polysome peaks. If TDP-43 is in polysomal fractions due to association with ribosomal complexes, we should observe a corresponding shift of V5-tagged TDP-43 to the lighter fractions, as well. After running the polysome profiles, we saw that while the polysomes were not completely dissociated after puromycin treatment, they did show a strong reduction (Fig 3.10). Additionally, when we probed the isolated protein using V5 antibody, we saw a definite shift of TDP-43 from the heavy fractions to the lighter fractions (Fig 3.11), supporting a specific association with translating ribosomes. Similarly, L7a protein was moderately shifted to the lighter fractions in a manner such that would be expected for partially dissociated polysomes.

It is important to note that the first few fractions of any polysome profile are usually made up of free mRNA and protein. In other words, these proteins or mRNAs are not associated with the ribosomal subunits or translating ribosomes. This explains why there is a strong band for TDP43-V5 in the lighter fractions (as TDP-43 is often localized in the nucleus) while there is nearly no L7a band found in the light fractions, since most L7a would be associated with the large ribosomal subunit, 80S, or polysomes.

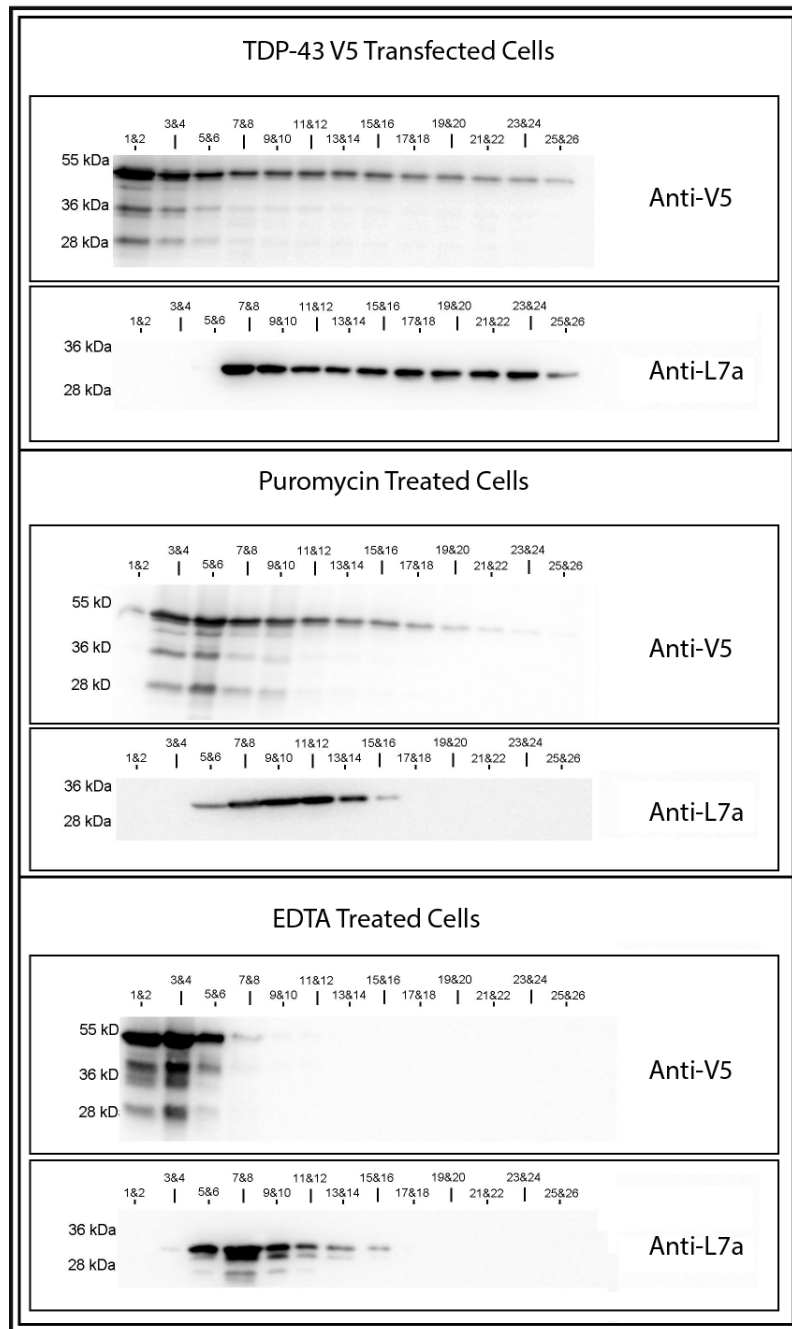


Figure 3.11 Western blots generated from polysome profiles show that TDP-43 shifts with the ribosome
 Protein was isolated from the fractions of the polysome profiles and probed by western blot for TDP-43 using a V5 antibody, and for ribosomes using the large ribosomal protein L7a antibody. Under normal conditions, TDP-43 is found in all fractions, including the polysome fractions, whereas when EDTA dissociates the ribosomes, TDP-43 is only found in the very lightest fractions. When puromycin, a translation inhibitor that causes ribosomal subunit dissociation from mRNAs, is used to treat the cells, TDP-43 shows an intermediate distribution, similar to the alteration in L7a. This provides further support for the idea that some portion of TDP-43 is associated with ribosome-mRNA complexes in the polysome fractions. Western blot lane labels (e.g. 1&2) indicate the combined polysome fractions that protein was isolated from. Smaller numbers indicate lighter fractions.

The amount of TDP-43 in each fraction was quantified using ImageJ to assess the intensity of the V5 bands (See Materials and Methods 2.11), and were normalized to the total intensity of V5 protein present in each western (Fig 3.12). These quantities were plotted to emphasize the quantifiable shift of TDP-43 protein from associating with all fractions – heavy fractions in particular – under normal conditions to associating with the lighter fractions in conditions that disrupt polysomes and cause the ribosomal subunits to shift to lighter fractions, such as puromycin and EDTA treatment. Only the major band (~47 kDa) was measured. The lower bands are likely C-terminal fragments, as many sizes of C-terminal fragments can at times be identified when probing for TDP-43 (Arai et al., 2006; Neumann et al., 2006). Taken together, these graphs along with the raw polysome profile data indicate that TDP-43 is associated with actively translating polysomes.

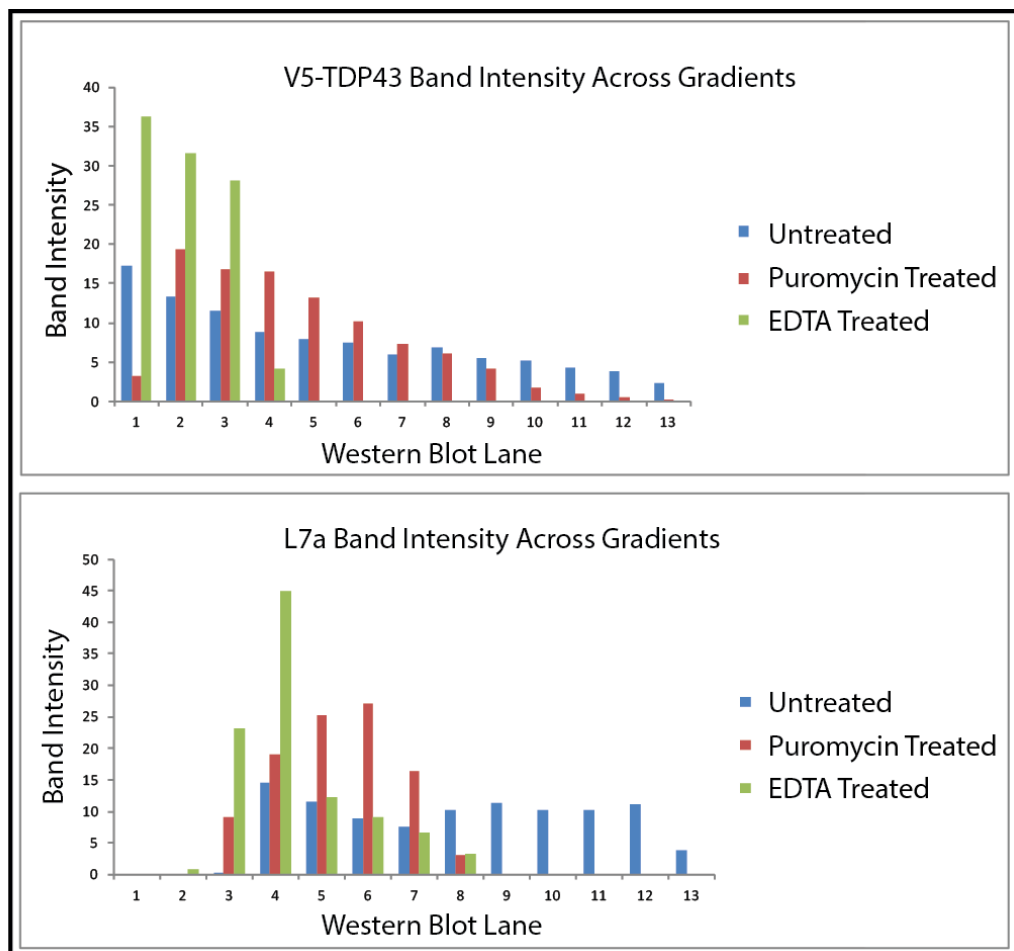


Figure 3.12 Quantification of TDP-43 and L7a distribution across the gradients

Both the V5 and the L7a band intensities shifted toward the lighter fractions after addition of Puromycin, and shift more dramatically due to the addition of EDTA. This quantification helps to illustrate that TDP-43 in the polysomal fractions shifts in a manner largely similar to the ribosomal protein L7a under multiple different treatment paradigms (see Materials and Methods 2.11).

3.4.2 GFP-TAGGED RIBOSOMAL PROTEIN L10a EXPRESSED IN MOUSE ChAT-POSITIVE NEURONS IS INCORPORATED INTO RIBOSOMES

There are many possible ways to look for translational changes occurring after TDP-43 expression has been altered. While it is possible to view these types of changes by probing a cDNA library generated from the fractions of polysome profiles, we chose two additional, complex but highly informative experimental techniques to explore genome-wide possibilities. One is the BacTRAP method, described below, and the other is the ribosomal footprinting technique, which is described in detail in section 3.5.

BacTRAP, or bacterial chromosome translating ribosome affinity purification, makes use of the fact that ribosomes are attached to the mRNAs that they are translating (Heiman et al., 2008). By immunoprecipitating ribosomes out of cell or tissue lysate, any mRNA that is also purified was probably bound by the ribosome, and is therefore likely to have been in the process of being translated. Rather than purifying all ribosomes from all cell types, the BacTRAP method allows for spatial and temporal specificity by expressing a GFP-tagged large ribosomal subunit protein L10a (GFP-L10a) under cell-type specific promoters. Because of this, it is possible to purify only the GFP-tagged ribosomes and their associated mRNAs from the specific cell types that express GFP-L10a (Fig 3.13; for a more in depth methodology, see section 2.15).

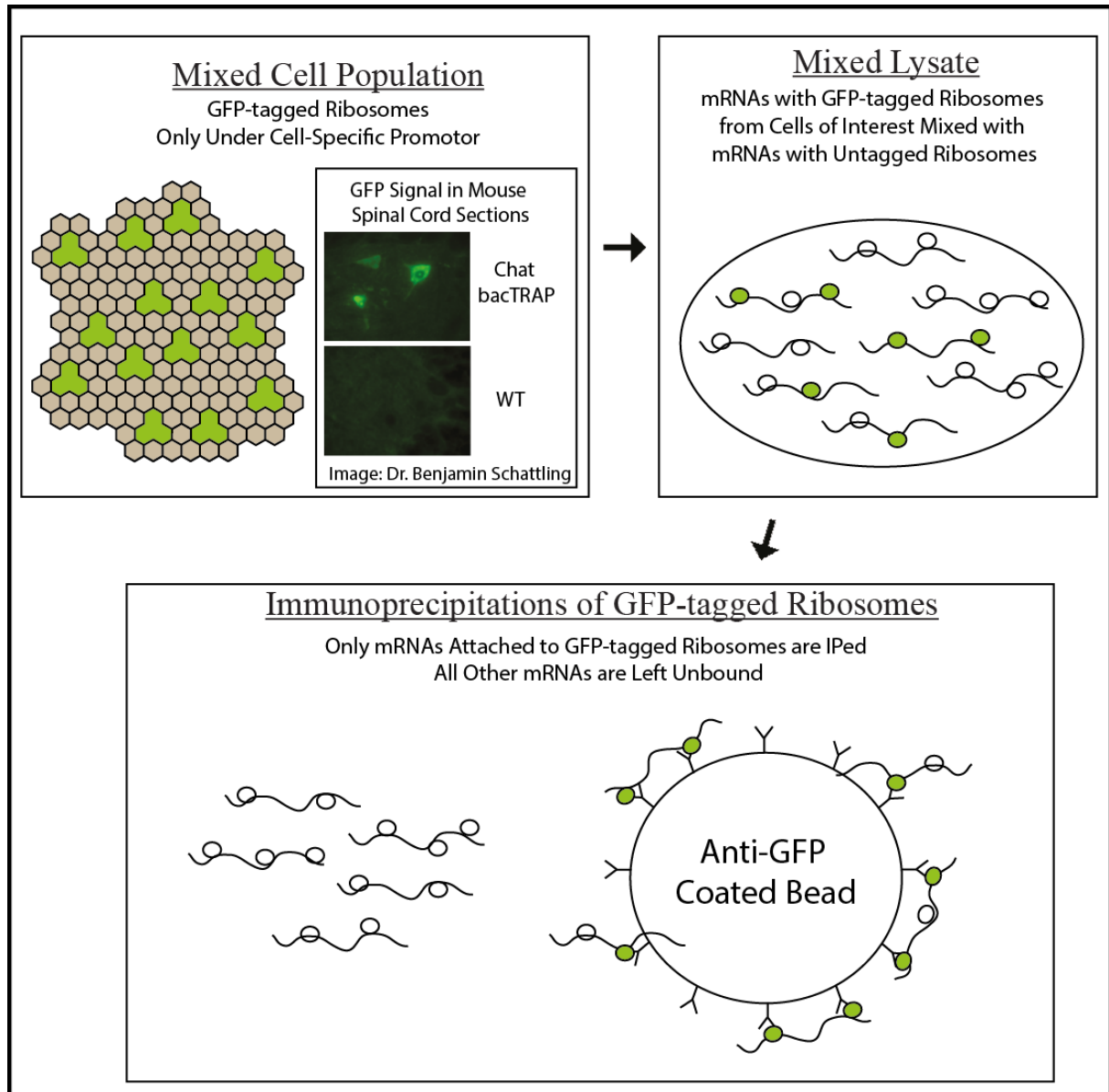


Figure 3.13 Overview of the BacTRAP method

GFP-tagged ribosomal protein L10a is expressed under a cell-specific promoter, in this case ChAT, which produces GFP-L10a in a subset of cells in the mouse nervous system. When tissue lysate is created, many different cells are mixed together, with both GFP-L10a-containing ribosomes and regular ribosomes in the mix. After immunoprecipitation using an anti-GFP antibody, only the GFP-L10a-containing ribosomes and their associated mRNAs will be purified, leaving any ribosomes/mRNAs from other cell types in the runoff. This allows purification of mRNAs bound by ribosomes from a specific cell type in vivo.

We are particularly interested in translational regulation that occurs in motor neurons, as they are the major cell type affected in ALS. We therefore performed all following mouse experiments using BacTRAP mice expressing GFP-L10a under the choline acetyltransferase (ChAT) promoter. These mice were generated by the Heintz laboratory (Heiman et al., 2008), and kindly provided to us by Prof. Manuel Friese. ChAT is expressed largely in motor

neurons, and is therefore frequently used as an immunohistochemical marker of motor neurons.

Before attempting immunoprecipitation experiments, we wanted to confirm that GFP-L10a was indeed expressed in the tissue of interest. Dr. Benjamin Schattling and Constantin Volkmann in the Friese laboratory at ZMNH performed this experiment, and Fig 3.13 shows that in BacTRAP tissue, cells were GFP-positive, whereas WT mice did not have GFP-positive cells.

It was also important to identify whether the GFP-L10a protein expressed was actually incorporated into the functional ribosome. Because of the GFP-tag size, it is possible that the addition of the tag could prevent the expressed GFP-L10a protein from associating with the rest of the ribosome. In order to check whether GFP-L10a was incorporated into ribosomes capable of translation, we established a protocol to generate polysome profiles from mouse brainstems (For method, see section 2.9).

We first generated polysome profiles from ChAT BacTRAP mice and from WT control littermates, and then isolated the protein from the fractions across the gradients and probed using an anti-GFP antibody (Fig 3.14). As expected, there was a GFP band visible through the polysome fractions of the ChAT BacTRAP profile, and no band visible for the WT control littermate profile. L7a ribosomal protein staining was used as a positive control for the protein isolation from each fraction, and since both L7a and L10a are associated with the large ribosomal subunit, it would follow that their western blot expression patterns should look relatively similar for the ChAT BacTRAP polysomes, which they do. These experiments indicate that the ChAT BacTRAP mice express GFP-L10a under the correct promoter, and that the GFP-L10a produced in these mice is incorporated into translating ribosomes. This means that these mice are suitable for BacTRAP immunoprecipitation experiments.

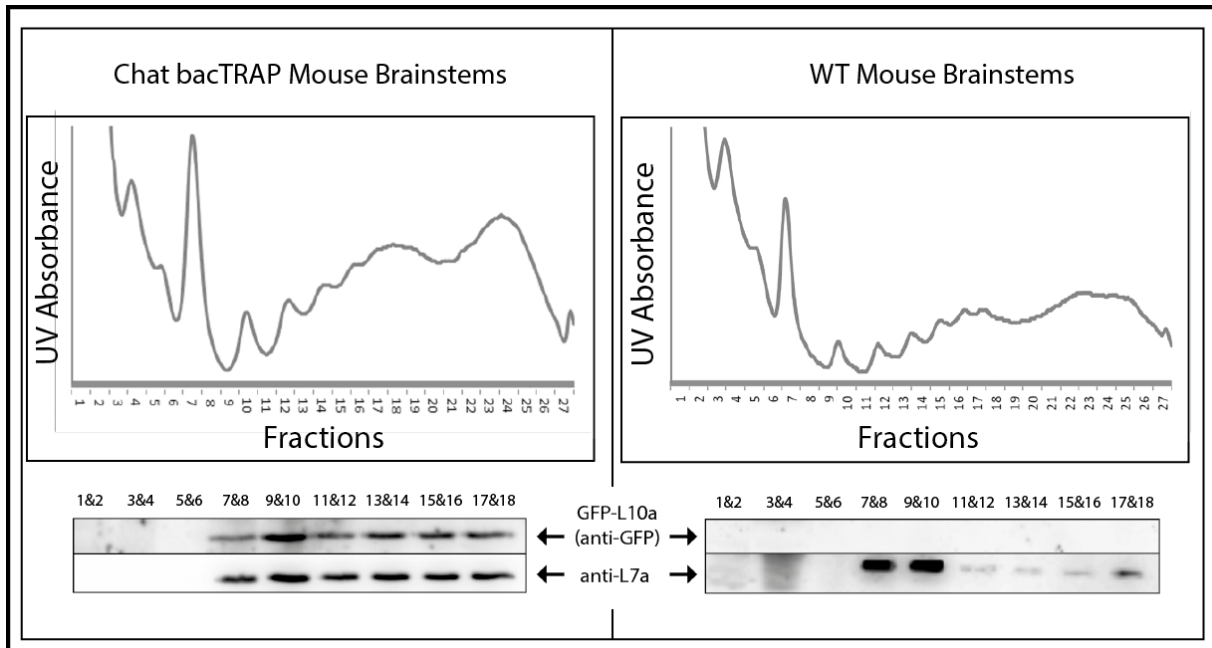


Figure 3.14 GFP-L10a is incorporated into the translating ribosome

Polysome profiles were generated from both ChAT BacTRAP and WT mouse brainstems. Protein was isolated from fractions, and probed by western blot for either GFP-L10a using an anti-GFP antibody or for L7a using an anti-L7a antibody. Western blot lane labeling (e.g. 1&2) corresponds to the polysome profile fractions that the protein was isolated from. L7a and GFP-L10a are both parts of the large ribosomal subunit, and therefore should have very similar distribution patterns across the gradient. Indeed, in the ChAT BacTRAP western blots, they have nearly identical distributions. No GFP band is visible, as expected, in the WT mouse western blots. While the L7a isolated from the fractions had a slightly different distribution across the polysomes in the WT mouse polysomes, its strong band intensity in fractions 7&8 and 9&10 with a corresponding lack of GFP indicates that no GFP-L10a is detected in the WT mouse brainstems, as expected.

3.4.3 IMMUNOPRECIPITATION OF GFP-TAGGED L10a FROM TRANSIENTLY TRANSFECTED MN1 CELLS IS HIGHLY EFFICIENT

Since we have established that the ChAT BacTRAP mice appropriately express GFP-L10a for immunoprecipitation experiments, we next wanted to set up the proper conditions to immunoprecipitate these ribosomes from mouse brainstems. As we were in contact with the originator of this method, we were able to procure an optimized method for both cellular and mouse brainstem immunoprecipitations from Prof. Myriam Heiman. This method was expanded upon for our specific needs. We decided to establish this method first by transiently transfecting the expression plasmid for the GFP-L10a protein into our MN1 cells. The reasons behind using the MN1 cell line for this establishment rather than the mouse brainstem

directly were twofold: First, the MN1 cells express the plasmid at a higher level and more uniformly across the cells than the mouse line does (only a small percentage of cells in the mouse brainstem are ChAT-positive cells). This would allow us to better assess by multiple methods – including western blot, nanodrop, and real-time PCR – whether the immunoprecipitation was robustly functioning. Second, by performing this in cells, we avoid using additional mice during our experimental optimization process.

The immunoprecipitation of the transiently expressed GFP-L10a from MN1 cells was highly efficient, as can be seen in the western blot analysis (Fig 3.15 B). Cells transfected with either GFP alone or with an empty transient transfection were used as controls, and show no band for GFP-L10a immunoprecipitation, as expected.

In order to verify that the immunoprecipitation was precipitating RNA species as well, we purified RNA from our immunoprecipitated samples and checked by nanodrop for the RNA concentration (Fig 3.15 A). RNA was much enriched in the GFP-L10a transfected immunoprecipitation compared to GFP alone or empty transfection, indicating that there is RNA (presumably ribosomes) co-precipitating with the protein.

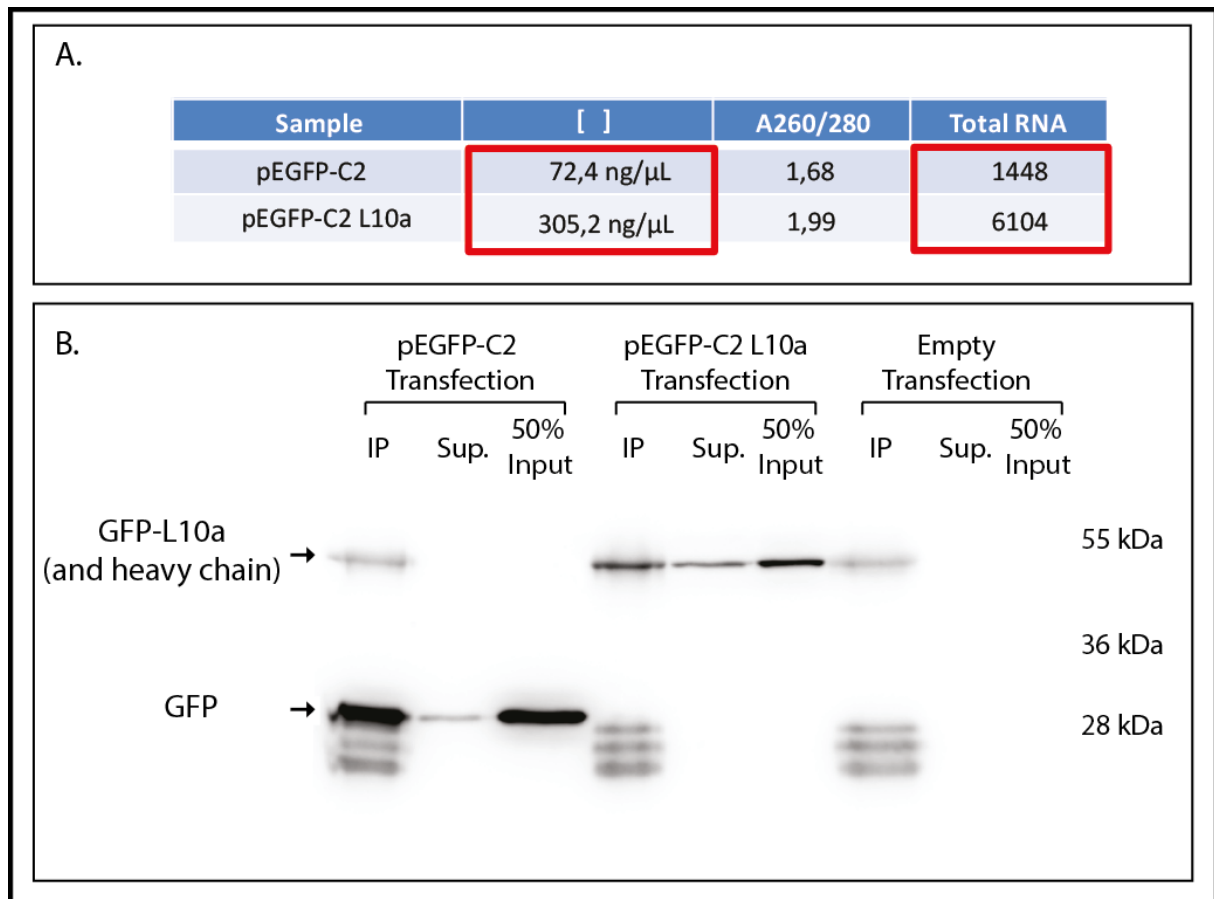


Figure 3.15 Functioning immunoprecipitation of GFP-tagged ribosomes from MN1 cells

A. RNA purification from immunoprecipitations from MN1 cells transiently transfected with either GFP alone (pEGFP-C2) or with GFP-L10a (pEGFP-C2 L10a) show that there is a large increase in the amount of RNA precipitated in the GFP-L10a samples. B. Western blot analysis shows that immunoprecipitation of GFP-L10a is specific and robust. Although the heavy chain IgG band is found at a similar weight as GFP-L10a, there is a clear band in the GFP-L10a IP, while no clear band is found in either the GFP IP or the empty transfection IP.

3.4.4 REAL-TIME PCR OF SELECTED SET OF GENES SHOWS CLEAN AND ROBUST IMMUNOPRECIPITATION FROM ChAT BacTRAP MOUSE BRAINSTEMS

Once we had established a robust method for immunoprecipitation of GFP-L10a along with associated RNAs, we performed this immunoprecipitation from ChAT BacTRAP mouse brainstems, using WT mouse brainstems as a negative control. When we optimized the polysome profiling method for mouse brainstems, we needed approximately 3-5 brainstems to clearly see the profiles. We assumed that this would be an ideal starting place to produce

enough material for the BacTRAP method as well, and to be able to identify specific mRNAs associated with ribosomes. Mice were sacrificed using a CO₂ chamber, decapitated, and quickly dissected in dissection media containing cycloheximide. This immediate addition of cycloheximide should help to chemically freeze the ribosomes on the mRNAs that they were translating in the cells prior to dissection and lysis. Dissected brainstems were incubated in trypsin containing cycloheximide at 37°C for 45 min before being crushed with a Dounce homogenizer in lysis buffer containing cycloheximide. This trypsinization and Dounce homogenization ensured that the brainstem was well dissociated and lysed prior to the immunoprecipitation.

GFP-tagged ribosomes were pulled down from brainstem lysate using a combination of GFP antibodies. RNA was then purified from the precipitation as well as from a percentage of the input lysate for normalization purposes. Although we know that GFP-L10a is expressed under the ChAT promoter, and is detectable in motor neurons by immunohistochemistry, we wanted to verify that our immunoprecipitation method pulled down only ribosomes and their bound mRNAs specifically from ChAT-positive neurons. Since immunoprecipitations can sometimes be nonspecific, this experiment could have resulted in contamination with RNAs from other cell types commonly found in the brainstem, such as astrocytes. To check this, we performed real-time PCR on a number of genes to assess the RNA quality of the immunoprecipitation as well as the cell specificity of the immunoprecipitation. These genes were:

- 1) Choline acetyl transferase – ChAT. We expected a large enrichment of ChAT mRNA in these immunoprecipitations, since the GFP-L10a gene is expressed under the ChAT promoter.

- 2) 18S and 28S ribosomal RNA – rRNA components of the small and large ribosomal subunits, respectively. Since we hope to be pulling down mostly intact ribosomes, we expect that both the small and large subunit should be represented in equal proportions. Therefore the rRNAs from each subunit should have been approximately equally detectable if the full ribosome was immunoprecipitated.

- 3) Potassium Channel – KCNN1 is a channel expressed ubiquitously in neurons, and since the GFP-L10a under the ChAT promoter is expressed in neuronal cell types, we expected to find this gene enriched in our immunoprecipitation targeting motor neurons.

4) Glial fibrillary acidic protein – GFAP is found in astrocytes and is frequently used as an immunohistochemical and real-time PCR marker for astrocytes. Since we are focused on immunoprecipitating ribosomes from ChAT-positive cell types, mainly motor neurons, GFAP mRNA should not have been present in our immunoprecipitation, as this would indicate that our immunoprecipitations were contaminated with astrocyte RNA.

Real-time PCRs were run for input and IP of both ChAT BacTRAP and WT mouse brainstem lysate. Prior to RNA isolation in all cases, *in vitro* transcribed luciferase RNA was spiked in for real-time PCR normalization purposes. Additionally, the respective input values were normalized to 1, and enrichment was shown as a comparative increase (Fig 3.16). We found a high enrichment – nearly 250x – of ChAT mRNA in the BacTRAP immunoprecipitation, as well as enrichment of KCNN1, 18S rRNA, and 28S rRNA. The 18S and 28S rRNAs were approximately equal in their enrichment, indicating that full ribosomes were likely being immunoprecipitated. Conversely, GFAP was not enriched at all in the immunoprecipitations, indicating that the immunoprecipitation was highly specific and was not contaminated with ribosomes or mRNA purified from other cell types, such as astrocytes.

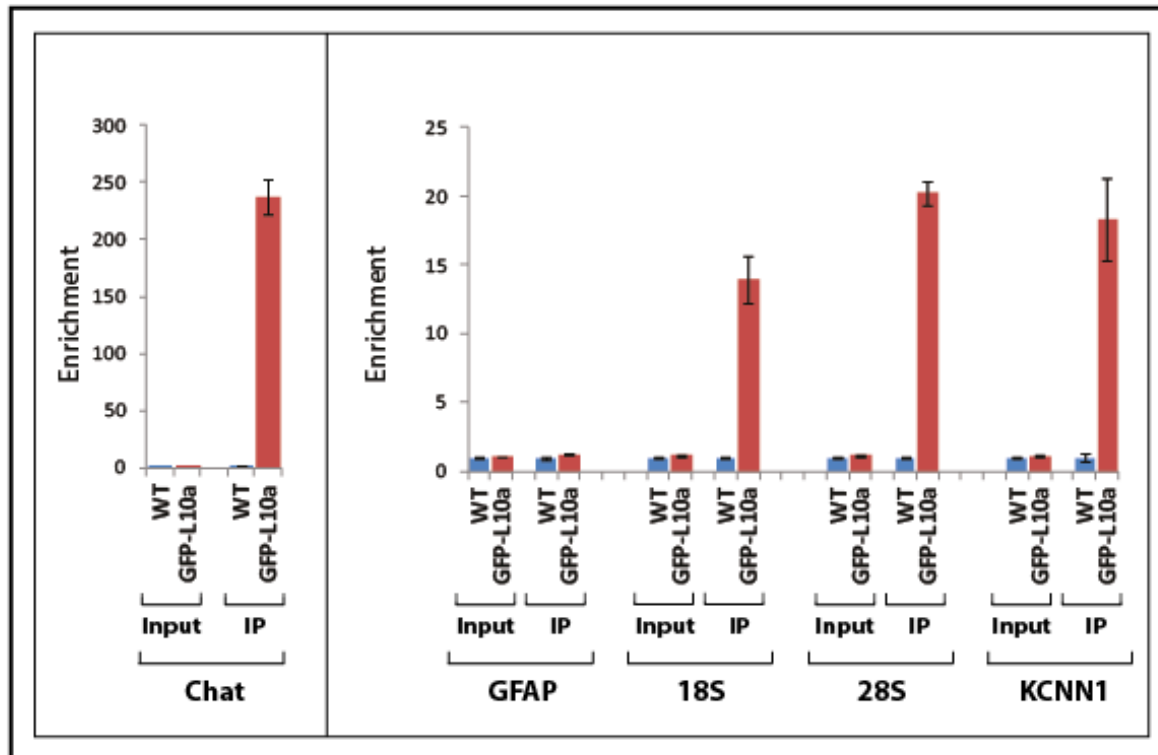


Figure 3.16 Expected mRNAs are enriched after BacTRAP immunoprecipitation

After immunoprecipitation from BacTRAP brainstems, real-time PCR was performed on isolated RNA pools to detect enrichment of specific mRNAs. ChAT was found to be highly enriched, as would be expected from immunoprecipitation from ChAT-positive cells. 18S and 28S ribosomal RNAs were both found to be enriched to around the same amount, as was neuronal channel KCNN1. GFAP, an astrocyte marker, was not found to be enriched at all, which indicates that the immunoprecipitation was very clean and did not include ribosomes from non-motor neuron cells such as astrocytes. Experimental-triplicate data ($n = 3$) are presented as mean \pm SEM.

This method can be used to generate a genome-wide library of mRNAs that are associated with ribosomes in ChAT-positive cells. By crossing ChAT BacTRAP mice with different variants of ALS mice, immunoprecipitating GFP-tagged ribosomes, purifying RNA, and running next-generation sequencing to identify any changes, it should be possible to identify mRNAs that have altered associations with the ribosome with different mouse backgrounds.

3.4.5 CO-IMMUNOPRECIPITATION OF V5-TAGGED TDP-43 WITH GFP-TAGGED L10a INDICATES THAT TDP-43 ASSOCIATES WITH RIBOSOMES

We have previously shown, for the first time without the addition of a stressor such as sodium arsenite, that TDP-43 associated with the polysome fractions in MN1 cells. This information

is of high interest to the field of TDP-43-associated disease research. We had run two control polysome profiles to verify that TDP-43 was actually associated with polysomes and not co-migrating with the polysome fractions, but due to the possible significance of this result, we wanted to additionally validate this finding using a second, independent method. Since our GFP-L10a immunoprecipitation is highly robust, we set out to confirm whether TDP-43 was associating with ribosomes by using this immunoprecipitation method.

Because of the low levels of detectable protein that are immunoprecipitated using this method, we decided to use exogenously expressed TDP-43 with a V5-tag. This would allow us to probe our immunoprecipitations using a highly specific and strong V5 antibody. We performed transient co-transfection of MN1 cells with GFP-tagged L10a as well as with V5-tagged TDP-43. After immunoprecipitating the GFP-tagged L10a as described previously, we ran western blots to probe with GFP and V5 antibodies (Fig 3.17 A). Clearly, and repeatedly, a light band for the V5-tagged TDP-43 was visible in the immunoprecipitated sample. GFP-tagged L10a transfected cells without V5-tagged TDP-43 did not have this band. This indicates that TDP-43 is in fact associated with ribosomes.

We then decided to try probing for endogenous TDP-43 (3.17 B). We transiently transfected MN1 cells with either GFP alone (pEGFP) or GFP-L10a (pEGFP-L10a). In addition to probing with anti-GFP and anti-TDP-43, we also probed with anti-L7a to identify whether the full ribosome was being immunoprecipitated, or only the GFP-L10a protein. L7a co-immunoprecipitated with GFP-L10a, but did not co-immunoprecipitate with GFP alone, indicating that the GFP-L10a is able to pull down the ribosome. Additionally, endogenous TDP-43 was co-immunoprecipitated with GFP-L10a, but not with GFP alone. This further supports the idea that TDP-43 associates with ribosomes.

It is not yet clear whether this association is direct or indirect, since TDP-43 could be binding to mRNA that is associated with the ribosome, and this should be looked into. However, regardless of whether TDP-43 is associated with polysomes directly or indirectly, the fact that TDP-43 is associated with ribosomes indicates that TDP-43 may likely have a function with regards to translation, and that this function may be altered under disease conditions. Further research following up on these findings may turn out to be extremely important for the creation of disease therapies.

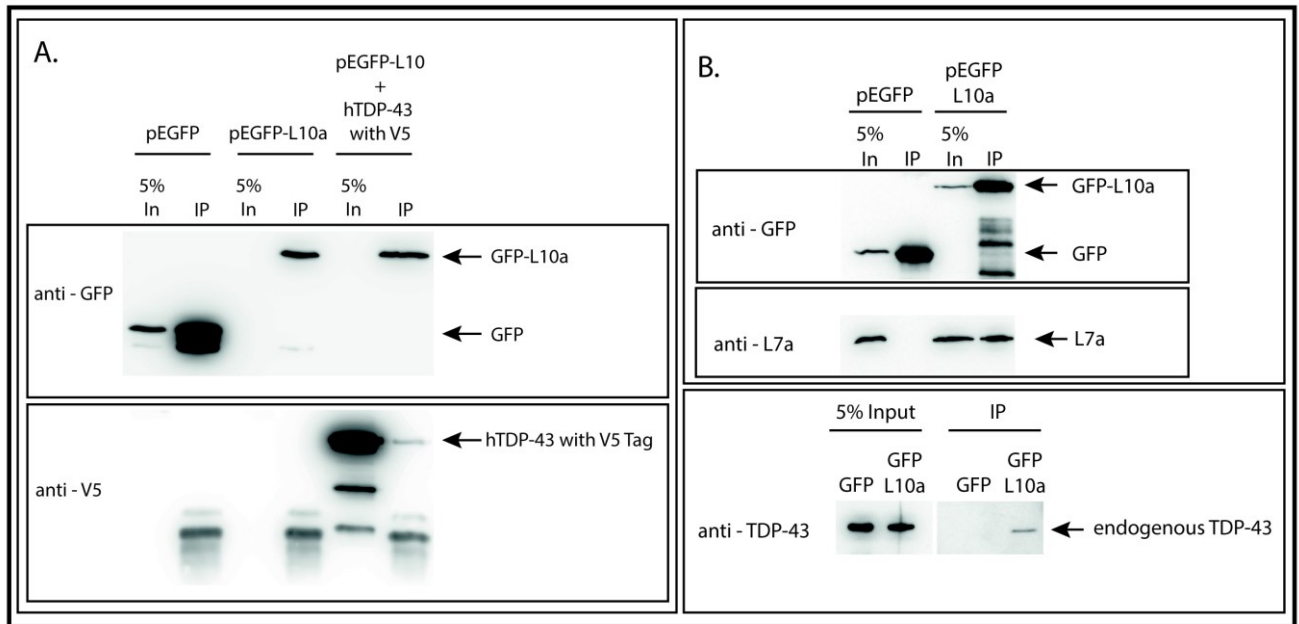


Figure 3.17 TDP-43 co-immunoprecipitates with the ribosome

A. MN1 cells were transfected with GFP alone (pEGFP), GFP-L10a (pEGFP-L10a), or GFP-L10a and V5-tagged TDP-43 (pEGFP-L10+hTDP-43 with V5). Lysate was immunoprecipitated using an anti-GFP antibody. A band for V5-tagged TDP-43 was visible only in the IP from the co-transfected pEGFP-L10a/V5-tagged TDP-43 cell lysate, as expected. Lower bands visible in the V5 blot are likely light-chain.

B. Cells were transfected with either GFP (pEGFP) or GFP-L10a (pEGFP L10a) to check for co-immunoprecipitation of endogenous TDP-43. L7a, a large ribosomal subunit protein, co-immunoprecipitated with GFP-L10a, but not GFP alone, which supported the idea that the immunoprecipitation had pulled down the full ribosome. Endogenous TDP-43 was found to co-immunoprecipitate with GFP-L10a, but not GFP alone. This gives strong evidence supporting the idea that TDP-43 associates with ribosomes.

3.5 RIBOSOME FOOTPRINTING METHOD IN MN1 CELLS AFTER TDP-43 KNOCKDOWN CAN BE USED AS AN ADDITIONAL GENOME-WIDE APPROACH

Since we have established that TDP-43 associates with ribosomes, it is important to identify whether altered TDP-43 may have an effect on translation of specific mRNAs. We have determined that TDP-43 does not show general translational regulation under normal conditions in MN1 cells upon either knockdown of TDP-43 or transient expression of several TDP-43 variants. Additionally, we were unable to detect altered translational regulation in a

selected subset of mRNAs that were selected due to the existence of TDP-43 binding sites in their 3'UTR. However, TDP-43 binds to 30% percentage of the transcriptome (Polymenidou et al., 2011). Thus, it might be easier to identify possible candidate genes that are translationally regulated by TDP-43 by using a genome-wide functional approach.

One such method for a genome-wide approach would be immunoprecipitation from ChAT-positive cells in the mouse brainstem using the BacTRAP method described above (see section 3.4.5). This has the advantage of using a full animal model rather than looking in cell culture, and it still allows for cell specificity. However, one major drawback is that the animal models for TDP-43 ALS research that are currently available are not ideal for this type of research. In order to effectively compare different variants of TDP-43 in a mouse model, it would be important that these mice use the same promoter to express these variants and that the mice be on the same genetic background as the Chat BacTRAP mice. The only set of available mouse models that met these criteria expressed TDP-43 under the prion protein (Prp) promoter. In principle, this should allow us to compare WT-hTDP43 to A315T-hTDP43. Unfortunately, after we imported these lines from Jackson Labs, a paper was published revealing that these A315T mice develop severe gastrointestinal problems which are not a common signature of ALS in humans (Esmaeili, Panahi, Yadav, Hennings, & Kiaei, 2013). This indicates that these mice are not reconstituting normal ALS pathology. Accordingly, it is therefore likely to be challenging to detect disease-relevant alterations in translational profiles using this specific mouse model.

Another method for genome-wide analysis of translational regulation is the ribosome footprinting method (Fig 3.18; for a more in depth method description, see section 2.16). This highly complex, multi-step method relies on digestion of mRNAs with a low concentration of RNaseI, which digests only the mRNA that is unprotected by ribosomes bound to it. A peak for the ribosomes along with the mRNA that are sitting in the mRNA channel of the ribosomes can be visualized by polysome profiling after digestion. The fractions containing the ribosomes/mRNA fragments can be purified, and the mRNA fragments can be isolated through size selection, since the protected mRNA fragments are known to be 28-34bp in length. With the addition of linkers, the mRNA can be circularized and PCR amplified, generating a next-generation sequencing compatible cDNA library that allows genome-wide sequencing of these fragments. After fragments are aligned, it is possible to identify mRNAs that show altered translation under different conditions.

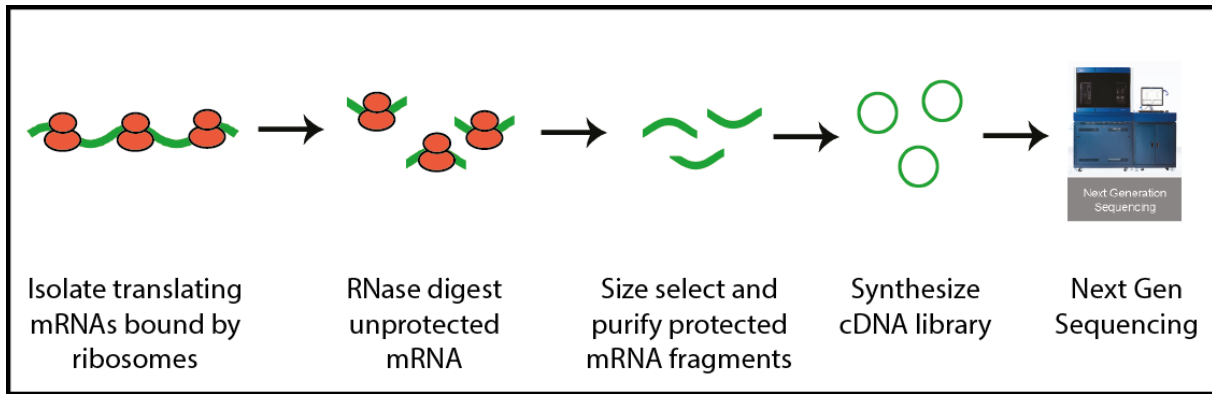


Figure 3.18 Overview of ribosome footprinting method

Cellular lysate is treated with a low concentration RNase I digestion to digest unprotected mRNA, while mRNA fragments protected by ribosomes bound to them are unaffected. RNA fragments are size selected, linker ligated, circularized and PCR amplified to generate a cDNA library compatible with next generation sequencing.

This method has several advantages over alternative methods. First, because of the use of next generation sequencing rather than microarray analysis on full mRNA, it is possible to identify alterations in splice variant expression. Since TDP-43 is involved in alternative splicing as well, this may be of particular interest in this project. Additionally, ribosome footprinting relies on the mRNAs that are protected by ribosomes. This gives additional information about where the ribosomes are sitting on the mRNA as they are translating. Because of this, ribosome footprinting has been shown to be particularly efficient in identifying ribosome-binding sites in unique open reading frames, including upstream open reading frames (uORFs), which would not be identified by traditional methods, including polysome fractionation.

We were able to establish the ribosome footprinting method through the step of library generation using MN1 cells. This extended method relies on several steps of gels and purifications to go from the first step of polysome profile generation after RNaseI digestion (Fig 3.19 A) to a PCR amplified cDNA library (Fig 3.19 B). In between, mRNA is size selected, linker ligated, circularized, and reverse transcribed. After these many steps, bands of the expected size were detectable in the last steps of purification (Fig 3.19 B, red boxes).

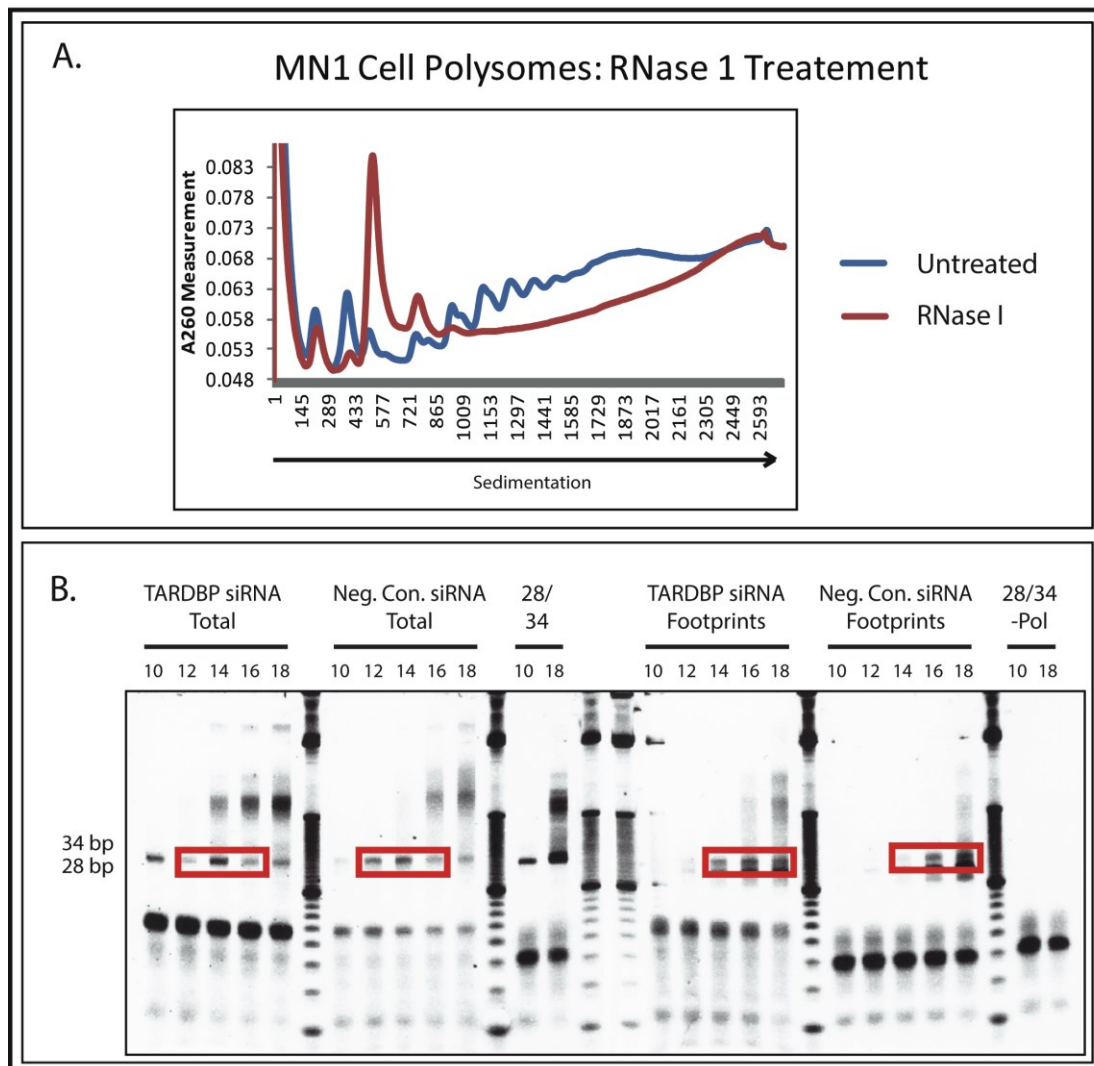


Figure 3.19 Early and late steps of ribosome footprinting show that method is functioning

A. After RNaseI digestion, lysate was run on a sucrose gradient and fractionated to view polysome profiles. Undigested lysate was used as a control. The RNaseI-treated lysate shows a distinct increase in the 80S peak with a striking decrease in the polysome peaks, indicating that the digestion generated monosomes from polysomes. B. Staining of an RNA gel shows that bands of the expected size (red boxes) were generated after the PCR amplification step to generate a cDNA library. These bands can be excised and purified before being sent in for sequencing. Lower bands are likely primer dimers.

Although the ribosome footprinting method is complicated, it would allow a wide-range of comparisons to be made on TDP-43 alterations. For this experiment, cells treated with TARDBP and scrambled negative control siRNAs were used. It would be possible to compare transient expression of TDP-43 variants, as well as MN1 cells under various stress conditions. As this method is functioning in the Duncan laboratory, it will undoubtedly shed much light on the question of whether TDP-43 regulates translation, under what conditions this regulation occurs, and what TDP-43's role in ALS may be.

4 DISCUSSION – TDP-43

In the present study, we demonstrated for the first time that TDP-43 associates with ribosomes and polysomes in the absence of cellular stress, indicating that TDP-43 may have a role in translation. Further studies revealed no alteration in general translational regulation after TDP-43 knockdown or expression of hTDP-43 variants in MN1 cells. Additionally, we found no translational regulation of a specific subset of genes. Multiple complex and precise genome-wide methods have been established to identify which mRNAs may be translationally regulated by TDP-43. There are several interesting questions raised by these results, and many interesting directions that this research can lead to in the future.

4.1 TDP-43 ASSOCIATES WITH RIBOSOMES/POLYSOMES

TDP-43 has been shown to shuttle between the nucleus and the cytoplasm under normal conditions, and to largely shift its localization from the nucleus to the cytoplasm under disease conditions. While much of the research previously performed has been focused on the nuclear function of TDP-43, the focus of this thesis was to study the possible cytoplasmic function of TDP-43, in particular with respect to translation.

When identifying the protein interaction partners of TDP-43, Freibaum et al., (2010) showed that TDP-43 had two major groups of interacting partners: a nuclear-splicing cluster, and a cytoplasmic-translation cluster. While many people have speculated that TDP-43 may have a function in translational regulation, only a few preliminary studies have been pursued. First, it was shown that TDP-43 could alter the splicing of the ribosomal S6 kinase 1 (S6K1) Aly/REF-like target (SKAR), a protein that is involved in the pioneer round of translation (Fiesel, Weber, Supper, Zell, & Kahle, 2012). More directly, TDP-43 was found to associate with polysomes in cultured cells after inducing stress, indicating that TDP-43's association with the translational machinery may be injury or stress related (Higashi et al., 2013).

For the first time, we have shown that TDP-43 associates with polysomes without the addition of a chemical agent such as sodium arsenite. Motor neuron like cells transiently transfected with a tagged variant of TDP-43 showed that TDP-43 co-migrates with the polysome-

containing fractions of polysome profiles (Figs 3.10, 3.11, 3.12). Two control experiments support the concept that this is a true ribosome association rather than co-migration in polysome fractions. First, TDP-43 was completely shifted to the light fractions of the profile when we added EDTA, a magnesium chelator known to dissociate the ribosomal subunits. As expected, all visible 80S and polysomes were dissociated into the 40S and 60S subunits by our EDTA treatment. To rule out the possibility that TDP-43 co-migrates with polysomes via association with some other EDTA-sensitive complex, we tested the effects of puromycin. Under our conditions, puromycin had a less dramatic effect on polysomal complex dissociation than EDTA. Nevertheless, puromycin treatment caused TDP-43 migration to be shifted toward the lighter, non-polysome fractions in a similar proportion to the reduction of polysome peaks. Together, these results strongly support the idea that the co-migration of TDP-43 with polysomes is due to an association with the translational machinery rather than a false positive co-migration due to an association with species that sediment at the same rate. Whether this association occurs via an indirect interaction with ribosome-bound mRNAs or involves direct physical interaction with the translation machinery requires further research.

Additional support for the idea that TDP-43 associates with the translational machinery comes from our data showing that TDP-43 co-immunoprecipitates with ribosomes (Fig 3.17). By co-transfection of cells with GFP-tagged ribosomal protein L10a as well as a tagged variant of TDP-43, we pulled down the ribosome using anti-GFP antibody. TDP-43 was found to associate with the GFP-tagged ribosome. We additionally checked whether endogenous TDP-43 could be co-immunoprecipitated with GFP-tagged ribosomes. We first showed that immunoprecipitation of GFP-tagged L10a also pulls down another ribosomal protein, large ribosomal protein L7a, supporting the idea that the ribosome itself is being immunoprecipitated, and not just protein L10a. L7a was not co-immunoprecipitated when the cells were transfected with GFP alone. Importantly, endogenous TDP-43 was also found to co-immunoprecipitate with the GFP-tagged ribosome, whereas no co-immunoprecipitation was detectable from the control cells transfected with GFP alone.

Taken together, our data reveal for the first time that TDP-43 can associate with the ribosome and with polysomes without the addition of stress-inducing agents such as sodium arsenite. This very importantly suggests that TDP-43 may play a role in translation even when cells are not stressed. Whether TDP-43 associates with ribosomes directly or indirectly has not yet been clarified. Since TDP-43 binds to a large number of mRNAs, it seems likely that TDP-43 may be indirectly associating with polysomes as a trans-acting factor bound to mRNA.

However, the protein interaction study carried out by Freibaum et al., (2010) suggests that TDP-43 might directly interact with the translational machinery. This line of study should be followed up on in the future to clarify whether TDP-43's association with ribosomes is a direct or an indirect interaction. In either case, our data reveal a new aspect of TDP-43 biology in the cytoplasm and provide further support for a functional role in translational control.

Since a previous study has shown that TDP-43 association with polysomes is visible upon addition of oxidative stress through sodium arsenite addition (Higashi et al., 2013), it would be interesting to assess whether the co-immunoprecipitation that we identified is also affected by stress conditions. It is possible, and perhaps even likely, that TDP-43's association with ribosomes exists under normal conditions and is increased after the addition of stress-inducing agents. By comparing directly the amount of TDP-43 co-immunoprecipitated under normal conditions to that co-immunoprecipitated after the addition of sodium arsenite, it would be possible to understand whether TDP-43 alters its association with the translational machinery under stress conditions. It would be of additional interest to widen the pool of stress conditions tested to see how different conditions might affect this kind of association differently. In particular, since TDP-43 was shown to relocate to the cytoplasm after axotomy of a mouse motor neuron (Moisse et al., 2009), it would be interesting to see how injury affects TDP-43's association with the translational machinery. It would potentially be possible to grow motor neuron-like cells in a microfluidic chamber and to perform an axotomy on them before immunoprecipitating GFP-tagged ribosomes and assaying the amount of TDP-43 that co-immunoprecipitates.

Also of interest would be to identify whether TDP-43's association with polysomes is universal or whether it is cell-type specific. Since we were using motor neuron-like cells, it could be possible that we identified the association of TDP-43 with polysomes due to the cell type we were assaying. Whether TDP-43 associates with polysomes under non-stress conditions in non-neuronal cells types would be of interest to study as well. One might also consider the use of induced pluripotent stem cells in pursuit of this information.

4.2 KNOCKDOWN OF TDP-43 IN MN1 CELLS DOES NOT ALTER GENERAL TRANSLATION

We found the interesting result that TDP-43 associates with polysomes and ribosomes, which supports the theory that TDP-43 is involved in translational regulation. However, it is important to distinguish whether translational regulation by TDP-43 actually occurs, and if so, whether regulation takes place at the level of general translation or at the level of mRNA-specific translation.

General translational control refers to factors that can alter the translation of a large subset of mRNAs. An example of this would be eukaryotic initiation factor 4E-binding protein (4E-BP), which is phosphorylated under normal conditions rendering it unable to bind to eukaryotic initiation factor 4E (eIF4E). However, under certain conditions where translational control is needed, 4E-BP is not phosphorylated, allowing it to bind to eIF4E. This binding prevents eIF4E from assisting in mRNA circularization, thus down regulating the step of translation initiation.

By using the powerful method of polysome profiling, we are able to visualize the distribution of 40S and 60S ribosomal subunits, 80S monosomes, and polysomes of cells. This allows us to easily see how translation might be changed under different conditions. For instance, if altered cellular conditions cause the 80S peak of the polysome profile to increase in height, while the polysome peaks decrease in height, this would indicate that a translation initiation defect is taking place. Alternatively, if the polysome peaks jump in height, while the 80S gets smaller, this would indicate that there is a translation elongation defect.

In order to assay general translation using the polysome profiling method, we chose to continue to work with MN1 cells, since these cells are motor neuron-like, which might give us insight into ALS disease etiology. MN1 cells have also been immortalized, and allow us to generate a large amount of starting material relatively easily. We were also able to generate a robust and reproducible knockdown of TDP-43 protein levels in MN1 cells to less than 20% of starting levels.

Previous research showed that TDP-43 levels are incredibly important for maintaining healthy animal models (Fiesel et al., 2011; Xu et al., 2010). TDP-43 expressed at levels lower than

normal or higher than normal both resulted in motor phenotypes and altered development. Additionally, in ALS and FTL, TDP-43 is found in aggregates in affected cell types. This might indicate that TDP-43 being titrated away from its normal cytoplasmic function may result in disease progression. With this in mind, we wanted to assay how a large-scale reduction of TDP-43 levels might affect general translation.

During repeated assays where we knocked down TDP-43 levels in MN1 cells and compared polysome profiles of MN1 cells with TDP-43 knocked down to MN1 cells treated with nonsense scrambled negative control siRNAs, we were unable to find any significant alteration in the polysome to monosome ratio between the profiles (Fig 3.4). In order to verify that translation rates were unaltered, we ran a nascent protein assay using Click chemistry (Fig 3.4). Again, we found no significant alteration in nascent protein synthesis when comparing TDP-43 knockdown with negative control cells.

There are many possible reasons why knockdown of TDP-43 may not have shown any alterations in polysome profiles. First, it may be that knockdown of TDP-43 does not actually have any effects on general translation, as appears to be the case for our system in MN1 cells. It is possible that knockdown of TDP-43 may affect general translation in other cell lines or tissues. For instance, the previous studies that showed that a reduction in TDP-43 levels resulted in motor deficits and death were done in animal models (Kabashi et al., 2010; Sephton et al., 2010). Although no *in vivo* models have yet shown effects on general translation, it may be that reduction of TDP-43 results in general translational effects only in a full model system. Since a previous study showed that TDP-43 is directed to dendrites in motor neurons after motor neuron stimulation, it is also possible that knockdown of TDP-43 may affect general translation only after stimulation of motor neurons.

Another possibility is that reduction of TDP-43 may result in altered translational regulation only under stress or injury conditions. A previous study has shown increased TDP-43 association with polysomes after addition of sodium arsenite stress (Higashi et al., 2013). It is also possible that TDP-43 associates with polysomes under normal conditions only at a low level, and may result in translational regulation of only a small number of mRNAs, the regulation of which would not be expected to lead to a visible effect in our polysome profiling assay. However, if TDP-43 associates more readily with polysomes under stress conditions,

and thereby increases its regulation of translation, it would be highly interesting to study how added stress to these cells affects the general translational profiles of TDP-43.

One other possibility is that our reduction of TDP-43, even to less than 20% of normal endogenous levels, is still not enough to see general translational regulation in a cellular model. If most of TDP-43 is localized in the nucleus with only a small amount in the cytoplasm in normal conditions, reduction of TDP-43 levels might need to be nearly complete before any translational effects are seen. This is an unavoidable caveat of a knockdown approach.

4.3 TRANSIENT EXPRESSION OF TDP-43 VARIANTS – INCLUDING hTDP-43, hTDP-43 WITH AN EXTRA NES, AND hTDP-43 WITH THE A315T PATIENT MUTATION – IN MN1 CELLS DOES NOT ALTER GENERAL TRANSLATION

Although reduction in TDP-43 protein expression levels did not result in general translational regulation in MN1 cells, altered expression of TDP-43 in other manners might be involved in translational regulation. We were interested in assaying whether human TDP-43 (hTDP-43) expressed in MN1 cells, or certain variants of hTDP-43, might have an effect on general translation.

We chose three variants of hTDP-43 to assay. The first was human TDP-43 with no modifications other than 5'- and 3'-tags. This was done to assay whether overexpression of TDP-43 or expression of human TDP-43 in particular might affect general translation. We also generated hTDP-43 with an extra NES in order to see whether TDP-43 directed to the cytoplasm might affect translation. We did this because in disease, TDP-43 is often relocalized from the nucleus to the cytoplasm, and we were interested to know whether TDP-43 in the cytoplasm is enough to generate regulation. Finally, we generated hTDP-43 with one of the ALS patient mutations, A315T. Since more than 30 patient mutations have been identified in ALS patients, we were curious whether one of the more commonly occurring mutations might have an effect on translation.

As mentioned previously, altered TDP-43 expression levels are known to cause disease-like phenotypes (Fiesel et al., 2011; Xu et al., 2010). We therefore wanted to generate a stable, inducible cell line to express these TDP-43 variants at the same levels, in order to remove expression levels as a reason for altered translational regulation. However, the stable cell line that we generated expressed our variants at such a low level that it did not make sense to use it in this particular assay. Instead, we chose to transiently transfect our cells and to verify that our variants were being expressed at similar levels in our MN1 cells line.

Once consistently similar expression levels of TDP-43 variants were established, we ran polysome profiles on these MN1 cells. Similar to the results that we obtained after TDP-43 knockdown, we found that transient expression of hTDP-43 did not noticeably alter the polysome to monosome ratios found in cells transiently transfected with hTDP43, hTDP-43 + NES, or hTDP-43 A315T (Fig 3.8).

Why hTDP-43 variants showed no global translational regulation could be explained by several different hypotheses. Again, it is possible that TDP-43 is not at all involved in global translational regulation, but rather involved in the regulation of a specific subset of mRNAs, or that TDP-43 variants need additional stress, such as hypoxia or nerve injury in order to stimulate altered translational regulation.

It is also possible that aging may be involved in causing altered translational regulation in cells for this gene. Neurodegenerative diseases such as ALS have a very strong age component; most patients are diagnosed between 55 and 70 years of age. It is possible that by using a cell culture-based system, we are not able to appropriately assay the result of an aging system on general translational regulation by TDP-43. This problem could potentially be solved by using an animal model. By monitoring translational regulation in neurons in mice with altered TDP-43 expression, and comparing changes in young versus old mice, it would be possible to conclude whether TDP-43 is regulating general translation.

4.4 REAL-TIME PCR ASSAY FOR SELECTED GENES AFTER TDP-43 KNOCKDOWN SHOWED NO ALTERED POLYSOME ASSOCIATION

Since we found no altered general translational regulation through either knockdown of TDP-43 or expression of hTDP-43 variants in MN1 cells, we were interested to see whether

translation of specific genes was altered. Previously, using the HITS-CLIP method, the set of mRNAs that TDP-43 interacts with was determined (Polymenidou et al., 2011; Tollervay et al., 2011). This was a very large set of mRNAs – approximately 30% of the mouse transcriptome – and many of these mRNAs were found to be regulated by TDP-43 at the splicing step in the nucleus. When researchers focused on the cytoplasmic fraction of mRNAs bound by TDP-43, they found that it was enriched for mRNAs with at least one TDP-43 binding site at the 3'UTR, which is a known interaction site for RBPs that regulate translation of mRNAs. We selected a number of the mRNAs that TDP-43 binds at the 3'UTR, and particularly selected for genes that may be of additional interest for TDP-43-associated diseases. For instance, we checked the regulation of TARDBP itself, as well as FUS/TLS, the other major RBP identified in aggregates of both ALS and FTLN patients. We also looked at GRN, a gene implicated in FTLN, Gria2, a gene involved in neuronal signal processing, and Nefl, a gene shown to be involved in ALS pathogenesis.

Interestingly, when we focused on the location in polysomes of the TARDBP mRNA after TDP-43 knockdown, we saw that TARDBP definitively moved from the heavy fractions to the light fractions of the gradient (Fig 3.9). This indicates that TARDBP may be translated less efficiently after TDP-43 knockdown. However, this information is complicated by the fact that TDP-43 knockdown may affect the ability of ribosomes to initiate translation due to breakdown of TARDBP mRNAs.

Whether TARDBP mRNA translation is actually regulated by TDP-43 or not, the fact that TARDBP mRNA shifted from heavy fractions to light fractions in our real-time PCR analysis is proof that this method functions robustly. In other words, we are in fact able to use real-time PCR across the polysome fractions to visualize altered polysome association of specific mRNAs. We therefore applied this method to our other candidate genes.

We did not find any altered polysome association for any of the other genes (FUS/TLS, GRN, Gria2, or Nefl). This may not be entirely surprising, since although we selected a particularly interesting subset of genes to study, TDP-43 binds to around 30% of the transcriptome under normal conditions. It may be that TDP-43 only binds to the mRNAs that it regulates translationally under stress or injury conditions, or it may be that mRNAs that TDP-43 binds to mostly in the nucleus may be additionally regulated cytoplasmically. Furthermore, TDP-43 may be regulating translation through a method other than binding to the 3'UTR of mRNAs.

Other RBPs have been shown to alter translation by binding to the 5'UTR of mRNAs (For a review, see Gebauer & Hentze, (2004)); alternatively, TDP-43 may regulate translation not through its RNA-binding ability, but rather through direct interactions with the translational machinery.

Since we have established that TDP-43 associates with ribosomes and polysomes, we have a reasonable motivation to believe that TDP-43 may be involved in translation. However, monitoring TDP-43's regulation of a selected subset of mRNAs may not be the most efficient method for determining whether TDP-43 regulates translation, and if so, how, and which mRNAs. It is likely more direct to use a genome-wide method of analysis to assess which mRNAs TDP-43 translationally regulates, and then determine from this set how this regulation functions.

4.5 ESTABLISHMENT OF SEVERAL GENOME-WIDE METHODS FOR FURTHER ANALYSIS OF TDP-43 TRANSLATIONAL REGULATION

There are many different methods that can be used to assess genome-wide what effect TDP-43 has on translation. Several of these methods have been established in our laboratory in relationship with this thesis. These include polysome profiling, ribosome footprinting, and BacTRAP analysis.

We established the method of polysome profiling in our laboratory for several purposes. As shown in this thesis, this method was used to identify possible general translational changes caused by altered TDP-43. It is also possible to isolate mRNA or protein from individual fractions generated by polysome profiling and to monitor the altered location of specific mRNAs or proteins under different conditions, as shown in figures 3.9 and 3.11, respectively.

In order to move polysome profiling to a genome-wide approach, one would need to determine how best to pool fractions in order to generate an ideal dataset. Running deep sequencing on each individual fraction of a polysome profile would be highly expensive. Consequently, there are two common compromises for genome-wide polysome profiling. One is to compare total mRNAs to mRNAs in all of the polysome fractions combined, thus showing the overall alterations in ribosome association. The second is to compare pooled "light" polysomes to "heavy" polysomes, which gives some additional information about

possible shifts of mRNAs within the polysome fractions. The first approach requires that translationally regulated mRNAs are done so in a binary fashion (“either the mRNAs are translated or they are not”). However, ribosome association is not always binary. Rather, much regulation occurs on a sliding scale (“mRNAs may be translated by few ribosomes or by many ribosomes, thus determining the amount of protein produced). Such mRNAs will be missed in the first approach, but would more likely be detected by the second.

This concept of “ribosome occupancy” – the binary concept of whether mRNAs are being translated or not under a certain condition – versus “ribosome density” – how many ribosomes are bound to mRNA under different conditions – is of great importance for how translational analysis is assessed. Importantly, a robust method for identifying ribosome density was created by Ingolia et al., (2009), and we were able to successfully establish this method in our laboratory. Ribosome footprinting relies on the protection of mRNA fragments by the ribosomes that remain bound to the mRNAs after a light RNase digestion. These fragments are deep-sequenced, and provide information about how many ribosomes are bound to an mRNA. Importantly, it also reveals where the ribosomes are preferentially associated with the mRNA. Thus, it has allowed researchers to identify regulated ribosome pause sites, and a large number of open reading frames (ORFs), including upstream ORFs that were not known to previously exist. While this method is of particular interest because of the amount of information it can provide, it is not inexpensive, and relies on a highly-complex process to produce the final material. However, despite the complexity of the method, we have successfully established ribosome footprinting in the laboratory. It would be extremely interesting to follow up on TDP-43’s translational regulation via the ribosome footprinting method.

The third method that was established in relation to this thesis is the BacTRAP method. Using mice that express GFP-tagged ribosomal protein L10a under a cell specific promoter (Heiman et al., 2008), we are able to isolate mRNAs that are bound by ribosomes in these cells by affinity purification of GFP from tissue lysate. These mRNAs are likely being translated in these cells.

The BacTRAP method, while very powerful, still has some distinct problems for assessing translational control. A key issue is that it is difficult to establish a “total” mRNA pool from the cell type of interest to compare to the “translational” mRNA pool. This means that it is hard to tell whether an increase or decrease in mRNA is due to increased or decreased mRNA transcription, degradation, or other alterations in mRNA processing, or whether it is due to an

actual increase in translation. Additionally, this method does not give information about the number of ribosomes bound to an mRNA. However, it has the very strong advantage that it is used *in vivo* in mammals. The ability to target mRNAs that are bound by ribosomes in an animal model addresses a number of issues, such as visualizing translational alteration in properly functioning motor neurons, as well as allowing the ability to assess translational regulation after aging of mice.

If the BacTRAP method were to be used in order to monitor altered mRNA association with ribosomes under altered TDP-43 expression, it would be imperative that the correct TDP-43 animal model be used. Thus far, many of the TDP-43 animal models are not easily compared. For one, many of the animal models use different promoters, and therefore cannot be compared outright. Secondly, one of the few sets of models that use the same promoter, the prion protein (Prp) promoter, promoting expression of hTDP-43 and hTDP-43 A315T mutation, the A315T mice develop a strong gastrointestinal problem. Since the GI tract should not be affected by motor neuron disease, it raises the question whether these models are correctly mimicking ALS. Most recently, a set of mice was created by the Cleveland laboratory that would allow comparison of hTDP-43 expression with hTDP-43 Q331K and hTDP-43 M337V expression (Arnold et al., 2013). However, these mice show highly varied expression levels of exogenous TDP-43, so it would be difficult to know whether any changes visualized are due to actual alterations in mRNA association with ribosomes or due to different levels of the TDP-43 variants.

The BacTRAP method would be of extreme interest to use for analysis of altered changes in mRNA association with ribosomes *in vivo*. However, until a TDP-43 mouse model set that shows a strong and predictable neurodegenerative phenotype and that expresses TDP-43 variants at similar levels is developed, this method may not be the ideal method for assaying TDP-43's effects on translational regulation.

4.6 GENERAL CONCLUSIONS

In this thesis, we showed for the first time that TDP-43 associates with ribosomes and with polysomes under normal conditions. This strongly supports the notion that TDP-43 may have a function related to translational regulation. We also showed that under conditions of TDP-43 knockdown or expression of hTDP-43 variants in MN1 cells, altered TDP-43 expression

does not regulate general translation. Additionally, although TDP-43 knockdown specifically altered the distribution pattern of TARDBP mRNA in relation to polysome profiling, none of the other mRNAs that we tested with TDP-43 binding sites in the 3'UTRs showed altered distribution.

The next steps would be to look genome-wide for translational alteration using one of the major methods that were established during this thesis. All three methods – polysome profiling, ribosome footprinting, and BacTRAP analysis – would give great insight into the question of whether TDP-43 regulates translation. Each method would create a large dataset that could then be further studied.

Next steps to be taken after this thesis would also include testing general and specific translational regulation in cells and tissues under stress or injury conditions. Since TDP-43 has been shown to alter its cellular localization in disease, as well as under stress and injury, it would be interesting to know whether the cause of this distribution might also have a direct effect on TDP-43's ability to perform translational regulation.

Overall, while much has yet to be done on this subject, this thesis has provided a strong motivation for continued research on TDP-43's association with translation, as well as a thorough starting point for genome-wide research on TDP-43's involvement in translational regulation. A compelling argument for TDP-43's involvement in translation can be made from the fact that TDP-43 is found to associate with ribosomes and polysomes (Figs 3.10, 3.11, 3.12, 3.17). Moreover, several methods that can be used for genome-wide analysis are established and robustly functional (Figs 3.2, 3.16, 3.19). Any datasets created with relation to this subject will undoubtedly be useful in furthering study of TDP-43-associated ALS, and will help to further establish what changes are occurring between TDP-43's normal function and its function in relation to disease.

5 INTRODUCTION - DOHH

5.1 HYPUSINATION

The highly unusual amino acid hypusine was identified in 1971 (Shiba, Mizote, Kaneko, Nakajima, & Kakimoto, 1971), and was found to occur in only one protein – eukaryotic initiation factor 5A (eIF5A) (Cooper, Park, & Folk, 1982). The process of generating hypusine on eIF5A uses two enzymes, deoxyhypusine synthase (DHS) and deoxyhypusine hydroxylase (DOHH) (Abbruzzese, Park, & Folk, 1986; M. H. Park, Cooper, & Folk, 1981). Strikingly, neither one of these enzymes has any known function other than to generate hypusine on eIF5A. This distinctive modification and the process of its generation have been heavily studied, since such a specific process would be a particularly useful target for drug therapies.

Hypusination occurs only on the 50th amino acid, lysine, of eIF5A. It appears that the sequence surrounding this lysine is highly important, likely due to the fact that it creates an exposed loop allowing the two functional enzymes to easily access the lysine residue. All three of the major proteins involved – eIF5A, DSH, and DOHH – are evolutionarily conserved, and eIF5A and DSH are essential for survival in all known model systems.

Also required for the hypusination reaction is the polyamine spermidine. Spermidine is synthesized from the precursor putrescine. In the hypusination reaction, DSH transfers the aminobutyl group from spermidine to the lysine residue (M. H. Park et al., 1981). This generates a deoxyhypusine residue. Next, DOHH catalyzes a hydroxylation reaction, generating hypusine (Abbruzzese et al., 1986). This hypusinated version of eIF5A is considered the active version of eIF5A.

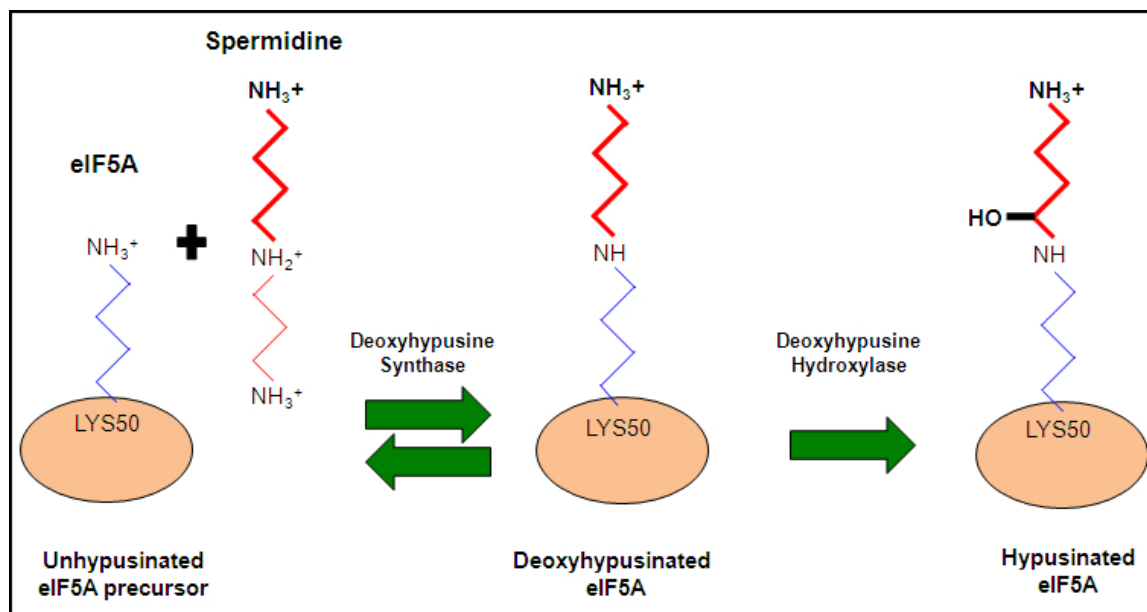


Fig 5.1 Hypusination

Hypusination occurs at only one amino acid (the lysine 50 residue) of only one protein (eIF5A). This process requires the polyamine spermidine, which is linked to the lys50 residue by the deoxyhypusine synthase enzyme (DHS), thereby creating the deoxyhypusinated form of eIF5A. The deoxyhypusine is converted to hypusine by the deoxyhypusine hydroxylase enzyme (DOHH). This generates the fully functional hypusinated version of eIF5A. Both DHS and DOHH have no other known functions other than to produce the hypusine amino acid on eIF5A. (Figure modified from Maier, Tersey, & Mirmira, 2010).

Importantly, both DHS and DOHH are needed for normal mammalian cell growth (M. H. Park, Nishimura, Zanelli, & Valentini, 2010; Sievert et al., 2014). Inhibition of DHS exerts a much stronger reduction in mammalian cell growth, but DOHH also strongly reduces growth. The need for the hypusine modification clearly evolved over time, as the DOHH gene is non-essential in yeast (J.-H. Park et al., 2006). However, the modification is essential in multicellular eukaryotes (Patel, Costa-Mattioli, Schulze, & Bellen, 2009). This indicates that while the hypusine modification was generated early in evolution, its function may have evolved over time.

5.2 eIF5A

In eukaryotes, eIF5A has two isoforms – eIF5A1 and eIF5A2 in humans. Interestingly, the expression of these two isoforms is different in mammals than in most other eukaryotes. In yeast, the homologues of these two proteins are alternately expressed under aerobic and anaerobic conditions, respectively (Schwelberger, Kang, & Hershey, 1993). In many other

eukaryotes, the two genes are co-expressed, and appear to have unique functions. However, in mammals, eIF5A-1 is highly expressed in all tissues whereas eIF5A-2 is not expressed at a detectable level under normal conditions, though it is found to be highly expressed in certain types of cancers (He et al., 2011). This indicates that despite the high conservation between the genes, eIF5A-1 and -2 may have different functions in mammals than in other species. Additionally, in a mouse knockout model of eIF5A-1, the mouse was embryonic lethal (Nishimura, Lee, Park, & Park, 2012), showing that eIF5A-1 is needed for mouse development.

eIF5A was initially identified as an initiation regulator, as indicated by its name. However, recent studies have suggested that the fully modified version of eIF5A may have a function more closely linked with elongation (Patel et al., 2009; Saini, Eyler, Green, & Dever, 2009) or that it may be involved with the first peptide bond formation at translation initiation (Blaha, Stanley, & Steitz, 2009).

5.3 DHS

The DHS enzyme has been found to be highly conserved in eukaryotes. Knockout of DHS causes a severe cell proliferation reduction, and through cellular proliferation regulation, DHS is found to be an essential gene in both yeast and mouse studies (Nishimura et al., 2012; Sasaki, Abid, & Miyazaki, 1996).

The chemical GC7 was identified as a potent and specific inhibitor of DHS. Addition of the chemical to cell culture prevents DHS from attaching spermidine to Lys50 of eIF5A. This creates a strong translation initiation defect in murine cells, as has been shown previously (Landau, Bercovich, Park, & Kahana, 2010).

5.4 DOHH

Similarly to DHS, DOHH was also shown to be highly conserved. However, whether DOHH is an essential gene or not is dependent on the organism. For instance, in yeast, DOHH is non-essential – when DOHH is knocked out, cell proliferation is only moderately affected (J.-H. Park et al., 2006). However, in *Drosophila melanogaster*, DOHH is an essential gene, and

knockout causes embryonic lethality (Patel et al., 2009). This difference in DOHH's "essentialness" indicates that the importance, and possibly the function, of the full hypusine modification may have evolved over time.

KO of the DOHH homolog Nero in *Drosophila* resulted in a translation elongation defect (Patel et al., 2009). This implied that the fully modified eIF5A is in fact an elongation factor, rather than an initiation factor or involved in first peptide synthesis, as originally thought (Benne, Brown-Luedi, & Hershey, 1978; Blaha et al., 2009). However, because of DOHH's different levels of "essentialness", it is not clear whether DOHH removal acts as an elongation inhibitor in all systems. It is of interest to identify how DOHH removal affects mammalian cells, and in particular, how it affects translational regulation.

5.5 GENERATION AND CHARACTERIZATION OF CONDITIONAL DOHH KNOCKOUT IN MICE AND 3T3 CELLS

While DOHH has been studied in several different model systems, until recently it was not studied in mammals. In collaboration with the Balabanov laboratory we worked to identify the function of DOHH in a conditional knockout mouse model. Generation of the conditional DOHH knockout under the CMV-Cre promoter, as well as characterization of the mouse and its cells was performed in the Balabanov laboratory (Sievert et al., 2014).

Homozygous mice were embryonic lethal between days E3.5 and E9.5. In order to further characterize the effects of DOHH KO in mammals, they then generated an immortalized 3T3 cell line. These cells were stably transfected with either a Cre expression plasmid or with an empty vector, so that the cells could inducibly knockout DOHH upon the addition of tamoxifen. DOHH knockout results in a reduced full hypusine modification. This takes approximately 8-10 days. (Sievert et al., 2014). These cells provide a powerful tool to find out how removal of DOHH affects translation. Due to their immortalization, they are easily manipulated, and are able to provide a large amount of material for experiments. By investigating the impact of DOHH's removal on translation in these 3T3 cells, we are the first group to examine this in a mammalian context.

5.6 HYPOTHESIS

Hypusine is a unique amino acid that occurs in only one known protein, eIF5A. The hypusine modification is created through a two-step process that utilizes the enzymes DHS and DOHH. The DOHH enzyme is inessential in yeast, but essential in *Drosophila* and mouse. Additionally, the removal of the DOHH enzyme in different organisms may lead to different translational effects. We therefore hypothesized that:

**The conditional removal of the DOHH enzyme from mouse cells
will have an effect on general translation.**

6 MATERIALS AND METHODS - DOHH

6.1 CELL CULTURE

3T3 cells were generated from mice to allow inducible knockout of DOHH. This allows us to work with an immortalized cell line that generates a large amount of material for research (Details about cell line and mouse generation can be found in Sievert et al., 2014). MEF cells were also generated by Sievert in the Balabanov laboratory to check that the effects that we saw in 3T3 cells were also visible in another cell type.

3T3 cells and MEF cells were cultured alike in DMEM supplemented with 10% fetal bovine serum, 50 U/ml penicillin, 50 µg/ml streptomycin, 25 µM β-mercaptoethanol, and 4 mM L-glutamine (37°C, 5% CO₂, humidified atmosphere). Cre- and Cre+ DOHH inducible-knockout cells were either left untreated, were treated with 100 nM tamoxifen for 8-10 days, or were treated with 100 nM tamoxifen for 8-10 days. Cells were then treated with 50 µg/ml cycloheximide for 30 min at 37°C prior to collection.

6.2 POLYSOME PROFILE GENERATION

To visualize the mRNAs bound to polysomes from the total mRNA pool, 3T3 cells were run through a gradient profiling system. Cells were treated with 50 µg/ml cycloheximide added dropwise to growth medium, and swirled to distribute. Cells were returned to the 37°C incubator for 30 min to allow cycloheximide to inhibit translocation.

During the incubation, sucrose gradients were formed and cooled. Fresh 50 ml sucrose solutions with 50% and 17.5% sucrose were made in gradient buffer containing 1.875 ml 2M KCl, 75 µl of 1M MgCl₂, and 500 µl of 1M Tris-HCl, and filter sterilized through a 0.22 micron filter.

Using a cannula, the bottom half of an Open-Top Polyclear Centrifuge Tube (Seton, Cat No: 7031) was filled with the light, 17.5%, sucrose solution. Using a second cannula, the heavy, 50%, sucrose solution was layered, slowly, below the light solution up to the halfway mark. Tubes were capped and formed into a gradient using the SHORT Sucr 17-50% wv setting on

the Gradient Master gradient former (BioComp, Model No 108). After rotating, tubes were stored at 4°C for 30 min to prechill.

After forming gradients, the plates containing the treated cells were removed from the 37°C incubator and immediately placed on ice. Growth medium was aspirated off and cells were washed twice with ice-cold PBS containing 50 µg/ml of cycloheximide. Cells were collected in polysome lysis buffer (20 mM Tris, 10 mM MgCl₂, 100 mM NaCl, 0.4% NP-40, Roche Complete Protease Inhibitor, 100 U/ml RNasin, cycloheximide 50 µg/ml in cycloheximide treated samples). Tubes were incubated on ice for 10 min, and then centrifuged for 10 sec to pellet the nuclei. The supernatant was transferred to a new eppendorf tube, and centrifuged for 10 min at 10,000 g at 4°C to pellet any residual debris. After the spin, lysate was transferred to a new tube.

Lysate was normalized as it was loaded onto sucrose gradients. The protein concentrations of all samples were measured by the BioRad Protein Assay, and were normalized across the protein concentrations. The samples were very carefully loaded onto the sucrose gradients on a balance, in order to carefully monitor the amount loaded. Gradients were ultracentrifuged in an SW40Ti rotor at 35,000 rpm for 2.5 hr at 4°C. Gradients were kept in 4°C room until fractionated.

Gradients were fractionated using a Piston Gradient Fractionator (BioComp, Model No: 152) (Fig 2-8). Samples were collected from top to bottom of the tubes. The piston was set to move at 0.3 mm/sec, with a distance of 3.00 per sample, with 27 samples total collected. This results in approximately 500 µl per fraction. As samples were removed from the top, they were passed through a Model EM-1 Econo UV Monitor (Bio-Rad, Cat No: 731-8160), which is set at 254 absorbance in order to measure RNA absorbance. Absorbance readouts were transmitted to and processed into graph form using the UV gradient profile program (BioComp, version 6.10).

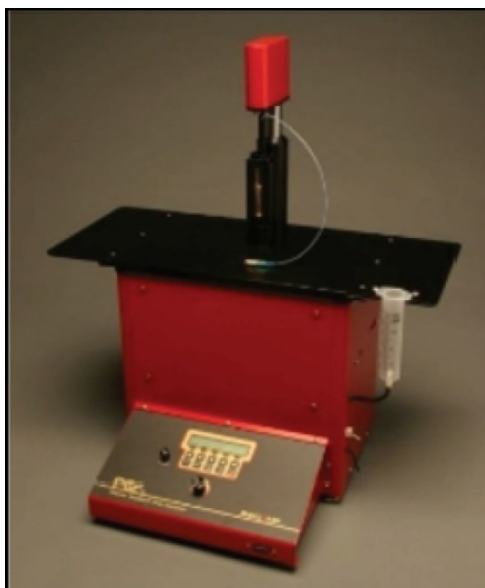


Fig 6-1: BioComp Piston Gradient Fractionator. The BioComp Piston Gradient Fractionator allows the fractionation of gradients (in the case of this project, sucrose), which are passed through a UV monitor to determine the RNA levels of each fraction. (Figure modified from Bor et al., 2006).

6.3 POLYSOME TO MONOSOME RATIO CALCULATION

Polysome to monosome ratios (P/M ratios) are calculated to provide information about how translation is being regulated. A standard P/M for a control sample must be taken for every experiment, since polysome profiles can be changed by very small alterations in cell and lysate preparation. All other runs from within the same experiment can be compared to this standard in order to verify whether the P/M ratio has increased (higher polysomes, lower monosome, or both) or decreased (lower polysomes, higher monosome, or both). An increased P/M ratio implies that there is a translation elongation defect and there are more ribosomes attached to the mRNAs as a result, whereas a decreased P/M ratio implies a translation initiation defect with more single ribosomes stuck at the start codon.

P/M ratios were calculated by drawing a line below the monosome peak across the polysome profile. A vertical line was drawn at the lowest point between the monosome and disome peaks. The area below the monosome curve (Fig 2-9, M) and the area below the polysomes (Fig 2-9, P) were measured using ImageJ to count the pixels. A ratio was taken of these two numbers and P/M ratios were compared.

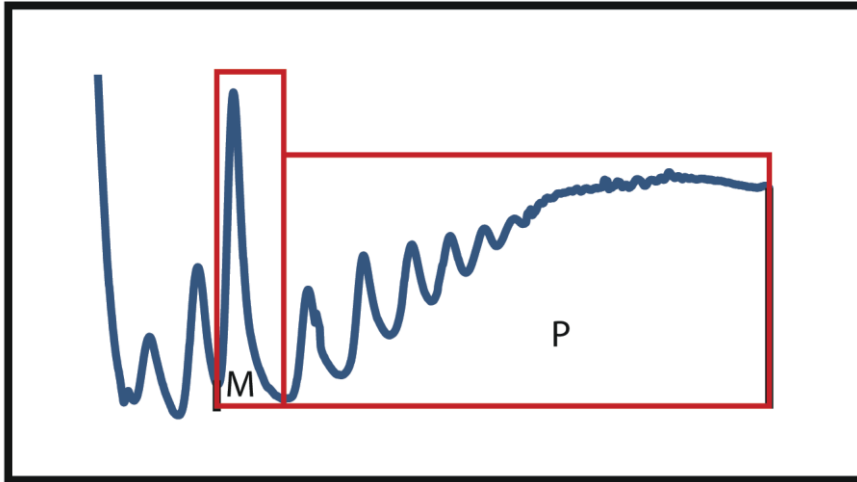


Fig 6-2: P/M ratio calculations. A representative polysome profile shown with sectioning of the monosome (M) and the polysomes (P) as done for P/M ratio calculations. The area M and the area P were measured by ImageJ in order to create a P/M ratio.

6.4 STATISTICAL ANALYSIS

For statistical analysis of P/M ratios, multiple runs were done for each polysome profile. Excel was used to calculate statistical significance using one-tailed type 3 t-tests. Data are presented as mean \pm SEM. * indicates a p-value of $p < 0.05$.

7 RESULTS – DOHH

7.1 DOHH KO IN 3T3 CELLS SHOWS A DEFECT IN TRANSLATION INITIATION

In order to identify what role DOHH plays in mouse cells, a 3T3 cell line was generated by Henning Sievert in the laboratory of Dr. Stefan Balabanov from the mouse model he previously generated. This cell line allows tamoxifen-inducible knockout of DOHH in these cells, which is measurable at the protein level after a period of approximately 8-10 days (shown in Sievert et al., 2014).

The cells used for this experiment were either Cre- or Cre+ DOHH inducible knockout cells. Cre is inducibly expressed in the Cre+ cell line upon the addition of tamoxifen. When Cre is expressed, DOHH is knocked out.

We ran polysome profiles on both cell lines that were untreated, treated just with tamoxifen, or treated with both tamoxifen and cycloheximide. This helped to identify whether any translational alterations were due specifically to the cycloheximide addition, since the effect of cycloheximide on the visualization of translational regulation by polysome profiling has on occasion been questioned. Cre+ DOHH inducible knockout cells induced with either tamoxifen or tamoxifen and cycloheximide showed a visible increase in the monosome peak when compared to Cre- cells treated in the same manner (Fig 7.1 A). This difference was not visible when cells were untreated. An increase in the monosome is indicative of a defect in translation initiation.

P/M ratios were calculated for repeated profiles generated under these conditions (Fig 7.1 B; see Materials and Methods 6.3 for an explanation for P/M ratio calculation). These ratios clearly indicate that there is a statistically measurable effect occurring on the monosome peaks of these profiles, and confirms that translation initiation is being altered under these cellular conditions.

This finding is particularly of interest since previously, the strongest evidence for DOHH's effect on translation was a publication that showed DOHH removal in fruit flies to cause a translation elongation defect, rather than a translation initiation defect (Patel et al., 2009). Others have suggested that eIF5A is involved in translation initiation or the first peptide bond formation (Benne et al., 1978; Blaha et al., 2009). This difference found in our data could be due to the fact that the experiments were run in different model systems. Since DOHH removal has not been previously assayed in a mammalian context, it is possible that DOHH removal in mice could have a different effect on translation than it does in fruit flies.

7.2 INHIBITION OF DHS SHOWS EXAGGERATED DEFECT IN TRANSLATION INITIATION

With the highly interesting results of the consequences of DOHH removal from 3T3 cells, it was important to verify that the 3T3 cells that were used behaved as expected under other conditions. We did this by running polysome profiles after inhibiting DHS, the enzyme that acts on eIF5A upstream of DOHH. DHS is easily inhibited chemically through the addition of GC7. GC7 inhibition of DHS is commonly performed in many cell lines, and has been used to confirm that DHS inhibition causes a strong translation initiation defect in mammalian cells (Landau et al., 2010). If the results we found after the removal of DOHH were non-artificial, these 3T3 cells should also show this known phenotype in response to DHS inhibition.

After addition of GC7 to the 3T3 cells, and generating polysome profiles, we found a very strong increase in the monosome, and decrease in the polysomes (Fig 7.1 C, D). This result was repeatable (n=3) and statistically significant (p=0.026). This showed that application of GC7 to 3T3 cells evokes the predicted phenotype, and indicated that the translation initiation defect found after knockdown of DOHH may be in fact due to the decrease in DOHH, and a unique phenotype found in mammalian cells, as compared to other cells types.

7.3 DEFECT IS NOT DUE TO A CELLULAR GROWTH PHENOTYPE

One possible suggestion for why a translation initiation defect was detected in 3T3 cells with induced knockout of eIF5A was that these cells showed a strong cellular growth phenotype.

Cells stopped proliferating quite quickly, and it may be that this reduction in proliferation is what was visible in the altered translational profile.

In order to verify that this was not the case, we treated the cells with doxorubicin, a chemical widely known to block cell proliferation, and used for this purpose for cancer treatments (Denard, Lee, & Ye, 2012). By running polysome profiling on these cells, we found a general reduction in translation, including reduced monosome and polysome peaks (Fig 7.1 E, F). This profile does not look similar to the profiles generated after DOHH knockout, and therefore supports the idea that the translation alteration that we identified is not due to a reduction in cellular growth.

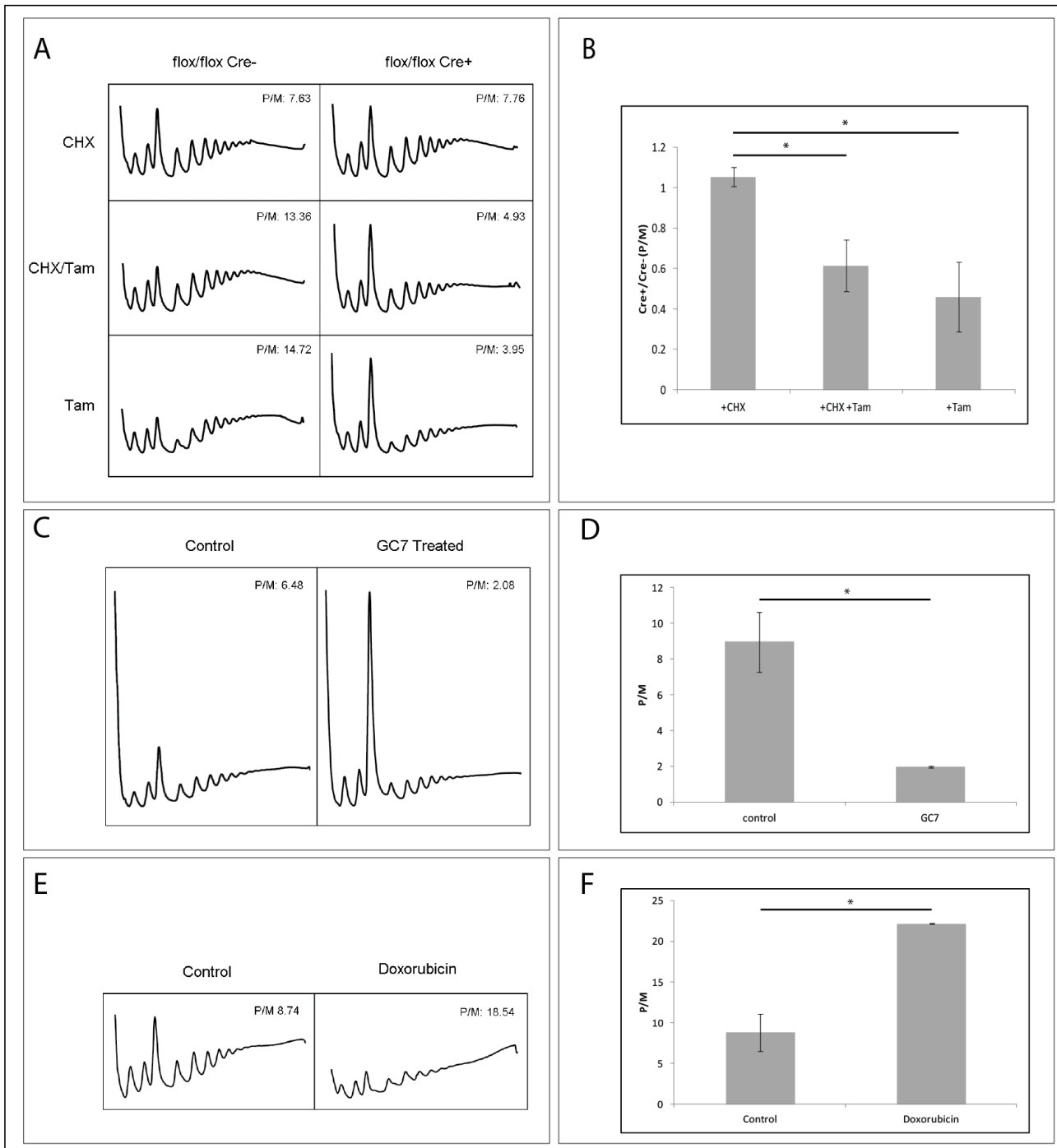


Fig 7.1 Removal of DOHH in conditional KO 3T3 cells shows translation initiation defect

Cells that were Cre-, and therefore would not remove DOHH upon tamoxifen addition, were compared with Cre+ cells that would remove DOHH upon addition of tamoxifen. Little difference was found in the polysome profiles generated by uninduced Cre- and Cre+ cells, or when the P/M ratios were compared between uninduced Cre- and Cre+. However, upon addition of tamoxifen either with or without cycloheximide (CHX), Cre+ 3T3 cells showed a significant reduction in the polysome to monosome ratio when compared to the P/M ratio of Cre- cells (A and B) (P-values: CHX to CHX/Tam: $p=0.03$; CHX to Tam: $p=0.033$; $n=3$; one-tailed, type 3 t-test). This effect was strongly enhanced upon the addition of the DHS inhibitor GC7 (C and D), thus supporting the

translational regulation event seen upon removal of DOHH, as DHS inhibition has been shown to cause initiation defects in mammalian systems (P-value: control to GC7-treated: $p=0.026$; $n=3$; one-tailed, type 3 t-test). In order to rule out an effect caused by reduced cell proliferation, doxorubicin was used to reduce cell proliferation in the same cells. Rather than causing a decreased P/M ratio, this caused a significantly increased P/M ratio, supporting the idea that the effect seen after DOHH removal is not due to a cell growth defect (P-value control to doxo: $p=0.013$; $n=3$; one-tailed, type 3 t-test; * indicates a p value of $p<0.05$). Biological-triplicate data ($n = 3$) are presented as mean \pm SEM. (Figure modified from Sievert et al., 2014).

7.4 SIMILAR TRANSLATION INITIATION DEFECT PHENOTYPE IS SEEN IN MEF CELLS AFTER REMOVAL OF DOHH

As this is the first time that DOHH removal has been linked to a translation initiation defect in mammalian cells, we wanted to confirm these findings using a second model. Since the DOHH inducible knockout 3T3 cells were several passages removed from the original cells taken from the mouse model, we also checked translation in MEF cells generated in the Balabanov laboratory. These cells were generated from the same mice as the 3T3 cells, but were less well established, and showed a less complete removal of DOHH upon tamoxifen induction (Personal communication with the Balabanov laboratory). These cells were either floxed DOHH Cre⁺ (which would remove DOHH upon the addition of tamoxifen) or wildtype (+/+) Cre⁺ (which would not remove DOHH). The cells were treated with tamoxifen, and we then lysed these cells and ran polysome profiles to compare floxed DOHH with +/+.

Similar to our 3T3 cells, we saw a trend towards an increase in the monosome peak for the floxed DOHH in MEF cells (Fig 7.2). This increase was not as drastic as the increase found after knockout of DOHH in the 3T3 cells, but this could likely be due to the fact that the removal of DOHH protein in the MEF cells was less complete than in the 3T3 cells (Personal communication with the Balabanov laboratory). Although it did not reach statistical significance, the trend found in MEF cells clearly supports the likelihood that the translation initiation defect found was a true effect of the removal of DOHH from mammalian cells.

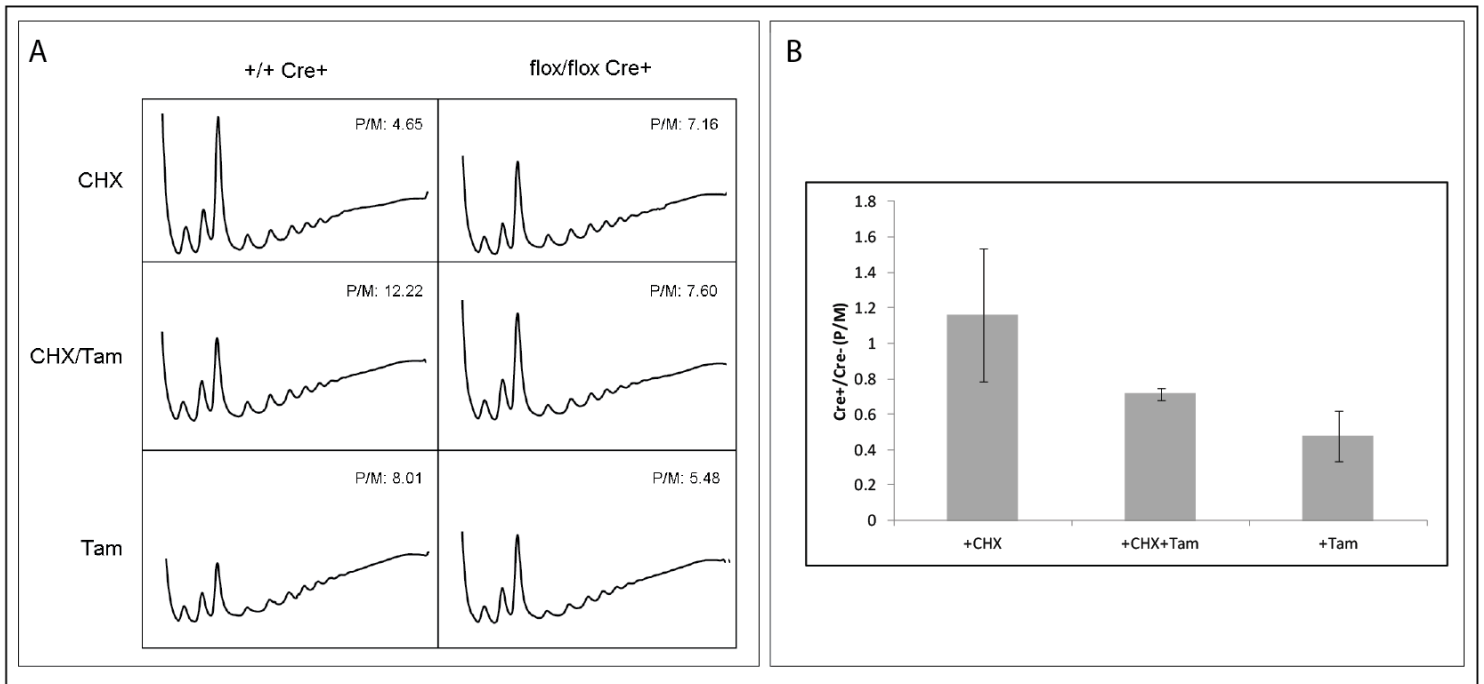


Fig 7.2 Knockout of DOHH in MEF cells shows similar trend in P/M ratio adjustments

A. Similar polysome profiling experiments were run in MEF cells with DOHH inducibly removed. An increase in the monosome peak was seen upon tamoxifen or tamoxifen/cycloheximide addition to the Cre⁺ cells. B. This decrease in the polysome to monosome ratio was not statistically significant, but definitely trending toward the same relationship as found in the 3T3 cells (P-values: Cycloheximide (CHX) to CHX/Tam: $p=0.222$; CHX to Tam: $p=0.147$; $n=3$; one-tailed, type 3 t-test; * indicates a p value of $p<0.05$). Biological-triplicate data ($n = 3$) are presented as mean \pm SEM.

8 DISCUSSION - DOHH

In the present study, we demonstrated through polysome profiling in cell culture experiments that removal of DOHH in a mammalian system causes an initiation defect. This is the first time that DOHH has been removed in a mammalian system, and the first time that the translational effect of DOHH removal in a mammalian system has been assayed.

8.1 DOHH REMOVAL FROM 3T3 AND MEF CELLS CAUSES AN INITIATION DEFECT

The polysome to monosome ratio is consistently used in the field of translation research to monitor global translational changes. A decrease in the polysome to monosome ratio indicates a likely initiation defect, while an increase in the polysome to monosome ratio indicates a likely elongation defect.

Using 3T3 cells that were derived in the Balabanov laboratory from the DOHH Cre KO mouse, we were able to inducibly remove DOHH upon tamoxifen addition to cell culture media. Cells with DOHH knocked out showed an increase in the 80S monosome and a statistically significant decrease in the polysome to monosome ratio (Fig 7.1 A, B). This indicates a likely initiation defect.

In order to further confirm our findings, we checked how the addition of GC7 (a DHS inhibitor) affected our 3T3 cells. GC7 has been shown previously to induce a strong initiation defect in mammalian cells (Landau et al., 2010). Our findings also confirm a highly significant decrease in the polysome to monosome ratio, consistent with an initiation defect (Fig 7.1 C, D). This result showed that application of GC7 to 3T3 cells evoked the predicted phenotype, and suggested that the similar translation initiation defect found after knockdown of DOHH may be a result of the decrease in DOHH, and a unique phenotype found in mammalian cells, as compared to other cells types.

Since our DOHH knockout results could have been due to the growth defect that is induced by removal of DOHH, we also checked the polysome profiles of our 3T3 cells after the

addition of doxorubicin – a known proliferation inhibitor. While doxorubicin did visibly inhibit cell proliferation (data not shown), it did not produce an initiation defect in the cells. Rather it reduced the monosome peak, and showed an increased polysome to monosome ratio, suggesting an elongation defect (Fig 7.1 E, F). This indicates that the initiation defect that we saw after removal of DOHH was not specifically due to the growth defect that DOHH removal causes.

We further confirmed our 3T3 cell findings by testing MEF cells derived by the Balabanov laboratory from the same mouse cell line. When polysome profiles were run on MEF cells with DOHH knocked out, the profiles showed a decreased polysome to monosome ratio, though not statistically significant (Fig 7.2). This did, however, support the idea that the result we found in 3T3 cells was not specific to these cells, but may have been a general consequence of DOHH removal in mammalian cells.

All of these findings are highly interesting, as this is the first time that DOHH removal has been studied in a mammalian context. Previously, knockout of DOHH in *Drosophila* suggested an elongation defect, rather than the initiation defect that we observed (Patel et al., 2009). This difference in results can be explained in several different ways. The most likely reason is that DOHH function has evolved over time, and that the hypusine function has evolved different functions in different species. For instance, DOHH is non-essential in yeast, while removal of DOHH in *Drosophila* or mice is embryonic lethal. This suggests that the full hypusine modification generated by DOHH may have a different function in yeast than it does in multicellular eukaryotes. Additionally, eIF5A1 and 2 have altered expression patterns in different species, indicating that their functions may be different across species. Since mammals have complex cellular systems that can differ from other models, it is possible that the hypusine modification in eIF5A imparts a different function in mammals than in *Drosophila* or yeast.

In order to confirm the fact that an initiation defect occurs in all mammalian cells, and not specifically in our cell culture, there are several experiments that could be performed. The first, and likely easiest, would be to generate polysome profiles from tissue taken from the DOHH-KO mouse line. This would show that the altered polysome to monosome ratio is not a consequence of some characteristics of the cell line, but rather a specific mammalian occurrence.

Additionally, using a method such as ribosome footprinting, it would be possible to identify where the ribosomes are sitting on mRNAs that are being translated. If ribosome footprints are found at the mRNA start codon, rather than piling up as is seen with elongation defects, this would further confirm the initiation defect.

8.2 GENERAL CONCLUSION

This was the first time that the effect on translation incurred by removal of DOHH was studied in a mammalian context. Interestingly, we determined that DOHH removal in murine 3T3 cells generated a translation initiation defect. This effect differs from the elongation defect reported for other eukaryotes, such as *Drosophila*, and suggests that the full hypusine modification in the mammalian context has evolved to have a different function than in other eukaryotes. Importantly, eIF5A would be an exceptional drug target, due to the fact that it is the only known protein to contain the unique amino acid hypusine. Further study on how the hypusine modification regulates eIF5A's function in translation will be of great interest both at the level of general science and with regard to drug therapies.

9 REFERENCES

- Abbruzzese, A., Park, M. H., & Folk, J. E. (1986). Deoxyhypusine hydroxylase from rat testis. Partial purification and characterization. *The Journal of Biological Chemistry*, *261*(7), 3085–9. Retrieved from <http://www.ncbi.nlm.nih.gov/pubmed/3949761>
- Arai, T., Hasegawa, M., Akiyama, H., Ikeda, K., Nonaka, T., Mori, H., ... Oda, T. (2006). TDP-43 is a component of ubiquitin-positive tau-negative inclusions in frontotemporal lobar degeneration and amyotrophic lateral sclerosis. *Biochemical and Biophysical Research Communications*, *351*(3), 602–11. doi:10.1016/j.bbrc.2006.10.093
- Arai, T., Hasegawa, M., Nonaka, T., Kametani, F., Yamashita, M., Hosokawa, M., ... Akiyama, H. (2010). Phosphorylated and cleaved TDP-43 in ALS, FTLD and other neurodegenerative disorders and in cellular models of TDP-43 proteinopathy. *Neuropathology: Official Journal of the Japanese Society of Neuropathology*, *30*(2), 170–81. doi:10.1111/j.1440-1789.2009.01089.x
- Arnold, E. S., Ling, S.-C., Huelga, S. C., Lagier-Tourenne, C., Polymenidou, M., Ditsworth, D., ... Cleveland, D. W. (2013). ALS-linked TDP-43 mutations produce aberrant RNA splicing and adult-onset motor neuron disease without aggregation or loss of nuclear TDP-43. *Proceedings of the National Academy of Sciences of the United States of America*, *110*(8), E736–45. doi:10.1073/pnas.1222809110
- Ayala, V., Granado-Serrano, A. B., Cacabelos, D., Naudí, A., Ilieva, E. V., Boada, J., ... Portero-Otin, M. (2011). Cell stress induces TDP-43 pathological changes associated with ERK1/2 dysfunction: implications in ALS. *Acta Neuropathologica*, *122*(3), 259–70. doi:10.1007/s00401-011-0850-y
- Ballard, C., Gauthier, S., Corbett, A., Brayne, C., Aarsland, D., & Jones, E. (2011). Alzheimer's disease. *Lancet*, *377*(9770), 1019–31. doi:10.1016/S0140-6736(10)61349-9
- Barmada, S. J., Skibinski, G., Korb, E., Rao, E. J., Wu, J. Y., & Finkbeiner, S. (2010). Cytoplasmic mislocalization of TDP-43 is toxic to neurons and enhanced by a mutation associated with familial amyotrophic lateral sclerosis. *The Journal of Neuroscience: The Official Journal of the Society for Neuroscience*, *30*(2), 639–49. doi:10.1523/JNEUROSCI.4988-09.2010
- Benajiba, L., Le Ber, I., Camuzat, A., Lacoste, M., Thomas-Anterion, C., Couratier, P., ... Brice, A. (2009). TARDBP mutations in motoneuron disease with frontotemporal lobar degeneration. *Annals of Neurology*, *65*(4), 470–3. doi:10.1002/ana.21612
- Benne, R., Brown-Luedi, M. L., & Hershey, J. W. (1978). Purification and characterization of protein synthesis initiation factors eIF-1, eIF-4C, eIF-4D, and eIF-5 from rabbit reticulocytes. *The Journal of Biological Chemistry*, *253*(9), 3070–7. Retrieved from <http://www.ncbi.nlm.nih.gov/pubmed/641055>
- Ben-Shem, A., Garreau de Loubresse, N., Melnikov, S., Jenner, L., Yusupova, G., & Yusupov, M. (2011). The structure of the eukaryotic ribosome at 3.0 Å resolution. *Science (New York, N.Y.)*, *334*(6062), 1524–9. doi:10.1126/science.1212642

- Blaha, G., Stanley, R. E., & Steitz, T. A. (2009). Formation of the first peptide bond: the structure of EF-P bound to the 70S ribosome. *Science (New York, N.Y.)*, 325(5943), 966–70. doi:10.1126/science.1175800
- Blobel, G., & Sabatini, D. (1971). Dissociation of mammalian polyribosomes into subunits by puromycin. *Proceedings of the National Academy of Sciences of the United States of America*, 68(2), 390–4. Retrieved from <http://www.pubmedcentral.nih.gov/articlerender.fcgi?artid=388945&tool=pmcentrez&rendertype=abstract>
- Bor, Y. C., Swartz, J., Li, Y., Coyle, J., Rekosh, D., & Hammarskjold, M.-L. (2006). Northern Blot analysis of mRNA from mammalian polyribosomes. *Protocol Exchange*, 1–16. doi:10.1038/nprot.2006.216
- Brody, E., & Abelson, J. (1985). The “spliceosome”: yeast pre-messenger RNA associates with a 40S complex in a splicing-dependent reaction. *Science (New York, N.Y.)*, 228(4702), 963–7. Retrieved from <http://www.ncbi.nlm.nih.gov/pubmed/3890181>
- Brookmeyer, R., Johnson, E., Ziegler-Graham, K., & Arrighi, H. M. (2007). Forecasting the global burden of Alzheimer’s disease. *Alzheimer’s & Dementia: The Journal of the Alzheimer’s Association*, 3(3), 186–91. doi:10.1016/j.jalz.2007.04.381
- Buratti, E., Dörk, T., Zuccato, E., Pagani, F., Romano, M., & Baralle, F. E. (2001). Nuclear factor TDP-43 and SR proteins promote in vitro and in vivo CFTR exon 9 skipping. *The EMBO Journal*, 20(7), 1774–84. doi:10.1093/emboj/20.7.1774
- Chaudhury, A., Chander, P., & Howe, P. H. (2010). Heterogeneous nuclear ribonucleoproteins (hnRNPs) in cellular processes: Focus on hnRNP E1’s multifunctional regulatory roles. *RNA (New York, N.Y.)*, 16(8), 1449–62. doi:10.1261/rna.2254110
- Chen-Plotkin, A. S., Lee, V. M.-Y., & Trojanowski, J. Q. (2010). TAR DNA-binding protein 43 in neurodegenerative disease. *Nature Reviews. Neurology*, 6(4), 211–20. doi:10.1038/nrneurol.2010.18
- Christopher K. Mathews, Kensal E. van Holde, D. R. Appling, S. R. A.-C. (2012). *Biochemistry (4th Edition)* (p. 1368). Prentice Hall.
- Colombrita, C., Zennaro, E., Fallini, C., Weber, M., Sommacal, A., Buratti, E., ... Ratti, A. (2009). TDP-43 is recruited to stress granules in conditions of oxidative insult. *Journal of Neurochemistry*, 111(4), 1051–61. doi:10.1111/j.1471-4159.2009.06383.x
- Cooper, H. L., Park, M. H., & Folk, J. E. (1982). Posttranslational formation of hypusine in a single major protein occurs generally in growing cells and is associated with activation of lymphocyte growth. *Cell*, 29(3), 791–7. Retrieved from <http://www.ncbi.nlm.nih.gov/pubmed/6817926>
- D’Ambrogio, A., Buratti, E., Stuani, C., Guarnaccia, C., Romano, M., Ayala, Y. M., & Baralle, F. E. (2009). Functional mapping of the interaction between TDP-43 and hnRNP A2 in vivo. *Nucleic Acids Research*, 37(12), 4116–26. doi:10.1093/nar/gkp342

- Davie, C. a. (2008). A review of Parkinson's disease. *British Medical Bulletin*, *86*, 109–27. doi:10.1093/bmb/ldn013
- DeJesus-Hernandez, M., Mackenzie, I. R., Boeve, B. F., Boxer, A. L., Baker, M., Rutherford, N. J., ... Rademakers, R. (2011). Expanded GGGGCC hexanucleotide repeat in noncoding region of C9ORF72 causes chromosome 9p-linked FTD and ALS. *Neuron*, *72*(2), 245–56. doi:10.1016/j.neuron.2011.09.011
- Denard, B., Lee, C., & Ye, J. (2012). Doxorubicin blocks proliferation of cancer cells through proteolytic activation of CREB3L1. *eLife*, *1*, e00090. doi:10.7554/eLife.00090
- Duncan, K., Grskovic, M., Strein, C., Beckmann, K., Niggeweg, R., Abaza, I., ... Hentze, M. W. (2006). Sex-lethal imparts a sex-specific function to UNR by recruiting it to the msl-2 mRNA 3' UTR: translational repression for dosage compensation. *Genes & Development*, *20*(3), 368–79. doi:10.1101/gad.371406
- Elden, A. C., Kim, H.-J., Hart, M. P., Chen-Plotkin, A. S., Johnson, B. S., Fang, X., ... Gitler, A. D. (2010). Ataxin-2 intermediate-length polyglutamine expansions are associated with increased risk for ALS. *Nature*, *466*(7310), 1069–75. doi:10.1038/nature09320
- Esmaili, M. a, Panahi, M., Yadav, S., Hennings, L., & Kiaei, M. (2013). Premature death of TDP-43 (A315T) transgenic mice due to gastrointestinal complications prior to development of full neurological symptoms of amyotrophic lateral sclerosis. *International Journal of Experimental Pathology*, *94*(1), 56–64. doi:10.1111/iep.12006
- Feldman, H., Levy, a. R., Hsiung, G.-Y., Peters, K. R., Donald, a., Black, S. E., ... Rockwood, K. (2003). A Canadian Cohort Study of Cognitive Impairment and Related Dementias (ACCORD): Study Methods and Baseline Results. *Neuroepidemiology*, *22*(5), 265–274. doi:10.1159/000071189
- Feng, Y., Absher, D., Eberhart, D. E., Brown, V., Malter, H. E., & Warren, S. T. (1997). FMRP associates with polyribosomes as an mRNP, and the I304N mutation of severe fragile X syndrome abolishes this association. *Molecular Cell*, *1*(1), 109–18. Retrieved from <http://www.ncbi.nlm.nih.gov/pubmed/9659908>
- Fiesel, F. C., Schurr, C., Weber, S. S., & Kahle, P. J. (2011). TDP-43 knockdown impairs neurite outgrowth dependent on its target histone deacetylase 6. *Molecular Neurodegeneration*, *6*, 64. doi:10.1186/1750-1326-6-64
- Fiesel, F. C., Weber, S. S., Supper, J., Zell, A., & Kahle, P. J. (2012). TDP-43 regulates global translational yield by splicing of exon junction complex component SKAR. *Nucleic Acids Research*, *40*(6), 2668–82. doi:10.1093/nar/gkr1082
- Fraser, C. S., & Doudna, J. a. (2007). Structural and mechanistic insights into hepatitis C viral translation initiation. *Nature Reviews. Microbiology*, *5*(1), 29–38. doi:10.1038/nrmicro1558
- Freibaum, B. D., Chitta, R. K., High, A. A., & Taylor, J. P. (2010). Global analysis of TDP-43 interacting proteins reveals strong association with RNA splicing and translation machinery. *Journal of Proteome Research*, *9*(2), 1104–20. doi:10.1021/pr901076y

- Gebauer, F., & Hentze, M. W. (2004). Molecular mechanisms of translational control. *Nature Reviews. Molecular Cell Biology*, 5(10), 827–35. doi:10.1038/nrm1488
- Geser, F., Lee, V. M.-Y., & Trojanowski, J. Q. (2010). Amyotrophic lateral sclerosis and frontotemporal lobar degeneration: a spectrum of TDP-43 proteinopathies. *Neuropathology: Official Journal of the Japanese Society of Neuropathology*, 30(2), 103–12. doi:10.1111/j.1440-1789.2009.01091.x
- Gilbert, W. V. (2010). Alternative ways to think about cellular internal ribosome entry. *The Journal of Biological Chemistry*, 285(38), 29033–8. doi:10.1074/jbc.R110.150532
- Goldstein, J. L., Beaudet, a L., & Caskey, C. T. (1970). Peptide chain termination with mammalian release factor. *Proceedings of the National Academy of Sciences of the United States of America*, 67(1), 99–106. Retrieved from <http://www.pubmedcentral.nih.gov/articlerender.fcgi?artid=283173&tool=pmcentrez&rendertype=abstract>
- He, L.-R., Zhao, H.-Y., Li, B.-K., Liu, Y.-H., Liu, M.-Z., Guan, X.-Y., ... Xie, D. (2011). Overexpression of eIF5A-2 is an adverse prognostic marker of survival in stage I non-small cell lung cancer patients. *International Journal of Cancer. Journal International Du Cancer*, 129(1), 143–50. doi:10.1002/ijc.25669
- Heiman, M., Schaefer, A., Gong, S., Peterson, J. D., Day, M., Ramsey, K. E., ... Heintz, N. (2008). A translational profiling approach for the molecular characterization of CNS cell types. *Cell*, 135(4), 738–48. doi:10.1016/j.cell.2008.10.028
- Higashi, S., Kabuta, T., Nagai, Y., Tsuchiya, Y., Akiyama, H., & Wada, K. (2013). TDP-43 associates with stalled ribosomes and contributes to cell survival during cellular stress. *Journal of Neurochemistry*, 126(2), 288–300. doi:10.1111/jnc.12194
- Iida, Y. (1996). Strength of translation initiation signal sequence of mRNA as studied by quantification method: effect of nucleotide substitutions upon translation efficiency in rat preproinsulin mRNA. *Nucleic Acids Research*, 24(17), 3313–3316. doi:10.1093/nar/24.17.3313
- Ingolia, N. T., Ghaemmaghami, S., Newman, J. R. S., & Weissman, J. S. (2009). Genome-wide analysis in vivo of translation with nucleotide resolution using ribosome profiling. *Science (New York, N.Y.)*, 324(5924), 218–23. doi:10.1126/science.1168978
- Jackson, R. J., Hellen, C. U. T., & Pestova, T. V. (2010). The mechanism of eukaryotic translation initiation and principles of its regulation. *Nature Reviews. Molecular Cell Biology*, 11(2), 113–27. doi:10.1038/nrm2838
- Jensen, K. B., Dredge, B. K., Stefani, G., Zhong, R., Buckanovich, R. J., Okano, H. J., ... Darnell, R. B. (2000). Nova-1 regulates neuron-specific alternative splicing and is essential for neuronal viability. *Neuron*, 25(2), 359–71. Retrieved from <http://www.ncbi.nlm.nih.gov/pubmed/10719891>
- Johannes, G., & Sarnow, P. (1998). Cap-independent polysomal association of natural mRNAs encoding c-myc, BiP, and eIF4G conferred by internal ribosome entry sites. *RNA (New York, N.Y.)*, 4(12), 1500–13. Retrieved from

<http://www.pubmedcentral.nih.gov/articlerender.fcgi?artid=1369721&tool=pmcentrez&endertype=abstract>

- Kabashi, E., Lin, L., Tradewell, M. L., Dion, P. a, Bercier, V., Bourguoin, P., ... Drapeau, P. (2010). Gain and loss of function of ALS-related mutations of TARDBP (TDP-43) cause motor deficits in vivo. *Human Molecular Genetics*, *19*(4), 671–83. doi:10.1093/hmg/ddp534
- Kabashi, E., Valdmanis, P. N., Dion, P., Spiegelman, D., McConkey, B. J., Vande Velde, C., ... Rouleau, G. a. (2008). TARDBP mutations in individuals with sporadic and familial amyotrophic lateral sclerosis. *Nature Genetics*, *40*(5), 572–4. doi:10.1038/ng.132
- Keeling, P. J., & Inagaki, Y. (2004). A class of eukaryotic GTPase with a punctate distribution suggesting multiple functional replacements of translation elongation factor 1alpha. *Proceedings of the National Academy of Sciences of the United States of America*, *101*(43), 15380–5. doi:10.1073/pnas.0404505101
- Kiernan, M. C., Vucic, S., Cheah, B. C., Turner, M. R., Eisen, A., Hardiman, O., ... Zoing, M. C. (2011). Amyotrophic lateral sclerosis. *Lancet*, *377*(9769), 942–55. doi:10.1016/S0140-6736(10)61156-7
- Kozak, M. (1987). At least six nucleotides preceding the AUG initiator codon enhance translation in mammalian cells. *Journal of Molecular Biology*, *196*(4), 947–50. Retrieved from <http://www.ncbi.nlm.nih.gov/pubmed/3681984>
- Kwiatkowski, T. J., Bosco, D. a, Leclerc, a L., Tamrazian, E., Vanderburg, C. R., Russ, C., ... Brown, R. H. (2009). Mutations in the FUS/TLS gene on chromosome 16 cause familial amyotrophic lateral sclerosis. *Science (New York, N.Y.)*, *323*(5918), 1205–8. doi:10.1126/science.1166066
- Lagier-Tourenne, C., Polymenidou, M., & Cleveland, D. W. (2010). TDP-43 and FUS/TLS: emerging roles in RNA processing and neurodegeneration. *Human Molecular Genetics*, *19*(R1), R46–64. doi:10.1093/hmg/ddq137
- Landau, G., Bercovich, Z., Park, M. H., & Kahana, C. (2010). The role of polyamines in supporting growth of mammalian cells is mediated through their requirement for translation initiation and elongation. *The Journal of Biological Chemistry*, *285*(17), 12474–81. doi:10.1074/jbc.M110.106419
- Liachko, N. F., Guthrie, C. R., & Kraemer, B. C. (2010). Phosphorylation promotes neurotoxicity in a *Caenorhabditis elegans* model of TDP-43 proteinopathy. *The Journal of Neuroscience: The Official Journal of the Society for Neuroscience*, *30*(48), 16208–19. doi:10.1523/JNEUROSCI.2911-10.2010
- Liu-Yesucevitz, L., Lin, A. Y., Ebata, A., Boon, J. Y., Reid, W., Xu, Y.-F., ... Wolozin, B. (2014). ALS-linked mutations enlarge TDP-43-enriched neuronal RNA granules in the dendritic arbor. *The Journal of Neuroscience: The Official Journal of the Society for Neuroscience*, *34*(12), 4167–74. doi:10.1523/JNEUROSCI.2350-13.2014

- Logroscino, G., Traynor, B. J., Hardiman, O., Chiò, A., Mitchell, D., Swingler, R. J., ... Beghi, E. (2010). Incidence of amyotrophic lateral sclerosis in Europe. *Journal of Neurology, Neurosurgery, and Psychiatry*, *81*(4), 385–90. doi:10.1136/jnnp.2009.183525
- Mackenzie, I. R. a, Bigio, E. H., Ince, P. G., Geser, F., Neumann, M., Cairns, N. J., ... Trojanowski, J. Q. (2007). Pathological TDP-43 distinguishes sporadic amyotrophic lateral sclerosis from amyotrophic lateral sclerosis with SOD1 mutations. *Annals of Neurology*, *61*(5), 427–34. doi:10.1002/ana.21147
- Maier, B., Tersey, S. A., & Mirmira, R. G. (2010). Hypusine: a new target for therapeutic intervention in diabetic inflammation. *Discovery Medicine*, *10*(50), 18–23. Retrieved from <http://www.ncbi.nlm.nih.gov/pubmed/20670594>
- Malys, N., & McCarthy, J. E. G. (2011). Translation initiation: variations in the mechanism can be anticipated. *Cellular and Molecular Life Sciences: CMLS*, *68*(6), 991–1003. doi:10.1007/s00018-010-0588-z
- McKee, A. C., Gavett, B. E., Stern, R. A., Nowinski, C. J., Cantu, R. C., Kowall, N. W., ... Budson, A. E. (2010). TDP-43 proteinopathy and motor neuron disease in chronic traumatic encephalopathy. *Journal of Neuropathology and Experimental Neurology*, *69*(9), 918–29. doi:10.1097/NEN.0b013e3181ee7d85
- Moisse, K., Volkening, K., Leystra-Lantz, C., Welch, I., Hill, T., & Strong, M. J. (2009). Divergent patterns of cytosolic TDP-43 and neuronal progranulin expression following axotomy: implications for TDP-43 in the physiological response to neuronal injury. *Brain Research*, *1249*, 202–11. doi:10.1016/j.brainres.2008.10.021
- Mori, K., Weng, S.-M., Arzberger, T., May, S., Rentzsch, K., Kremmer, E., ... Edbauer, D. (2013). The C9orf72 GGGGCC repeat is translated into aggregating dipeptide-repeat proteins in FTL/ALS. *Science (New York, N.Y.)*, *339*(6125), 1335–8. doi:10.1126/science.1232927
- Munroe, D., & Jacobson, A. (1990). mRNA poly(A) tail, a 3' enhancer of translational initiation. *Molecular and Cellular Biology*, *10*(7), 3441–55. Retrieved from <http://www.pubmedcentral.nih.gov/articlerender.fcgi?artid=360780&tool=pmcentrez&rendertype=abstract>
- Muthukrishnan, S., Both, G. W., Furuichi, Y., & Shatkin, A. J. (1975). 5'-Terminal 7-methylguanosine in eukaryotic mRNA is required for translation. *Nature*, *255*(5503), 33–7. Retrieved from <http://www.ncbi.nlm.nih.gov/pubmed/165427>
- Nakashima-Yasuda, H., Uryu, K., Robinson, J., Xie, S. X., Hurtig, H., Duda, J. E., ... Trojanowski, J. Q. (2007). Co-morbidity of TDP-43 proteinopathy in Lewy body related diseases. *Acta Neuropathologica*, *114*(3), 221–9. doi:10.1007/s00401-007-0261-2
- Nalavadi, V. C., Muddashetty, R. S., Gross, C., & Bassell, G. J. (2012). Dephosphorylation-induced ubiquitination and degradation of FMRP in dendrites: a role in immediate early mGluR-stimulated translation. *The Journal of Neuroscience: The Official Journal of the Society for Neuroscience*, *32*(8), 2582–7. doi:10.1523/JNEUROSCI.5057-11.2012

- Napoli, I., Mercaldo, V., Boyd, P. P., Eleuteri, B., Zalfa, F., De Rubeis, S., ... Bagni, C. (2008). The fragile X syndrome protein represses activity-dependent translation through CYFIP1, a new 4E-BP. *Cell*, *134*(6), 1042–54. doi:10.1016/j.cell.2008.07.031
- Nazar, R. N. (2004). Ribosomal RNA processing and ribosome biogenesis in eukaryotes. *IUBMB Life*, *56*(8), 457–65. doi:10.1080/15216540400010867
- Neary, D., Snowden, J., & Mann, D. (2005). Frontotemporal dementia. *Lancet Neurology*, *4*(11), 771–80. doi:10.1016/S1474-4422(05)70223-4
- Neumann, M., Sampathu, D. M., Kwong, L. K., Truax, A. C., Micsenyi, M. C., Chou, T. T., ... Lee, V. M.-Y. (2006). Ubiquitinated TDP-43 in frontotemporal lobar degeneration and amyotrophic lateral sclerosis. *Science (New York, N.Y.)*, *314*(5796), 130–3. doi:10.1126/science.1134108
- Nishimura, K., Lee, S. B., Park, J. H., & Park, M. H. (2012). Essential role of eIF5A-1 and deoxyhypusine synthase in mouse embryonic development. *Amino Acids*, *42*(2-3), 703–10. doi:10.1007/s00726-011-0986-z
- Ou, S. H., Wu, F., Harrich, D., García-Martínez, L. F., & Gaynor, R. B. (1995). Cloning and characterization of a novel cellular protein, TDP-43, that binds to human immunodeficiency virus type 1 TAR DNA sequence motifs. *Journal of Virology*, *69*(6), 3584–96. Retrieved from <http://www.pubmedcentral.nih.gov/articlerender.fcgi?artid=189073&tool=pmcentrez&rendertype=abstract>
- Park, J.-H., Aravind, L., Wolff, E. C., Kaevel, J., Kim, Y. S., & Park, M. H. (2006). Molecular cloning, expression, and structural prediction of deoxyhypusine hydroxylase: a HEAT-repeat-containing metalloenzyme. *Proceedings of the National Academy of Sciences of the United States of America*, *103*(1), 51–6. doi:10.1073/pnas.0509348102
- Park, M. H., Cooper, H. L., & Folk, J. E. (1981). Identification of hypusine, an unusual amino acid, in a protein from human lymphocytes and of spermidine as its biosynthetic precursor. *Proceedings of the National Academy of Sciences of the United States of America*, *78*(5), 2869–73. Retrieved from <http://www.pubmedcentral.nih.gov/articlerender.fcgi?artid=319460&tool=pmcentrez&rendertype=abstract>
- Park, M. H., Nishimura, K., Zanelli, C. F., & Valentini, S. R. (2010). Functional significance of eIF5A and its hypusine modification in eukaryotes. *Amino Acids*, *38*(2), 491–500. doi:10.1007/s00726-009-0408-7
- Patel, P. H., Costa-Mattioli, M., Schulze, K. L., & Bellen, H. J. (2009). The *Drosophila* deoxyhypusine hydroxylase homologue nero and its target eIF5A are required for cell growth and the regulation of autophagy. *The Journal of Cell Biology*, *185*(7), 1181–94. doi:10.1083/jcb.200904161
- Pestova, T. V., & Kolupaeva, V. G. (2002). The roles of individual eukaryotic translation initiation factors in ribosomal scanning and initiation codon selection. *Genes & Development*, *16*(22), 2906–22. doi:10.1101/gad.1020902

- Pisarev, A. V, Skabkin, M. A., Pisareva, V. P., Skabkina, O. V, Rakotondrafara, A. M., Hentze, M. W., ... Pestova, T. V. (2010). The role of ABCE1 in eukaryotic posttermination ribosomal recycling. *Molecular Cell*, 37(2), 196–210. doi:10.1016/j.molcel.2009.12.034
- Polymenidou, M., Lagier-Tourenne, C., Hutt, K. R., Huelga, S. C., Moran, J., Liang, T. Y., ... Cleveland, D. W. (2011). Long pre-mRNA depletion and RNA missplicing contribute to neuronal vulnerability from loss of TDP-43. *Nature Neuroscience*, 14(4), 459–68. doi:10.1038/nn.2779
- Renton, A. E., Majounie, E., Waite, A., Simón-Sánchez, J., Rollinson, S., Gibbs, J. R., ... Traynor, B. J. (2011). A hexanucleotide repeat expansion in C9ORF72 is the cause of chromosome 9p21-linked ALS-FTD. *Neuron*, 72(2), 257–68. doi:10.1016/j.neuron.2011.09.010
- Ritson, G. P., Custer, S. K., Freibaum, B. D., Guinto, J. B., Geffel, D., Moore, J., ... Taylor, J. P. (2010). TDP-43 mediates degeneration in a novel *Drosophila* model of disease caused by mutations in VCP/p97. *The Journal of Neuroscience: The Official Journal of the Society for Neuroscience*, 30(22), 7729–39. doi:10.1523/JNEUROSCI.5894-09.2010
- Rosen, D. R., Siddique, T., Patterson, D., Figlewicz, D. A., Sapp, P., Hentati, A., ... Deng, H. X. (1993). Mutations in Cu/Zn superoxide dismutase gene are associated with familial amyotrophic lateral sclerosis. *Nature*, 362(6415), 59–62. doi:10.1038/362059a0
- Russell, P. J. (2009). *iGenetics: A Molecular Approach*, 3/E (p. 848). Benjamin Cummings.
- Saini, P., Eyler, D. E., Green, R., & Dever, T. E. (2009). Hypusine-containing protein eIF5A promotes translation elongation. *Nature*, 459(7243), 118–21. doi:10.1038/nature08034
- Salazar-Grueso, E. F., Kim, S., & Kim, H. (1991). Embryonic mouse spinal cord motor neuron hybrid cells. *Neuroreport*, 2(9), 505–8. Retrieved from <http://www.ncbi.nlm.nih.gov/pubmed/1751804>
- Sasaki, K., Abid, M. R., & Miyazaki, M. (1996). Deoxyhypusine synthase gene is essential for cell viability in the yeast *Saccharomyces cerevisiae*. *FEBS Letters*, 384(2), 151–4. Retrieved from <http://www.ncbi.nlm.nih.gov/pubmed/8612813>
- Schwelberger, H. G., Kang, H. A., & Hershey, J. W. (1993). Translation initiation factor eIF-5A expressed from either of two yeast genes or from human cDNA. Functional identity under aerobic and anaerobic conditions. *The Journal of Biological Chemistry*, 268(19), 14018–25. Retrieved from <http://www.ncbi.nlm.nih.gov/pubmed/8314769>
- Sephton, C. F., Good, S. K., Atkin, S., Dewey, C. M., Mayer, P., Herz, J., & Yu, G. (2010). TDP-43 is a developmentally regulated protein essential for early embryonic development. *The Journal of Biological Chemistry*, 285(9), 6826–34. doi:10.1074/jbc.M109.061846
- Shiba, T., Mizote, H., Kaneko, T., Nakajima, T., & Kakimoto, Y. (1971). Hypusine, a new amino acid occurring in bovine brain. Isolation and structural determination. *Biochimica et Biophysica Acta*, 244(3), 523–31. Retrieved from <http://www.ncbi.nlm.nih.gov/pubmed/4334286>

- Sievert, H., Pällmann, N., Miller, K. K., Hermans-Borgmeyer, I., Venz, S., Sendoel, A., ... Balabanov, S. (2014). A novel mouse model for inhibition of DOHH mediated hypusine modification reveals crucial function for embryonic development, proliferation and oncogenic transformation. *Disease Models & Mechanisms*, (May). doi:10.1242/dmm.014449
- Slegers, K., Cruts, M., & Van Broeckhoven, C. (2010). Molecular pathways of frontotemporal lobar degeneration. *Annual Review of Neuroscience*, 33, 71–88. doi:10.1146/annurev-neuro-060909-153144
- Sreedharan, J., Blair, I. P., Tripathi, V. B., Hu, X., Vance, C., Rogelj, B., ... Shaw, C. E. (2008). TDP-43 mutations in familial and sporadic amyotrophic lateral sclerosis. *Science (New York, N.Y.)*, 319(5870), 1668–72. doi:10.1126/science.1154584
- Taylor, D. J., Nilsson, J., Merrill, A. R., Andersen, G. R., Nissen, P., & Frank, J. (2007). Structures of modified eEF2 80S ribosome complexes reveal the role of GTP hydrolysis in translocation. *The EMBO Journal*, 26(9), 2421–31. doi:10.1038/sj.emboj.7601677
- Tollervey, J. R., Curk, T., Rogelj, B., Briese, M., Cereda, M., Kayikci, M., ... Ule, J. (2011). Characterizing the RNA targets and position-dependent splicing regulation by TDP-43. *Nature Neuroscience*, 14(4), 452–8. doi:10.1038/nn.2778
- Traynor, B. J., Codd, M. B., Corr, B., Forde, C., Frost, E., & Hardiman, O. M. (2000). Clinical features of amyotrophic lateral sclerosis according to the El Escorial and Airlie House diagnostic criteria: A population-based study. *Archives of Neurology*, 57(8), 1171–6. Retrieved from <http://www.ncbi.nlm.nih.gov/pubmed/10927797>
- Tsukiyama-Kohara, K., Iizuka, N., Kohara, M., & Nomoto, a. (1992). Internal ribosome entry site within hepatitis C virus RNA. *Journal of Virology*, 66(3), 1476–83. Retrieved from <http://www.pubmedcentral.nih.gov/articlerender.fcgi?artid=240872&tool=pmcentrez&rendertype=abstract>
- Ule, J., Jensen, K. B., Ruggiu, M., Mele, A., Ule, A., & Darnell, R. B. (2003). CLIP identifies Nova-regulated RNA networks in the brain. *Science (New York, N.Y.)*, 302(5648), 1212–5. doi:10.1126/science.1090095
- Vance, C., Rogelj, B., Hortobágyi, T., De Vos, K. J., Nishimura, A. L., Sreedharan, J., ... Shaw, C. E. (2009). Mutations in FUS, an RNA processing protein, cause familial amyotrophic lateral sclerosis type 6. *Science (New York, N.Y.)*, 323(5918), 1208–11. doi:10.1126/science.1165942
- Voigt, A., Herholz, D., Fiesel, F. C., Kaur, K., Müller, D., Karsten, P., ... Schulz, J. B. (2010). TDP-43-mediated neuron loss in vivo requires RNA-binding activity. *PloS One*, 5(8), e12247. doi:10.1371/journal.pone.0012247
- Wang, I.-F., Wu, L.-S., Chang, H.-Y., & Shen, C.-K. J. (2008). TDP-43, the signature protein of FTLD-U, is a neuronal activity-responsive factor. *Journal of Neurochemistry*, 105(3), 797–806. doi:10.1111/j.1471-4159.2007.05190.x

- Warraich, S. T., Yang, S., Nicholson, G. a, & Blair, I. P. (2010). TDP-43: a DNA and RNA binding protein with roles in neurodegenerative diseases. *The International Journal of Biochemistry & Cell Biology*, 42(10), 1606–9. doi:10.1016/j.biocel.2010.06.016
- Wegorzewska, I., Bell, S., Cairns, N. J., Miller, T. M., & Baloh, R. H. (2009). TDP-43 mutant transgenic mice develop features of ALS and frontotemporal lobar degeneration. *Proceedings of the National Academy of Sciences of the United States of America*, 106(44), 18809–14. doi:10.1073/pnas.0908767106
- Wells, S. E., Hillner, P. E., Vale, R. D., & Sachs, a B. (1998). Circularization of mRNA by eukaryotic translation initiation factors. *Molecular Cell*, 2(1), 135–40. Retrieved from <http://www.ncbi.nlm.nih.gov/pubmed/9702200>
- Wilson, J. E., Powell, M. J., Hoover, S. E., & Sarnow, P. (2000). Naturally occurring dicistronic cricket paralysis virus RNA is regulated by two internal ribosome entry sites. *Molecular and Cellular Biology*, 20(14), 4990–9. Retrieved from <http://www.pubmedcentral.nih.gov/articlerender.fcgi?artid=85949&tool=pmcentrez&rendertype=abstract>
- Xu, Y.-F., Gendron, T. F., Zhang, Y.-J., Lin, W.-L., D'Alton, S., Sheng, H., ... Petrucelli, L. (2010). Wild-type human TDP-43 expression causes TDP-43 phosphorylation, mitochondrial aggregation, motor deficits, and early mortality in transgenic mice. *The Journal of Neuroscience : The Official Journal of the Society for Neuroscience*, 30(32), 10851–9. doi:10.1523/JNEUROSCI.1630-10.2010
- Yokota, O., Davidson, Y., Bigio, E. H., Ishizu, H., Terada, S., Arai, T., ... Mann, D. M. A. (2010). Phosphorylated TDP-43 pathology and hippocampal sclerosis in progressive supranuclear palsy. *Acta Neuropathologica*, 120(1), 55–66. doi:10.1007/s00401-010-0702-1
- Zaher, H. S., & Green, R. (2009). Fidelity at the molecular level: lessons from protein synthesis. *Cell*, 136(4), 746–62. doi:10.1016/j.cell.2009.01.036

10 STATEMENT OF CONTRIBUTION

MN1 cells were provided by Dr. Edgar Kramer. Southern blot was performed under the supervision of PD Dr. Irm Hermans-Borgmeyer. BacTRAP mice were provided by Prof. Manuel Friese. GFP-positive immunohistochemistry was performed by Dr. Benjamin Schattling and Constantin Volkmann. Updated BacTRAP immunoprecipitation protocol was provided by Prof. Myriam Heiman. pEGFP-C2 plasmid containing the sequence for L10a was provided by Dr. Froylan Calderon de Anda. 3T3 and MEF cells were cultured and induced by Dr. Henning Sievert and Dr. Nora Pällmann.

11 EIDESSTATTLICHE VERSICHERUNG

Hiermit erkläre ich an Eides statt, dass ich die vorliegende Dissertationsschrift selbst verfasst und keine anderen als die angegebenen Quellen und Hilfsmittel benutzt habe.

Hamburg, den 19. Juni 2014

Unterschrift

12 EIDESSTATTLICHE ERKLÄRUNG

Ich erkläre hiermit, dass ich mich bisher keiner weiteren Doktorprüfung unterzogen habe. Ich habe die Dissertation in der gegenwärtigen oder einer anderen Fassung an keiner anderen Fakultät eingereicht.

Hamburg, den 19. Juni 2014

Unterschrift